Design of Biomimetic Bone Substitutes: Role of Chemical Composition & Nanostructure

M. P. Ginebra^{1,2}

¹Biomaterials, Biomechanics & Tissue Engineering Group, Department of Materials Science & Metallurgy, Universitat Politècnica de Catalunya, Barcelona, ES, ²Insitute for Bioengineering of Catalonia, Barcelona Institute of Technolohgy, Barcelona, ES

KEYNOTE: Biomimicry seeks inspiration in nature for the design of more efficient solutions in science and technology. This approach can be applied to the design of synthetic bone Historically, calcium phosphate grafts. biomaterials have been proposed as synthetic bone grafts because they mimic the major inorganic component of bone, are bioactive and can form intimate and functional interfaces with neighbouring bone. However, not only composition matters. The mineral phase contained in the extracellular matrix of bone consists of a calcium phosphate compound, hydroxyapatite, with specific chemical. crystallographic and textural features that confer bone its special properties. Particularly, these specific features contribute to make it possible the bone remodelling cycle, since bone cells are able to control dissolution and reprecipitation of this mineral phase.

The design of bone substitutes that can enter the physiological bone turnover cycle, i.e., that can be resorbed and replaced with new bone the same way that impaired bone is replaced in the bone turnover process, is a great challenge. But how can this be achieved? What are the properties that should be modified to make a synthetic bone substitute more biomimetic? What is the impact of stoichiometry, crystallinity. nanostructure or carbonate content, in the performance of calcium phosphate bone substitutes?

We have shown, using different *in vitro and in vivo* models, that textural properties can modulate the biological performance of calcium phosphates in a very significant way, even outweighing the effect of other features such as the solubility of the compounds. Textural properties affect significantly the *in vitro* interaction with cells relevant for the bone regeneration cycle, like mesenchymal stem cells, osteoclasts and osteoblasts; and finally, they have a clear impact in the *in vivo* performance of calcium phosphate materials [1-2].

Specifically, we have shown using a canine model that nanocrystal size and morphology have a strong effect on the osteoinductive potential of hydroxyapatite foams, affecting also significantly scaffold degradation. But also chemical composition is important. Similar effects were obtained by doping the apatitic phase with carbonate, which resulted in small plate-shaped nanocrystals, accelerated both the intrinsic osteoinduction and the bone healing capacity, and significantly increased the cell-mediated resorption [3-4].

These results suggest that tuning the chemical composition and the nanostructural features, in a way that the material mimics better the natural bone mineral, allows entering the physiological bone remodelling cycle, promoting a tight synchronization between scaffold degradation and bone formation.

ACKNOWLEDGEMENTS: This work was supported by the Spanish Government through Project MAT2015-65601-R, co-funded by the EU through European Regional Development Funds. Support was received through the "ICREA Academia" prize, funded by the Generalitat de Catalunya.

REFERENCES: [1] J.M. Sadowska et al. Biomaterials 181 (2018): 318-332. [2] A. Diez-Escudero, et al. Tissue Engineering Part C, Methods, 23(2017):118-124. [3] A. Barba et al., ACS Applied Mater & Interfaces 2017, 9, 41722–41736. [4] A. Barba et al., Applied Mater & Interfaces 2019, in press.

Phase Separation in the Assembly of Biomolecular Materials M. B. Linder¹

¹Aalto University, Department of Bioproducts & Biosystems. Espoo, FI

KEYNOTE: Controlling and understanding the assembly of biomolecules into materials structures is a key aspect of any use, interaction, or manufacture of biological materials. An understanding is emerging within which liquid-liquid phase separations form essential intermediate steps within this assembly.

We have worked on the assembly process of highly engineered proteins that combine spider silk sequences with other functional domains. The protein architectures were inspired from the natural ones but the realization was completely synthetic. Studying the assembly of the engineered proteins we noted that fibres could be drawn from concentrated solutions of them. We noted that fibre assembles only occurred if the protein had previously undergone a phase transition in which a condensed protein phase had separated from a dilute aqueous phase. The condensed protein phase had several other interesting materials properties than fibre formation. For example, the condensed phase functioned as an adhesive with improved toughness properties. We further established various physical characteristics, including the thermodynamics of the protein condensation. We also established that there are multiple forms of condensed proteins and that only a subset of these had properties that were advantageous as adhesives or in fibre formations. Other variants of the condensates showed gel-like properties.

We performed molecular modelling that indicate mechanisms for the assembly of the engineered proteins. Based on our data we suggest an importance of multiple segments of the polymer that show weak interactions, forming so-called sticker interactions between chains.

We note that the overall concepts of a formation of condensed phases is widespread in biology and is often related to structure formation, especially in the case of proteins. In a cellular environment, condensates often form various membraneless organelles. These typically have a role in stress response and often protect different molecular species. A consequence of the packing of polymers in the condensates is

that they can start to interact strongly with each other. In some cases this leads to amyloid formation.

In other fields of research it has been found that condensate formation is an essential aspect of the formation of adhesive structures. One example is marine adhesives where very strongly adhesive plaques are formed.

Altogether a generality of condensates on biopolymer assembly is suggested. The mechanisms by which polymers interact, the thermodynamics behind interactions, and the effect on polymer properties are essential to understand in order to understand both pathological conditions as well as being able to utilize the assembly process for functional purposes.

REFERENCES: [1] Mohammadi, P., Beaune, G., Stokke, B., Timonen, J., Linder, M.B. (2018) Self-coacervation of a silk-like protein and its use as an adhesive for cellulosic materials ACS Macro Letters ACS Macro Lett. 1120-1125, 2018. 7, 10.1021/acsmacrolett.8b00527. [2] Lemetti, L., Hirvonen, S-P., Fedorov, D., Batys, P., Sammalkorpi, M., Tenhu, H., Linder, M.B., Aranko, S. (2018) Molecular crowding facilitates assembly of spidroin-like proteins through phase separation. European Polymer Journal, doi: 10.1016/j.eurpolymj.2018.10.010. [3] Mohammadi, P., Aranko, A.S., Lemetti, L., Cenev, Z., Zhou, O., Virtanen, S., Landowski, C.P., Penttilä, M., Fischer, W.J., Wagermaier, W., and Linder, M.B. (2018) Phase transitions as intermediate steps in the formation of molecularly engineered protein fibers. **Communications** Biology 1:86, doi: 10.1038/s42003-018-0090-y.

Dynamically Stiffening Hydrogels to Study Cellular Mechanobiology

A. Gunay, J. Silver, T. Ceccato, K. S. Anseth

Department of Chemical & Biological Engineering & BioFrontiers Institute, University of Colorado Boulder, CO, US

INTRODUCTION: Cells sense the mechanical properties of their microenvironment, which undergo significant changes upon injury and disease that occur over various timescales. Advances in hydrogels with on-demand control of material properties allow experimenters to probe the role of outside-in signalling on cellular fate. Here, we explore two different chemistries that enable hydrogel stiffening photochemical using cytocompatible conditions, specifically crosslinking dibenzocycloocytne (DBCO) groups dimerization of anthracenes (Ant). Results will demonstrate the benefits of each material system. Specifically, the DBCO crosslinking used to explore muscle mvoblast mechanotransduction in a dynamic 3-D microenvironment. while we explored mechanosensitive pathways in cardiac fibroblasts using Ant hydrogels by tracking their myofibroblast activation in real time.

METHODS: Poly(ethylene glycol)-based hydrogels were formed using a strain promoted azide/alkyne cycloaddition (SPAAC) reaction with excess DBCO groups. The pendant DBCO groups could be further crosslinked rapidly (< 120 s) in the presence of 365 nm light (5 - 10 mW/cm²) and photoinitiatior (LAP), thus enabling the in situ stiffening of cell-laden hydrogels.^[1] The initial and final hydrogel moduli was tuned via the initial stoichiometry of N₃/DBCO groups. As the SPAAC reaction is spontaneous, it permits cell encapsulation and studying mechanobiology in 3D matrices. In a complementary material system, photodimerization of Ant groups at 365 nm were used to prepare hydrogels without the of exogenous addition photoinitiaton^[2] Hydrogel moduli and stiffening were controlled by shuttering the photocrosslinking light on/off to achieve a broad range of hydrogel modulii (E'= 0.1 to 100 kPa).

RESULTS: Using the SPAAC hydrogels, mouse muscle myoblasts (C2C12s) and muscle myofibers were encapsulated in 3D microenvironments and their mechanosensitivity was assessed by their stiffness-dependent nuclear localization of a key

mechanosensor, yes-associated protein (YAP). C2C12 cells were cultured in hydrogels with a 2:1 DBCO/N₃ ratio that could be stiffened from G' = 710 Pa to 5050 Pa. A protease degradable (N₃-GPQGIWGQKG-N₃) crosslinker introduced into the network to further allow cellular remodelling before stiffening. At short time scales (1-day after stiffening), C2C12 cells remained rounded and YAP remained primarily in the cytosol. In contrast, when the cellular microenvironment was stiffened at a later time point (e.g., > 7day), the C2C12 cells exhibited a spread morphology and YAP became more localized in the nucleus. By using PEG-Ant hydrogels, we developed a hydrogel that can stiffen from E' = 10 to 50 kPa in 90 s. of irradiation to simulate the change in cardiac muscle stiffness upon a heart attack.[3] By using a real time reporter cardiac fibroblast cell line, we found that nuclear factor of activated T Cells (NFAT), a downstream target of calcium signalling translocates to the nucleus within 80 min. post-stiffening, but remains cytoplasmic on both E' = 10 and 50 kPa static hydrogels.

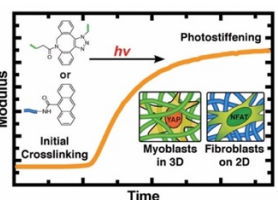


Fig. 1. DBCO crosslinking and anthracene dimerization both permit dynamically stiffening hydrogels. These hydrogels allow monitoring mechanoresponsive proteins, such as YAP in two or three dimensional microenvironments.

DISCUSSION & CONCLUSIONS: Cytocompatible, dynamically stiffening hydrogels with tailorable initial and final modulii allows experimenters to investigate outside-in mechanobiology. The hydrogels are useful to study cellular mechanotransduction either in two or a three-dimensional matrix.

ACKNOWLEDGEMENTS: NIH Grants HL132353-01 and DE016523.

REFERENCES: [1] Brown, TE *J Am Chem Soc* 2018, *140*, 11585. [2] Berry, MF *Am J Physiol Heart Circ Physiol*, 2006, *290*, 2196. [3] Zheng, Y *Macromolecules* 2002, *35*, 5228.

Regeneration of Human Cornea with Combined Strategy of Human Stem Cells & Biomaterial Solutions

H. Skottman¹, A. Mörö-Sorkio¹, L. Koivusalo¹, M. Vattulainen¹, M. Kauppila¹, O. P. Oommen¹, S. Miettinen¹, T. Ilmarinen¹

¹Faculty of Medicine & Health Technology, Tampere University, Tampere, FI

INTRODUCTION: Corneal blindness affects millions of people worldwide, and there is a constant shortage of high-quality donor tissue. Engineering a corneal transplant that could effectively restore functional limbal epithelial stem cells (LESC) and regenerate the corneal epithelium and stroma is an important goal. To achieve this, differentiation of LESCs from human pluripotent stem cells (hPSC-LESC) provides new approach for regenerative therapy. In addition, human adipose stem cells (hASCs) provide an appealing cell source for corneal stromal regeneration due to their capacity to differentiate towards corneal keratocytes, immunomodulatory properties and good availability from healthy adult donors. However, limited strategies exist for the delivery of therapeutic stem cells with tissuelike cellular organization to the anterior cornea.

METHODS: We have developed an efficient and clinically relevant method to produce LESC- like cells from hPSCs [1]. We succeeded in engineering cornea-mimicking 3D structures with corneal epithelium and stroma using hPSC-LESCs and hASCs by two different strategies, namely, laser-assisted bioprinting (LaBP) with combination of novel bioinks [2], and sequential cell plating in ECM mimetic hydrazone-crosslinked hyaluronic acid (HA) hydrogels [3], modified with tissue adhesive dopamine (DOPA) moieties. Here, cornea-mimicking cell stratification established by encapsulating hASCs inside the hydrogels, followed by surface conjugation of ECM-components and hPSC-LESC seeding on the hydrogel surface. The characteristics and functionality of the cells as well as organized 3D structures has been studied with molecular characterization of the cells, ex vivo porcine cornea organ culture model and recently LESCs also in vivo.

RESULTS: With our novel differentiation method, we are able to produce cells expressing clinically relevant corneal progenitor markers in defined and serum-free culture conditions and in high numbers, allowing their usage also for

3D bioprinting applications. The process of LaBP retained the expression of clinically relevant stem cell marker p63α/p40 and proliferation marker Ki67 in hPSC-LESCs. Both cell types had good viability after printing. Importantly, the printed hPSC-LESCs formed a stratified epithelium with apical expression of differentiation markers and basal expression of the progenitor markers. In the 3D bioprinted stroma, the hASCs organized horizontally in alternating layers as in the native corneal stroma. Ex vivo cornea model showed attachment and hASC migration of the 3D bioprinted structures to the host tissue. The HA-DOPA hydrogel system also maintained the characteristics of both cell types. Additionally, the tissue adhesive cell-containing hydrogels were successful implanted in the ex vivo cornea model.

DISCUSSION & CONCLUSIONS: With these studies, we have demonstrated for the first time the feasibility of 3D LaBP for corneal applications and that hPSC-LESC provide a useful model for studying the mechanisms of corneal development *in vitro* and importantly attractive cell population to be tested *in vivo* for limbal regeneration. We have developed a tissue adhesive HA-DOPA hydrogel and shown its proof-of-concept to deliver cells for regeneration of the corneal epithelium and the underlying stroma. Collectively, these results encourage sutureless implantation of functional stem cells as the next generation of corneal regeneration.

ACKNOWLEDGEMENTS: The research is supported by Business Finland, Academy of Finland, Sigrid Juselius foundation, Graduate School of Faculty of Medicine and Health Technology, Instrumentarium Science Foundation and Finnish Cultural Foundation.

REFERENCES: [1] Hongisto, H., et al., Stem Cell Research & Therapy, 2017, 8:291. [2] Sorkio, A., et al., Biomaterials, 2018. 171:57-71. [3] Koivusalo, L., et al., Materials Science & Engineering C, 2018, 85: 68–78.

Novel Bioceramics: Synthesis & Characterisation H. Engqvist

Applied Materials Science, Department of Engineering Science, Ångström Laboratory, Uppsala University, Uppsala, SE

KEYNOTE: Bioceramics have found it use as a bone substitute material, i.e. load bearing in joints and as artificial teeth or non-loadbearing as bone void fillers.

One clinical indication that has not been fulfilled is to combine loadbearing and bone regeneration. An implant design that has high enough biomechanical strength and good handling properties would represent a significant clinical benefit. One strategy to achieve such properties is to develop reinforced phosphate implants. calcium Both reinforcement and the calcium phosphate composition need to be carefully selected. Reinforcement using a metal (e.g. Ti) or a polymer mesh can provide the design with sufficient strength. The evaluated design includes a Ti mesh with monetite-based tiles, tested in cranioplasty. The results show bone formation, even in the center of large cranial defects.

A novel clinical indication relates to a new class of calcium phosphate based materials that can glue tissues together, and bond tissues to metallic and polymeric biomaterials. Surprisingly, alkaline phosphate cements modified with phosphorylated amino acid monomers of phosphoserine can bond tissues even stronger than commercial cyanoacrylates when cured in wet-field conditions. The addition of phosphoserine to a calcium phosphate cement formulation creates a new microstructure, in the set material, where the precipitated calcium phosphate particles are of nanoscale leading to very high surface energy. Interestingly, all components in the adhesive material are resorbable and biocompatible. The results presented show excellent adhesive properties in combination with an intriguing new cement microstructure.

ACKNOWLEDGEMENTS: Support from the Swedish Research Society and the Swedish Foundation for Strategic Research (RMA15-0110).

Peripheral & Central Nerve Repair Using Phosphate-Based Glass Fibres

J. C. Knowles¹⁻⁴, H.-W. Kim^{3,4}, J.-K. Hyun^{3,4}

¹Division of Biomaterials & Tissue Engineering, Eastman Dental Institute, University College London, London, UK, ²Discoveries Centre for Regenerative & Precision Medicine, UCL Campus, London, UK, ³Department of Nanobiomedical Science & BK21 PLUS NBM Global Research Center for Regenerative Medicine, Dankook University, Cheonan, KR, ⁴UCL Eastman-Korea Dental Medicine Innovation Centre, Dankook University, Cheonan, KR

KEYNOTE: Peripheral and central nerve damage are extremely debilitating for the patient and we currently have no adequate treatments available, in particular, for spinal cord damage. Our work has focused on acellular approaches to repair, initially utilising glass fibres as scaffolds to promote rapid repair and functional recovery. More recently our work has utilised the fibres as temporary sacrificial templates to allow the production of continuous discrete channels in polymers. This presentation will detail some of the work we have undertaken and also some of the more recent large animal studies we have performed.

We have worked on utilisation of fibres as scaffolds for neural regeneration, utilising the fibres as a topological use to direct neurite growth and subsequent repair⁽¹⁾. These fibres showed excellent compatibility and the appropriate cues to drive repair compared to the control. However during the course of this work it became clear that the parameter controlling the repair was the ability to present and maintain space within which the cells can grow and thus we then developed a new system whereby the fibres were used as a sacrificial template to form pores from one end of a polymer scaffold to the other (see Figure 1)

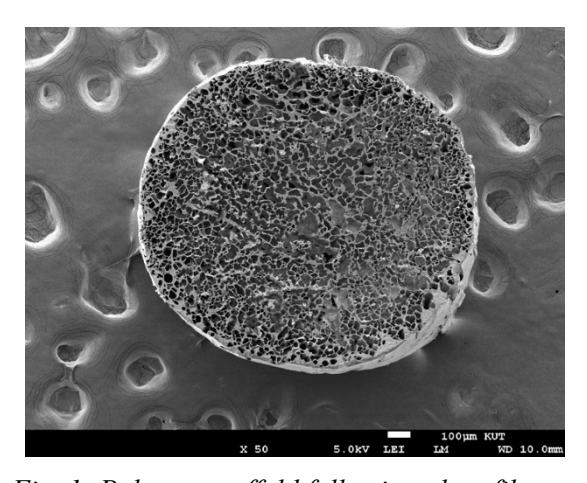


Fig. 1: Polymer scaffold following glass fibre removal via a dissolution process in water.

Further work has shown the highly porous nature of these conduits as evidences by axons seen throughout the constructs and also the presence of NGF to promote Schwann cell growth (See Figure 2)





Fig. 2: Top: Conduit without NGF. Bottom: with NGF. Tuj-1 (green) for axons and S100 (red) for Schwann cells Bar = 500µm)

In conclusion, the methods presented here offer a simple and yet highly effective method to drive nerve regeneration and lead to the all important function recovery. It can be seen that nerve repair can be achieved without the need for complex cell based interventions. However, the benefit of the presence of cells cannot be underestimated and future work may allow us to continue to improve these therapies by developing them in conjunction with cellular therapies, which are starting to show some promising results in early clinical trials.

REFERENCES: [1] Joo NY, Knowles JC, Lee GS, Kim JW, Kim HW, Son YJ, et al. Effects of phosphate glass fiber-collagen scaffolds on functional recovery of completely transected rat spinal cords. Acta Biomater. 2012;8(5):1802-12.

Additive Manufacturing of Trabecular Bone Structures

A. Diez-Escudero¹, A. Spanou¹, D. Wu¹, P. Isaksson², C. Persson¹

¹ BioMaterial Systems, Department of Engineering Sciences, Uppsala University, Uppsala, SE, ²Solid Mechanics, Department of Engineering Sciences, Uppsala University, Uppsala, SE

INTRODUCTION: One challenge when mimicking bone to achieve e.g. good synthetic regenerative scaffolds lies in its highly hierarchical conformation. The architecture of bone at the mm- to microlevel grants its optimal intrinsic mechanical properties, together with the arrangement of organic and inorganic phases at the micro- to nanolevel. Reproducing both the mechanical and morphological properties of bone can endow scaffolds optimal mechanical and biological performance. The aim of this work was to use 3D printing to obtain complex trabecular designs enabling their use as models for evaluation of new implants, as well as bone scaffolds using bioresorbable polymers and composites.

METHODS: Femoral trabecular bone images were obtained by synchrotron radiation X-ray CT with a pixel size of 3.25µm. A region of interest (ROI) of 4.6mm×7mm was cut out of trabecular bone, and used as a model for 3D printing. Images within the ROI were segmented, and converted to a printable mesh file using Matlab. Fused deposition modelling (Ultimaker 2+) was used to print the trabecular structures. Filaments of polylactic acid (PLA) and composites of PLA with different amounts (5-10-15%wt.) of hydroxyapatite (HA) were used for printing. Cylinders (6x12mm²) were used to determine the compressive strength and Young's modulus of the bulk composite materials, pure PLA was used as control material (n=3). Screw pull-out tests were performed on the printed trabecular structures using PLA-HA composites and polyurethane foam (Sawbone) as control (n=3). The structural reproducibility of the scaffolds was assessed by comparing µCT scans of the scaffolds to the original meshed images.

RESULTS: The incorporation of HA into the PLA matrices showed an enhancement in compressive strength and Young's moduli compared to the pristine PLA. The trabecular designs from the femoral scans printed in composite material showed an increase of 100-200N in pull-out force, for 5%HA and 10%HA

respectively, compared to Sawbone. Even though further printing optimization is needed, μ CT evaluation of bone volume fraction for the input geometry and the printed parts showed similar values, 39.4 and 35.7%, respectively (Fig 1).

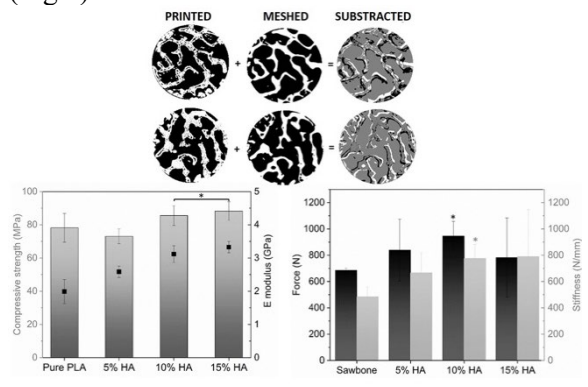


Fig. 1: Top: μ CT scans comparing printed and the meshed structures generated from synchrotron images. Bottom: Compressive strength of the printed bulk material to the left, and screw pull-out force and stiffness from the different trabecular composites to the right.

DISCUSSION & CONCLUSIONS:

Mimicking the trabecular structure of femoral bone was enabled by combining PLA/HA composites and 3D printing technology. Both materials, PLA and HA are known to be biocompatible and resorbable. Thus the synergy of the trabecular architecture with such materials is a promising strategy to develop bone mimicking materials. Furthermore, the mechanical properties of the trabecular designs demonstrated a more representative model of femoral samples than the currently used synthetic foams (SawBone)[1].

ACKNOWLEDGEMENTS: The authors thank Prof. Stefan Johansson for printer setup, Paul Scherrer Institute, for synchrotron radiation beamtime at TOMCAT and the Göran Gustafsson Foundation for financial support.

REFERENCES: [1] M. Pujari-Palmer, J. Mech. Behav. Biomed. Mater.,77 (2017).

"Mussel-Inspired" Biomimetic Polymer-Composite Bone Cement for Fracture Fixations: Synthesis, Characterization & ex-vivo Evaluation

K. Valová¹, L. Michlovská¹, K. Lysáková¹, J. Brtníková¹, M. Krtička², P. Poláček¹, K. Částková¹, L. Vojtová¹

¹Advanced Biomaterials, Brno University of Technology, CEITEC-Central European Institute of Technology, Brno, CZ, ²University Hospital Brno, Brno, CZ

INTRODUCTION: phosphate Calcium cements (CPCs) have been a subject of interests in bone tissue engineering mainly because of their attractive properties such as self-setting ability in vivo at physiological conditions, good injectability and cohesion [1]. However, they have still very important limitations like separation when injected through very thin needle and poor adhesion to bone, which is essential for fracture fixation via mini-invasive surgery. Therefore, modification of the CPCs with bioadhesive "mussel-inspired" dopamine seems to be a good solution. Up to now, dopamine has been used for coating different polymerization oxidative biomaterials bv exhibiting excellent adhesion to most of the surface even in wet environment [2].

METHODS: The polymer-composite bone cement was prepared according to our previous work [2] with light modification. Shortly, (Premier alpha-tricalcium phosphate Biomaterials, Ireland) and dopamine (Sigma-Aldrich, Pennsylvania) were mixed with aqueous solution of thermosensitive poly(D,Llactic acid-co-glycolic acid)-b-poly(ethylene glycol)-b-poly(D,L-lactic acid-co-glycolic acid) triblock copolymer (PLGA-PEG-PLGA) synthesized via Michlovská et al. [3]. Fig. 1 represents fast reaction of cement at 37°C due to the copolymer gelation followed by cement self-setting and dopamine polymerization. The rheological properties during setting reaction and thixotropy were observed using rotational rheometer AR-G2 (TA Instruments). Ex-vivo biomechanics in both compression and threepoint bending of bonded cadaverous femoral pig bones were evaluated on Zwick instrument.

RESULTS: Dopamine addition accelerated the CPC setting reaction (about 2 hours) while exhibiting very good injectability and cohesion. A porous structure of dopamine-modified bone cement is very important for promoting cell integration and faster bone regeneration. Moreover, dopamine based cement showed

better adhesion to bone and higher strain (elasticity) in comparison to unmodified one.

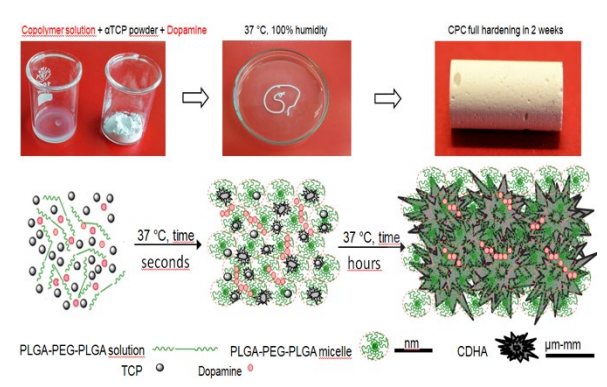


Fig. 1: Preparation of dopamine modified bone cement and scheme of the setting reaction.

DISCUSSION & CONCLUSIONS: Although the adhesion is an important parameter for potential use of CPC in traumatology, it is very important that additives must not negatively influence other parameters such as rheological and mechanical properties, biocompatibility and biodegradability. While rheological, morphological and ex-vivo testing have already showed promising results, in-vitro and in-vivo biocompatibility is being evaluated under collaboration with Motol university hospital in Prague. Anyhow, dopamine modified polymer-CPC has a great potential for future bone fracture fixation study in-vivo.

ACKNOWLEDGEMENTS: This work was supported by the CEITEC 2020 (LQ1601) with financial support from the MEYS of the Czech Republic under the National Sustainability Programme II, by the Ministry of Health (NV18-05-00379) and CEITEC VUT-J-19-6087.

REFERENCES: [1] L. Vojtová et al. *Int. J. Mol. Sci.* (2019), **20**(2), 391. [2] Y.Liu et al. *Chem. Rev.* (2014), 114(9), 5057-5115. [3] L. Michlovská et al. *Macromol. Symp.* (2010), 295, 119.

Vitamin K2 changes vitamin D induced mechanical properties of human 3D bone spheroids *in vitro*

M. Schröder¹, E. Riksen¹, B. H. Skallerud³, M. Møller⁴, A. M. Lian², J. E. Reseland¹

INTRODUCTION: Rotating bioreactors on a clinostat system create an environment that allows bone cells to aggregate into 3D multicellular spheroids and form bone-tissue like structures. These 3D in vitro analogs of human bone represent a new potential model for testing of various stimuli on bone formation and remodeling¹. The active vitamin D metabolite 1,25(OH)2D has a known function in bone homeostasis. Vitamin K2 is a cofactor of gamma-carboxylase, and essential for the pathway of gamma-carboxylation of vitamin Kdependent proteins like the bone matrix protein osteocalcin (OC) and matrix Gla protein (MGP), which inhibits soft tissue calcification in arteries and cartilage². In vivo, vitamin K₂ administration has been shown to improve bone strength and quality, reducing fracture risk, while there is no effect on bone mineral density³. In this study, the effect of vitamin K₂ alone and in combination with vitamin D₃ was tested in a rotary culture systems in the 3D bone model. Results are compared to effects in a 2D culture system.

METHODS: Human primary osteoblasts (hOBs) were cultures in 2D and in 3D (BioArray Matrix drive BAM v4, CelVivo, Blommenslyst, Denmark). Synthetic vitamin K_2 MK-4 (10 μM) and 1α ,25-dihydroxyvitamin D_3 (vitamin D_3) (10^{-8} M) were added alone and in combination. Untreated cells were used as control. After 21 days, osteospheres were characterized in terms of their mechanical response by nanoindentation (Hysitron, Minneapolis, USA) and expression of periostin and collagen type I by confocal microscopy. The secretion of cytokines and bone factors to the medium was analyzed by Luminex.

RESULTS: In a 2D culture system, the secretion of OC and osteopontin (OPN) from hOBs was enhanced by MK-4 alone and in combination with vitamin D₃. These are major non-collagenous proteins involved in bone matrix organization and deposition⁴. In the 3D

bone model, mechanical testing revealed that vitamin D_3 treatment alone increased osteosphere stiffness compared to the control while MK-4 supplementation, both alone and in combination with vitamin D_3 , induced a softer osteosphere.

DISCUSSION & CONCLUSIONS: Ex vivoderived 3D bone constructs are useful in vitro models in physiological studies of bone formation, remodeling and function. Vitamin K₂ modulates bone quality in 3D in vitro bone constructs via extracellular matrix synthesis and vitamin K-dependent proteins in the bone matrix.

ACKNOWLEDGEMENTS: The authors thank Krzysztof Wrzesinski (CelVivo, Blommenslyst, Denmark) for kindly providing the BioArray Matrix drive BAM v4. JE Reseland is a member of Cost action CA16119 CellFit.

REFERENCES: [1] M. S. Clark et al. (2013) *Acta biomaterialia* **9:** 7908-7916. [2] G. Lou et al. (1997) *Nature* **386:** 78-81. [3] M. H. J. Knapen, L. J. Schurgers and C. Vermeer (2007) *Osteoporos Int* **18:** 963-972. [4] S. Bailey (2017) Ann N Y Acad Sci. **1409:** 79–84.

Department of Biomaterials, Institute for Clinical Dentistry, University of Oslo, Oslo, NO,
 Oral Research Laboratory, Institute for Clinical Dentistry, University of Oslo, Oslo, NO,
 Department of Structural Engineering, Faculty of Engineering, Norwegian University of Science & Technology, Trondheim, NO, ⁴Axial Vita AS, Oslo, NO

Biofilm Interfacial Microenvironment Evaluation by pH Sensitive Nanoparticles

P. Merkl¹, G. A. Sotiriou¹

¹Department of Microbiology, Tumor & Cell Biology, Karolinska Institutet, Stockholm, SE

INTRODUCTION: associated **Implant** infections caused by biofilms are a major cause of implant rejection and, if not detected sufficiently early, may result in fatal sepsis (Shirtliff and Leid, 2009). Biofilms are dense microcolonies of bacteria which typically adhere to surfaces therefore, their detection and diagnosis can be difficult. Their extracellular matrix and the diverse roles which the bacteria can fulfill in the biofilm also lead to them being more tolerant of antibiotics and more easily developing resistance against them. promising strategy to help combat biofilms are "smart" anti-biofilm release surfaces. These surfaces are often loaded with antibiotics or other antimicrobials and respond to the creation of a microenvironment characteristic of biofilms by releasing their cargo (Koo et al. such 2017). One characteristic microenvironment is low pH, whereas in healthy tissue the pH should lie close to 7.4 at the biofilm substrate interface the pH can decrease to 5 and below even when biofilm is grown in buffered pH 7.4 medium (Schlafer et al. 2015).

METHODS: Calcium phosphate nanoparticles doped with europium were produced by flame spray pyrolysis and directly deposited as a film on silicon substrates. Their structure was analysed using SEM, XRD and FTIR and their luminescent properties were evaluated with a spectrometer. A sensor response calibration curve was measured using pH buffers and a variety of bacterial strains and species were allowed to form biofilms on the chips in M9 minimal media. The formation of biofilm was assesses using crystal violet staining.

RESULTS: These nanoparticles exhibited a pH dependent change in their luminescence intensity, whereby the emission peak at 616 nm undergoes a strong decrease compared with the 592 nm peak. This provides a ratiometric sensor response and known pH buffers were used as calibrants. A panel of clinically relevant biofilm forming bacteria were selected to measure their interfacial pH. These bacteria grown in buffered

media demonstrated low pH environments, however, differences between bacterial strains and species were observed.

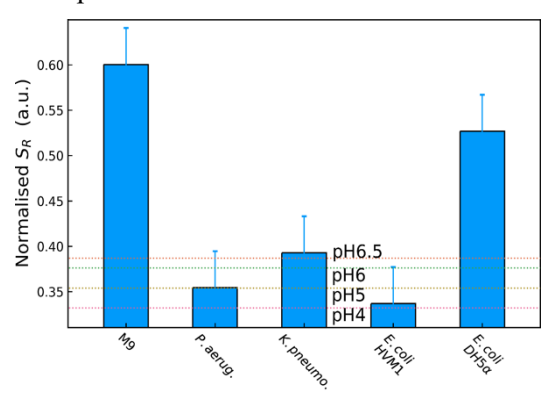


Fig. 1: Normalised sensor response (S_R) with 24 hr biofilm growth vs. clean growth medium (M9). Horizontal lines show the associated pHs derived from the calibration curve.

DISCUSSION & CONCLUSIONS: Here a novel ratiometric sensor which relies on the same processes for sensing as for potential antimicrobial release is presented in order to optically probe the interfacial biofilm surface pH. These pH responsive silicon chips can therefore be used to guide the development of anti-biofilm surfaces to target particular bacterial infections.

ACKNOWLEDGEMENTS: This project has received funding from the European Research Council (ERC) under the European Union's Horizon 2020 research and innovation programme (ERC Grant agreement n° 758705). Funding from the Karolinska Institutet Board of Research, the Swedish Research Council (2016-03471), the Jeansson Foundations (JS2016-0029) and the Åke Wiberg Foundation (M16-0098) is kindly acknowledged.

REFERENCES: [1] Shirtliff, M.; Leid, J. (2009) *The Role of Biofilms in Device-Related Infections*, Springer. [2] Koo, H et al. (2017) Nat. Rev. Microbiol, 15, 740–755. [3] Schlafer, S., et al. (2015) Appl. Environ. Microbiol. 81, 1267–1273.

Design & Development of a 3D in vitro Model for Alzheimer's Disease

V. D. Ranjan¹, L. Qiu², E. K. Tan², H. Weimin³, Y. Zhang³, L. Zeng²

¹HealthTech NTU, Interdisciplinary Graduate School, Nanyang Technological University, SG, ²Research Department, National Neuroscience Institute, SG, ³School of Mechanical & Aerospace Engineering, Nanyang Technological University, SG

INTRODUCTION: Three-dimensional (3D) cell culture platforms have been found to be more advantageous, compared to traditional 2D monolayer cultures, in mimicking native in vivo microenvironments with high physiological relevance especially for in vitro modelling of complex diseases such as Alzheimer's disease (AD). In this regard, a novel 3D culturing system comprised of human AD patient iPS cell derived neurons grown within a 3D electrospun nanofibrous scaffold was developed and optimized for modelling AD. A comparison of key characteristics between cells grown in 2D and 3D cultures was performed using this model to better understand the key differences in cellular phenotypes as well as progression of AD pathogenesis, including amyloid- β (A β) accumulation and tau hyperphosphorylation.

METHODS: Fabrication of a 3D biomaterial based nanofibrous scaffold was done via wet electrospinning technique. In addition, the 3D scaffold geometry was tuned by optimizing various parameters including polymer material, fiber diameter, pore size, porosity, wettability, stiffness etc., with the aim of promoting iPSCs differentiation towards neurons and enabling long-term survival of iPSC-derived neurons. Cellular phenotypes were then characterized by immunostaining followed by confocal microscopy, and further validated via quantitative PCR (qPCR) analysis.

RESULTS: The 3D nanofibrous scaffold allows for increased cell infiltration up to 2 mm inside, along with enabling a uniform distribution and space for cell growth. We found that iPSC-derived neurons from AD patients exhibit decreased proliferation and faster differentiation when cultured within the 3D nanofiber scaffold compared to 2D monolayer based culture. However, the cells also exhibited lower viability during longer term culture in 3D format compared to 2D culture.



Fig. 1: Scaffold geometry for different polymer materials studied: PCL(left), PLLA (middle), PLGA (right) fabricated via electrospinning

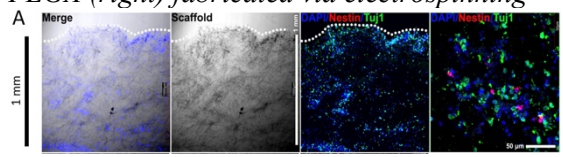


Fig. 2: iPS cell infiltration and distribution inside the 3D PLGA nanofiber scaffold

DISCUSSION & CONCLUSIONS: PLGA was found to be the most suitable among the 3 synthetic polymers studied for fabrication of 3D scaffold via electrospinning and, in terms of other physical features such as pore size controllability, porosity, hydrophilic property, mechanical stiffness and biocompatibility. The scaffold pore size could be tuned to an extent to enhance cell infiltration by modification of the seeding paradigm. The 3D nanofiber scaffold microenvironment was found to promote faster iPSC-derived NPC differentiation/maturation compared to that of 2D culturing system. However, 3D culture didn't magnify the Aβ phenotype compared with 2D culture.

REFERENCES: [1] Ranjan VD, Qiu L, Tan EK, Zeng L, Zhang Y. Modelling Alzheimer's disease: Insights from in vivo to in vitro three-dimensional culture platforms. J Tissue Eng Regen Med. 2018;1–15. https://doi.org/10.1002/term.2728.

Alignment of Chondrocytes using Carbon Nanotube Micropillars

L. Janssen¹, S. Muthusamy¹, O. Pitkänen¹, G. S. Lorite¹

¹Microelectronics Research Unit, University of Oulu, Oulu, FI

INTRODUCTION: Articular cartilage is an avascular tissue composed of only one type of cells (chondrocytes) surrounded by extracellular matrix (containing mainly collagen type II and proteoglycans such as aggrecan). The structure of articular cartilage can be divided into three layers (superficial, transitional and deep zone), which have each specific proprieties such as extracellular matrix content and chondrocyte orientation and morphology. One of the biggest challenges in cartilage tissue engineering is to obtain the required chondrocyte orientation and morphology in the different layers of the cartilage scaffold, in order to allow optimal mechanical and metabolic response by the cells. This work evaluates the use of multi walled carbon nanotube (MWCNT) templates to provide guidance for chondrocyte growth.

METHODS: 10 µm high vertically aligned MWCNT templates organized in different geometries were synthesized via chemical vapor-phase deposition. The designs included honeycomb forest as well as micropillared stripes, grids and spirals with center-to-center spacing varying between 10 and 220 µm. The micropatterns were fabricated by lift-off lithograph over Si/SiO2 surfaces, which was used as control samples. Primary chondrocytes at passage 3 were seeded on the various MWCNT templates at a density of 15 000 cells/cm² for 1, 3 and 7 days after which life/dead staining as well as immunostaining using anti-collagen type II and anti-aggrecan antibodies with fluorescent secondary antibody (FITC and NL557 respectively) were performed together with DAPI staining for the nuclei. Scanning electron microscopy was used to acquire high resolution images.

RESULTS: Immunostaining images clearly show that chondrocyte align in the MWCNT grid design (Fig. 1 middle row), displaying an elongated morphology, while they are spread and disorganized on flat Si/SiO₂ surface (Fig. 1 top row). Furthermore, the shape of chondrocytes can also be influenced by other designs such as the honeycomb MWCNT pattern (Fig. 1 bottom row). The expression of collagen II and aggrecan was unchanged between the different templates and controls

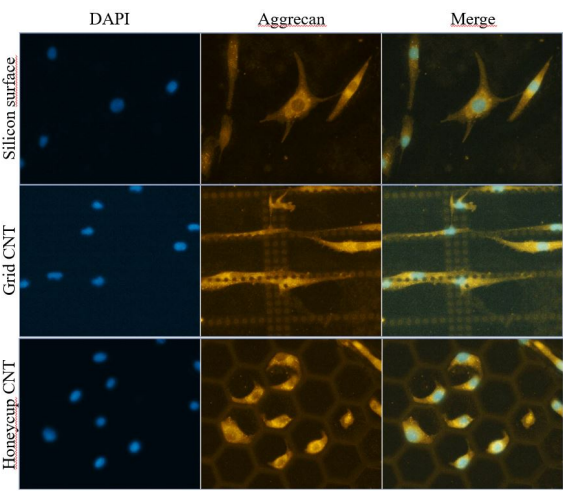


Fig. 1: Chondrocytes growing for 3 days on different MWCNT templates (honeycomb forest and micropillared grid design) versus control (Si/SiO₂ flat surface). Cells were stained with DAPI (blue) and anti-aggrecan (orange/red).

of this study was to evaluate the effect of MWCNT templates on chondrocytes alignment. Our results showed that by tailoring MWCNT templates it is possible to control the organisation and morphology of chondrocyte either achieving alignment (micropillared grid design) or confining the cells (honeycomb forest design). These results give new perspectives for the use of MWCNT in 3D scaffolds to guide cell orientation and morphology in order to mimic the different layers of the articular cartilage tissue.

ACKNOWLEDGEMENTS: This work was funded by EU project RESTORE (H2020-NMBP-TR-IND-2018-814558) and Academy of Finland (#317437 and #320090).

Platelet Lysate-Based Nanocomposite Biomaterials for Tissue Engineering & Regenerative Medicine

M. Gómez-Florit^{1,2}, B. B. Mendes^{1,2}, R. M. A. Domingues¹⁻³, R. L. Reis¹⁻³, M. E. Gomes¹⁻³

¹3B's Research Group, Research Institute on Biomaterials, Biodegradables & Biomimetics, University of Minho, Headquarters of European Institute of Excellence on Tissue Engineering & Regenerative Medicine, Guimarães, PT, ²ICVS/3B's-PT Government Associate Laboratory, Braga/Guimarães, PT, ³Discoveries Centre for Regenerative & Precision Medicine, Headquarters at University of Minho, Avepark, 4805-017 Barco, Guimarães, PT

INTRODUCTION: Platelet lysate (PL) has shown outstanding properties as an inexpensive source of growth factors, cytokines and extracellular matrix precursors (e.g. fibrinogen) currently being explored in several tissue engineering strategies. However, the proposed PL-based formulations show limited ability to retain/protect biological active biomolecules from degradation, exhibit extremely low mechanical properties and structural stability, as well as fast in vitro/in vivo degradation rates.1 In order to overcome these limitations and further enabling the use PL not only as a source of growth factors but also as a scaffolding biomaterial, we propose here reinforcing its protein content with cellulose nanocrystals (CNC). Using this strategy, we have been able to develop injectable hydrogels, bioinks and sponges, with unprecedented biomimetic and biofunctional characteristics with high potential in tissue engineering applications.

METHODS: CNC were modified to present surface aldehyde groups. PL/CNC materials were produced using standard double barrel syringes promoting the *in situ* PL-clotting via thrombin and calcium activation along with the CNC/protein covalent crosslinking.² While the sponges were obtained by freeze-drying of the injectable hydrogels, the bioink was 3D printed inside a support microparticles bath. Human adipose tissue-derived stem cells (hASCs) were used for all the tests.

RESULTS: The inclusion of CNC allowed to avoid extensive clot retraction typical from plain PL gels while remaining biocompatible. Furthermore, the CNC markedly increased the bulk hydrogels mechanical properties up to an impressive 2 orders of magnitude higher storage modulus compared to plain PL gels, while allowing to control growth factor release and to tune hASCs behaviour. In addition, using the bioink formulation, we were able to 3D print complex freeform cell-laden constructs with

outstanding biomimetism of the native tissues fibrillar extracellular matrix and unprecedented biofunctionality, which promoted fast cellularization and remodelling of the printed constructs. Regarding the PL/CNC sponges, they were biocompatible and showed better haemostatic properties than commercial gelatin sponges *in vivo*.

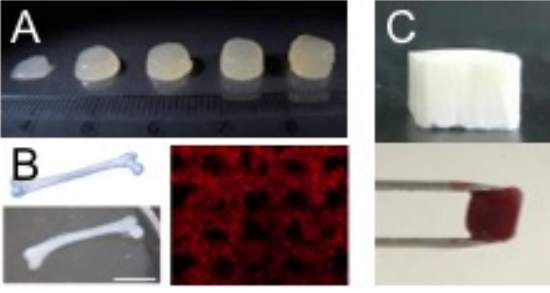


Fig. 1: PL/CNC nanocomposite biomaterials. A) Injectable hydrogels with increasing CNC content. B) A 3D printed human femur model (left) and a square lattice structure with encapsulated stem cells (right) produced using the bioink. C) The sponges (up) showed excellent haemostatic properties (bottom).

DISCUSSION & CONCLUSIONS: The combination of PL, a clinical-derived product, with CNC, the nature's "carbon nanotubes", has allowed to produce biomimetic biomaterials that explore the outstanding biological properties of PL for a wide range of applications in tissue engineering and regenerative medicine.

ACKNOWLEDGEMENTS: European Union's H2020 programme; European Research Council (ERC); Fundação para a Ciência e a Tecnologia (FCT); Hospital da Prelada (Portugal).

REFERENCES: [1] B.B. Mendes et al., Adv Drug Deliv Rev 129 (2018) 376. [2] B.B. Mendes et al., Nanoscale 10 (2018) 17388.

Air Gap Electrospun Templates with Blue Light Gradient for Engineered Cell Stimulation

D. Velasquez Pulgarin^{1,2}, B. Hambly¹, G. Bowlin¹

¹Department of Biomedical Engineering, University of Memphis, TN, US, ²Centre for Molecular Medicine, Karolinska Institutet, SE

INTRODUCTION: Anterior cruciate ligament reconstruction surgery has high repair failure, mostly due to the current inability to regenerate a properly functioning enthesis¹. The structural and mechanical gradients of entheses are critical for normal function and regenerating these gradients is a major challenge. The present study's goal is to develop a twocomponent system in which an electrospun template (component 1) will be used to deliver physicochemical cues to engineered adiposederived stem cells (ASCs) (component 2) to generate a countergradient of growth factors that will guide the regeneration of the enthesis. Air gap electrospinning generates aligned fibers that mimic the native ligament. For developing delivery of gradient stimuli, we chose blue light, expecting diffusion through the template according to Beer-Lambert's Law.

METHODS: Polycaprolactone (PCL) was dissolved overnight in 1,1,1,3,3,3 hexafluoro-2propanol at 100 mg/mL concentration and electrospun (+25KV, 10cm, 3ml/hr, collected on a rotating air gap mandrel). Fiber diameter measured using scanning electron microscopy (SEM), and analyzed (n = 300 measurements, FibraQuantTM 1.3 software). Uniaxial tensile testing (n=5) was performed with a TestResourcesTM frame (Model: 220Q). Dog-bone shaped samples were allowed to proceed to failure at a strain rate of 10mm/min, and force-elongation curves recorded with XY software. To analyze the gradient in blue light intensity along the longitudinal axes of the templates, samples (n=5) were illuminated from one end with an OpalDrive laser source and Laser Wire® guide (470nm wavelength) and images acquired with a Pariss Imaging Microscope. Pixel intensity was calculated with ImageJ software.

RESULTS: Templates had an average fiber diameter of 519nm±120nm. Fibers were aligned and presented similar morphology to ligament ECM (figure 1). Uniaxial tensile testing showed that templates exhibit similar characteristics to natural pig ligament. Particularly interesting is

the presence of an initial concave area, a linear range, and initial failure point in the force-elongation curves (figure 2). Blue light gradients were exhibited on the first 400µm of the template, and correspond to the desired range of enthesis depth - 200-500µm (figure 3).

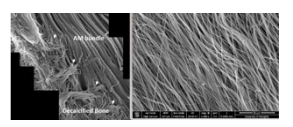


Fig. 1: Representative SEM of air gap electrospun template compared to pig ACL enthesis (L. Zhao, et al J. Anat (2014)).

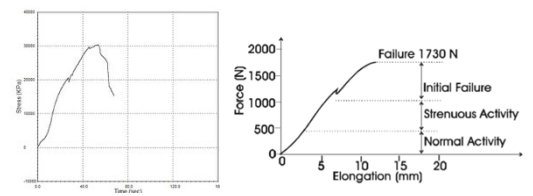


Fig. 2: Representative force-elongation curve of air gap electrospun template compared to typical ligament curve (S. Pal, Design of Artificial Human Joints & Organs).

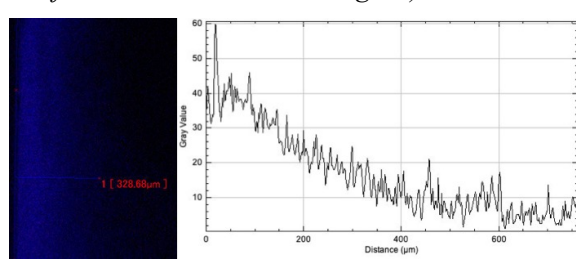


Fig. 3: Blue light gradient image and pixel intensity plot along template longitudinal axis.

DISCUSSION & CONCLUSIONS: The air gap electrospun templates have biomimetic characteristics (morphological and mechanical) and are amenable to the generation of a blue light gradient for optogenetic stimulation of engineered cells. This combination should be useful in the directed differentiation of cells to populate the enthesis. This study is the first to elucidate the possibility of presenting engineered cells with blue light stimulation in a gradient fashion for interfacial tissue engineering.

REFERENCES: [1] Font Tellado, et al. *Adv. Drug Deliv. Rev.* **94**, 126–140 (2015).

Peptide-Folding Mediated Self-Assembly of Dynamic Hydrogels

C. Aronsson¹, R. Selegård¹, S. Dånmark¹, J. Christoffersson², C.-F. Mandenius¹, **D. Aili**¹Laboratory of Molecular Materials, Division of Molecular Physics, Linköping University, Linköping, SE, ²Division of Engineering Biology, Department of Physics, Chemistry & Biology, Linköping University, Linköping, SE

INTRODUCTION: Extracellular matrix (ECM) mimicking hydrogels are widely used as scaffolds for 3D cell culture and tissue applications. including engineering bioprinting. Tunable and modular hydrogels can facilitate materials optimization and also enable dynamic and spatially confined modulation of materials properties. To this end, we have developed a range of peptide-based hybrid components for fabrication of hydrogels with properties that can be tailored and dynamically using specific peptide-folding modified mediated interactions.

METHODS: Peptides were synthesized on solid phase using Fmoc chemistry and were purified by reversed phase HPLC. Cysterminated peptides were conjugated to maleimide functionalized 4-armed star-shaped poly- (ethylene glycol) (PEG) and hydrogel self-assembly was induced by mixing PEGs with complementary peptides. Azide modified peptides were conjugated to bicyclo[6.1.0]nonyne (BCN) modified hyaluronic acid.

RESULTS: A versatile library of coiled coil peptides with excellent properties for tunable self-assembly of nanostructured materials has been designed and synthesized. (1,2) The peptides are random coils as monomers but are designed to heterodimerize and fold into well-defined αhelical motifs under physiological conditions. The dimerization process can be tightly controlled and large differences in dissociation constants (10 pM < Kd < 1 μ M) results in thermodynamic self-sorting.(2) When conjugated to a polymer backbone (star-shaped PEG and/or hyaluronan), dimerization and folding triggers rapid (< 30 sec) and specific self-assembly supramolecular into hydrogels. (1,3) The hydrogels were shear thinning and self-healing with storage modulus depends on affinities for peptide dimerization (Fig. 1). HepG2 cells encapsulated in the PEG-based hydrogels showed high viability and spheroid formation within 3-7 days. Moreover, by combining covalent and peptide-mediated crosslinking, it was possible to achieve robust but yet mechanically dynamic hydrogels. Triggering peptide homodimerization resulted in a rapid increase in storage modulus of the hydrogels and a dramatic reduction in swelling ratio, indicating of supramolecular cross-links. formation Moreover, pendant peptides enabled introduction of functional moieties (e.g. biotins or cell adhesion motifs) by means of peptide heterodimerization.

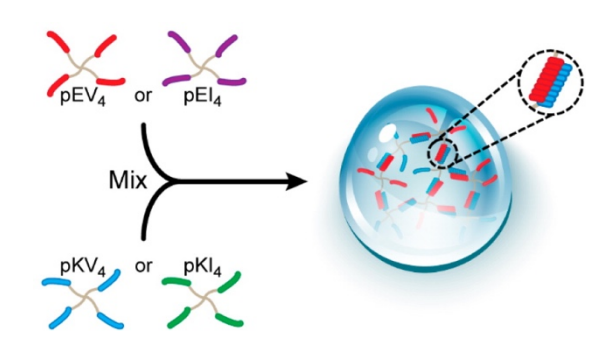


Fig. 1: Coiled-coil peptides conjugated to 4arm-PEG self-assemble into hydrogels with rheological properties dictated by the affinities for peptide dimerization.

DISCUSSION & CONCLUSIONS: We show that it is possible to use specific peptide-folding mediated interactions for tuning supramolecular cross-linking of cytocompatible hydrogels and for introducing new functional moieties in the hydrogels post synthesis. These strategies enable rational material optimization and facilitates studies of dynamic changes in material properties.

ACKNOWLEDGEMENTS: Funding from the Knut and Alice Wallenberg Foundation, and the Swedish Foundation for Strategic Research is acknowledged.

REFERENCES: [1] R. Selegård et al. *Sci. Rep.*, **2017**, 7, 7013. [2] C. Aronsson et al. *Sci. Rep.* **2015**, 5, 14063. [3] S. Dånmark et al. *Biomacromol.* **2016**, 17, 2260-2267.

Guided Outgrowth of Human Neuronal Cells Networks by Using Tailored 3D Micropillared Carbon Nanotube Templates

<u>G. S. Lorite</u>¹, <u>L. Ylä-Outinen</u>², <u>O. Pitkänen</u>¹, <u>T. Joki</u>², <u>J. T. Koivisto</u>³, <u>M. Kellomäki</u>³, <u>R. Vajtai</u>⁴, <u>S. Narkilahti</u>², <u>K. Kordas</u>¹

¹Microelectronics Research Unit, University of Oulu, Oulu, FI, ²NeuroGroup, BioMediTech, Faculty of Medicine & Health Technology, Tampere University, Tampere, FI, ³Biomaterials & Tissue Engineering Group, BioMediTech, Faculty of Medicine & Health Technology, Tampere University, Tampere, FI, ⁴Department of Materials Science & Nanoengineering, Rice University, Houston, TX, US

INTRODUCTION: The ability to control human neurite outgrowth opens up new horizons in neuroscience, ranging fundamental understanding of the nervous system development to exploiting strategies for repairing of injured central nervous system. Cells are able to sense and respond to the chemical and physical stimuli of environment. In the past vears. researchers have reported strong evidence that not only chemical cues but also physical ones such as topography and stiffness play important role on neuron cells morphology, growth and differentiation. In this work, we demonstrated the use of tailored carbon nanotube micropillars template to control orientation of human neurite outgrowth.

Micropillared **METHODS:** multi-walled carbon nanotubes (MWCNTs) were grown on Si/SiO₂ subtract by using lift-off lithography and chemical vapour-phase deposition. Three micropatterns different **MWCNTs** designed: squared arrays of pillars, pillars along spiral patterns and pillars arranged in stripes. In addition to flat Si/SiO2 surfaces, squared arrays of Si/SiO₂ pillars were fabricated by reactive ion etching. 3D micropillared templates were sterilized via oxygen plasma treatment. Commercial human neural precursor cells hNP1 were seeded at a density of 15,000 cells/cm². Cells were cultured for a total period of 21 days. The cell behaviour was analysed by means of live/dead staining, immunostaining (MAP-2 and β-tubulinIII) and scanning electron microscopy (SEM).

RESULTS: Our results showed that MWCNTs supported long-term survival of the cells when comparing to the control samples. While tight bundles were found wrapping the Si/SiO₂ pillars, single neurite outgrowth forming highly organized networks were observed on optimized MWCNT pillar dimensions and

spacing (Fig. 1). By arranging the optimized parameters, human neurites can be guided along any created patterns (such as spirals and stripes, Fig. 1B). Moreover, human neurites were found to interact with and anchor to MWCNTs pillars (Fig. 1C-D). The neurality of the cells were verified by immunocytochemical staining.

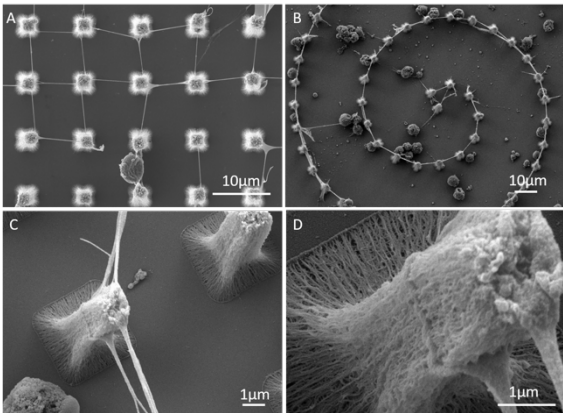


Fig. 1: (A) Organized human neural network on micropillared MWCNT arrays. (B) Guided human neurite along micropillared spirals. (C-D) Neurites interacting with and anchoring to MWCNT pillars.

DISCUSSION & CONCLUSIONS: micropillared MWCNTs templates provide not only micro- and nano-environment but also mechanically flexible and electrically conductive cues promoting the formation of high organized and well guided complex neuronal networks. Apart of relevance in neural tissue engineering, these results open new perspectives to develop CNT-based microelectrode arrays to study cell network electrophysiology.

ACKNOWLEDGEMENTS: This work was funded by Academy of Finland (# 317437, #286990, #312414, #312409), Finnish Cultural Foundation Pirkanmaa Regional Fund (#50151501) and the Central Fund (#00150312), and Business Finland (former Tekes, Human Spare Parts project).

Click-Type Bioconjugation Catalysed Simply by Salt Solution

J. Hilborn¹, O. Varghese¹, S. Wang¹, G. Nawale¹, S. Kadekar¹, O. P. Oommen², N. Jena³, S. Chakraborty³

¹Polymer Chemistry Division, Department of Chemistry, Ångström Laboratory, Uppsala University, Uppsala, SE, ²Bioengineering & Nanomedicine Lab, Faculty of Biomedical Sciences & Engineering, BioMediTech, Tampere University, Tampere, FI, ³Condensed Matter Theory, Materials Theory Division, Department of Physics & Astronomy, Ångström Laboratory, Uppsala University, Uppsala, SE

INTRODUCTION: Bioconjugation an expanding field of large importance biomaterials research. Reactions allowing for sitespecific derivatization of proteins, DNA, RNA, and carbohydrates have been developed for discovery of biological interaction, biochemical assays, diagnostics, in vivo imaging, highthroughput screening and even reactions to cell surface. Oxime formation is one of the most powerful coupling strategies for bioconjugation owing to its simplicity and efficiency. It is chemoselective and produces hydrolytic stability linking, making it a reaction of choice for biologists as an alternative to 'click-chemistry'. However, it suffers from low reaction rate, poor reactivity with keto substrates and the need of high substrate. Therefore, identifying biocompatible catalysts that can accelerate oxime formation at physiological pH is highly desirable.

METHODS: Oxime-formation kinetics was analyzed by ¹H NMR and UV-Vis spectrometry. The reaction of (aminooxy)methane and acetone/4-hydroxybenzaldehyde (4-HB) using different concentrations of NaCl in phosphate buffer was performed. We also performed the salt catalysed oxime-based bioorthogonal ligation to modify cell surface glycoproteins by generating an aldehyde on human colon cancer cell line (HCT116 cells) by periodate oxidation. A fluorescein-functionalized aminooxy derivative was used and live cell-surface label ling experiment was performed at pH 7.4.

RESULTS & DISCUSSION: For the first time it is shown that aqueous NaCl solution is capable of promoting the oxime reactions at physiological pH, Fig.1. This effect is attributed to the stabilization of the charged transition states that favour the key rate-limiting elimination (dehydration) step 4.

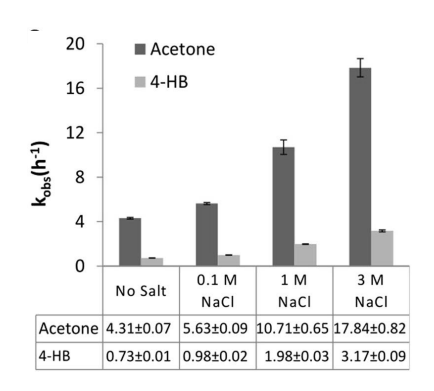
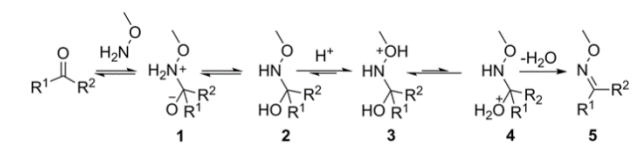


Fig. 1: Comparative oxime reaction kinetics.



R¹, R²=CH₃ (acetone)

R¹=H, R²=ArOH (4-hydroxybenzaldehyde)

The cell labelling showed efficient labelling on live cells to demonstrate the highly biocompatibility of the catalyst.

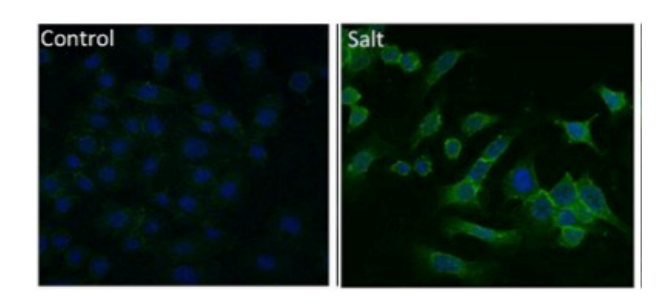


Fig. 2: Oxime labelling of periodate treated HCT116 cells with and without salt catalyst.

ACKNOWLEDGEMENTS: Support by Swedish strategic research grant 'StemTherapy' (139400126) and Swedish foundation for strategic research (SSF).

Optimizing Alginate Gelation Conditions for 3D Cell Culture

D. Zaytseva-Zotova¹, W.I. Strand¹, A. Akbarzadeh¹, R. Ruohola¹, H. Haslene-Hox², Ø. Arlov², A. Vikenes², A.D. Hoel², G. Klinkenberg², H. Sletta², B.L. Strand¹

¹Department of Biotechnology & Food Science, Norwegian University of Science & Technology, Trondheim, NO, ² Department of Biotechnology & Nanomedicine, SINTEF Industry, Trondheim, NO

INTRODUCTION: Alginate is considered as an attractive material for fabrication of extracellular environment for *in vitro* 3-dimensional (3D) cell culture. Internal gelation of alginate is a well-known strategy for formation of soft gels with homogenous and reproducible structure. This method allows to control over gelation kinetics of alginate and thus is suitable for robotic handling [1]. In this work we were aimed to adapt the internal gelation method for 96-well plate format and robotic handling, and studying how the encapsulation procedure affects viability of different cell lines.

METHODS: Sodium alginates with F_G 0.68 and MW 237-298 kDa were evaluated. Alginate was cross-linked by mixing sodium alginate (dissolved in a buffer) with CaCO₃ nanoparticles and slowly hydrolyzing acid glucono-δ-lactone [2]. Alginate gelation was controlled by addition of sodium citrate. To maximize cell survival during encapsulation procedure, a buffer composition was adjusted to physiological values of ionic strength and osmolarity. Buffer capacity and initial pH were varied to minimize pH changes in gelling solution. Gelation kinetics and mechanical properties of the hydrogels, formed at 4, 20 and 37°C, were characterized using oscillatory rheometry and compression measurements. Viability of 3 human cell lines, namely hepatocellular carcinoma HepG2, prostatic carcinoma PC3 and lung fibroblasts IMR90, within the hydrogels was examined using confocal laser scanning microscopy (CLSM) after staining cells with live/dead assay.

RESULTS: Gel formulation was optimized with respect to required gelation kinetics, i.e. sol-gel transition occurred after 15-30 minutes and gelling was completed to >70% within the first 2 hours. Gelation kinetics and gel strength depended upon temperature: hydrogels were formed slower and became stiffer with temperature decrease. Syneresis of the gels did not depend on gelation temperature, but was influenced by the buffer composition and was

significantly reduced in presence of NaCl. At maximum tested buffer capacity, pH of the gelling solution changed within the wide range (7.8 down to 6.5) within the first 2 hours of gelation at 37°C. This led to decrease in cell viability, even when additional washing steps were introduced. Reduction of temperature to 4°C during initial gelation allowed to increase cell survival, likely due to pH stabilization within the range of 7.4 to 7.9. Cell growth and viability within the hydrogels was found to be different for the 3 cell types examined (Fig.1).

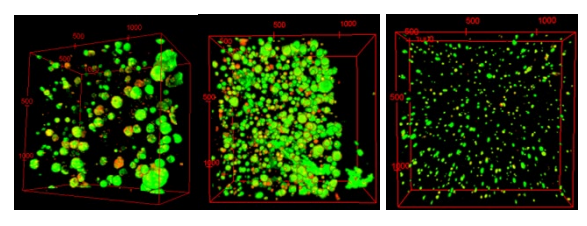


Fig. 1: 3D reconstruction of confocal z-stacks of HepG2 (left), PC3 (median) and IMR90 (right) cells cultured in 0.5% alginate gels for 2 weeks. Live cells (green), dead cells (red).

DISCUSSION & CONCLUSIONS:

Composition of gelling solution was optimized with regards to desired gelation kinetics for compatibility with the robotic system and required mechanical properties of the gels being within the range relevant for soft tissue. Initial evaluation of cell responses showed that cell viability depends on gelling solution composition, gel formation conditions and cell type.

ACKNOWLEDGEMENTS: This work is a part of 3DLife project within Center of Digital Life Norway, and is financed by the Research Council of Norway (project 269273).

REFERENCES: [1] T. Andersen, B.L. Strand, K. Formo, E. Alsberg, B.E. Christensen (2011) *Carbohydrate Chemistry* 37:227-258. [2] K.I. Draget, K. Østgaard, O. Smidsrød (1990) *Carbohydrate Polymers* 14:159-178.

Silicic Acid Mediated Formation of Tannic Acid Coatings

F. Weber¹, W.-C. Liao², A. Barrantes¹, M. Eden², H. Tiainen¹

¹<u>Department of Biomaterials</u>, Faculty of Dentistry, University of Oslo, NO, ²<u>Department of Material & Environmental Chemistry</u>, Stockholm University, SE

INTRODUCTION: Polyphenolic molecules. such as tannic acid (TA), are well known for their anti-oxidant properties, and metal ion and protein complexation.1 The resulting antiinflammatory and antimicrobial behavior of these molecules is of interest for biomedical applications, especially for creating advanced functionalized surfaces.² The coating formation however, depends on the type of polyphenolic molecule³ and is either mediated by oxidative polymerization or crosslinking via metal ions in so called metal phenolic networks.4 We found that TA continuously deposits on various surfaces in presence of silicic acid. Therefore we studied the interaction of silicic acid with TA to clarify whether the coating formation is based on catalyzed oxidative polymerization or a crosslinking mechanism.

METHODS: The coating formation was monitored in real-time using a quartz crystal microbalance (QCM-D). Chemical analysis of TA coatings and complexation / polymerization products was performed by means of EDS, XPS, UV-vis, FTIR, and solid-state NMR.

RESULTS: The formation of TA coatings in the presence of silicic acid (Si_{aq}) resulted in an in situ coating thickness of ~200 nm (24 h). Without supplementing Siaq a monolayer of 1.8 nm is formed at pH 7.8 until oxidative polymerization distorts the QCM-D signal after 3 h. The FTIR analysis of the TA oxidation product indicated that the structural integrity of TA was lost, whilst the spectrum of the precipitate obtained in presence of excess Siaq attested a similar structure compared to TA. The later result was confirmed by ¹³C NMR. Our XPS measurements of the chemical state of Si within the coating excluded the presence of SiO₂. The evidenced Si 2p peak was centered at 102.6 eV and exhibited a homogenous distribution. Further ²⁹Si NMR of coated TiO₂ particles showed peaks at -99 and -139 ppm, indicating a penta- and hexa-coordination of Si_{aq} binding 2/3 TA ligands.

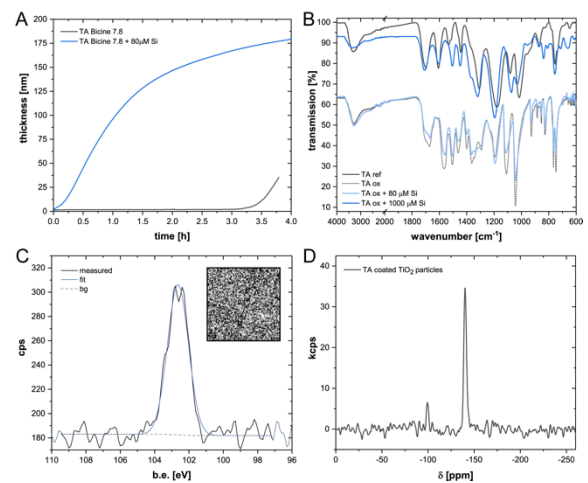


Fig. 1: TA coating formation monitored by QCM-D (A). FTIR characterization of TA ox. product and TA-Si precipitate (B). XPS map of Si 2p peak (C). Solid-state ²⁹Si NMR (D).

based on the formation of coordination complexes with Si_{aq}. The use of complexation networks maintains the structural integrity of TA within the coating, which may be beneficial for the functional properties of TA. Further, it enables the change of experimental conditions during the formation, allowing for a broader applicability of polyphenolic coatings.

ACKNOWLEDGEMENTS: This work was funded by the Faculty of Dentistry, UiO. WCL and ME acknowledge funding from the Carl Trygger Foundation (CTS 17:130).

REFERENCES: [1] Quideau, S.; Deffieux, D.; Douat-Casassus, C.; Pouységu, L., *Angew Chem Int Ed Engl* **2011**, *50* (3), 586. [2] Li, X.; Gao, P.; Tan, J.; Xiong, K.; Maitz, M. F.; Pan, C.; Wu, H.; Chen, Y.; Yang, Z.; Huang, N., *ACS Appl Mater Inter* **2018**, *10* (47), 40844. [3] Barrett, D. G.; Sileika, T. S.; Messersmith, P. B., *Chem Commun* **2014**, *50* (55), 7265. [4] Reitzer, F.; Allais, M.; Ball, V.; Meyer, F., *Adv Colloid Interfac* **2018**, *257*, 31.

Bone Formation by Porous Strontium-Loaded Bioactive Glass: A Macro- to Nano-Scale Characterisation

H. Autefage^{1,2}, F. Allen³, H. M. Tang¹, C. Kallepitis¹, E. Gentleman⁴, N. Reznikov¹, K. Nitiputri¹, A. Nommeots-Nomm¹, M. D. O'Donnell¹, C. Lange⁵, B. M. Seidt⁵, T. B. Kim¹, P. D. Lee^{1,7}, B. F. Pierce¹, W. Wagermaier⁵, P. Fratzl⁵, A. Goodship³, J. R. Jones¹, G. Blunn³, M. M. Stevens^{1,2}

¹Deptartment of Materials, Deptartment of Bioengineering, & Institute of Biomedical Engineering, Imperial College London, London, UK, ²Deptartment of Medical Biochemistry & Biophysics, Karolinska Institutet, Stockholm, SE, ³Institute of Orthopaedics & Musculoskeletal Science, University College London, London, UK, ⁴Centre for Craniofacial & Regenerative Biology, King's College London, London, UK, ⁵Max Planck Institute of Colloids & Interfaces, Dept. of Biomaterials, Potsdam, DE, ⁶Mechanical Engineering, University College London, UK

INTRODUCTION: While developing synthetic bone substitutes that exhibit adequate structural and biological cues to repair large bone defects that cannot endogeneously heal, is a well-established challenge, little is known regarding the quality of the bone that has been newly-formed in response to implantation, despite the importance of bone characteristics at the nano- to the macro-levels for its function. Here, we developed and implanted a porous three-dimensional strontium-containing bioactive glass in a critical-sized defect in an ovine model, and evaluated the material's outcome and quality of the new bone using a multiscale analysis.

METHODS: 3D porous pSrBG granules (1 – 3 mm) were produced by in situ hybridization¹, and implanted in critical-sized defects in the left medial femoral condyles in sheep. 45S5 particles (0.1-1 mm) were used as controls. At 6 and 12 weeks post-implantation, samples were analyzed by histology, histomorphometry, mechanical testing, Raman spectral imaging, X-ray fluorescence, small-angle X-ray scattering, and scanning electron microscopy imaging of focused ion beam-milled sections.

RESULTS: pSrBG displayed high osteoconductive properties, with a remarkable bone-to-material contact of nearly 100% after only 6 weeks of implantation, significantly higher than that of 45S5. The combination of materials-based characterisation techniques used to assess the newly-formed bone quality from macro- to nano-scales further showed that pSrBG promoted the formation of a well-organised lamellar bone with characteristics similar to those of a normal healthy bone.

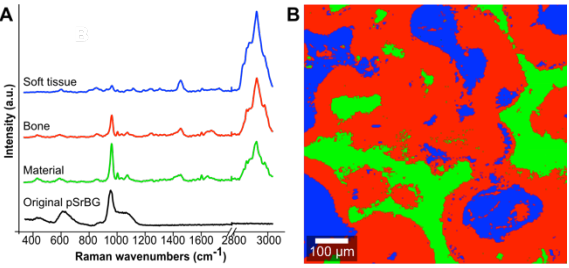


Fig. 1: Raman signature (left) and Raman spectral imaging (right) from K-means clustering of pSrBG induced new-formed bone after 12 weeks of implantation.

psrbG was able to promote the formation of a healthy native-like bone, containing small quantities of strontium, and displayed high osteoconductive properties in a critical-sized defect in sheep. This was likely the result of the combination of its composition and structural characteristics. Evaluating the quality of the newly-formed bone in response to materials, in association with conventional techniques, could open new questions regarding the mechanisms by which materials drive bone regeneration.

ACKNOWLEDGEMENTS: MMS thanks the Medical Engineering Solutions in Osteoarthritis Centre of Excellence funded by the Wellcome Trust and the EPSRC, the Technology Strategy Board, UK, the Rosetrees Trust, the Swedish Research Council (VR 4-478/2016) financial support. H.A. was partially funded by the VIP award from the Wellcome Trust Support Institutional Strategic Fund (097816/Z/11/B). E.G. was supported by a Research Career Development Fellowship from the Wellcome Trust.

REFERENCES: [1] Wu Z.Y. et al, *Acta Biomater.*, 2011, 7 (4): 1807–1816.

In vitro Degradation of Porous Bioactive Glass Scaffolds with a Polymer–Bioactive Glass Coating

P. Uppstu¹, S. Engblom¹, N. Moritz², L. Aalto-Setälä³, S. Inkinen¹, L. Hupa³, C.-E. Wilén¹

¹Laboratory of Polymer Technology, Åbo Akademi, Turku, FI, ² Turku Clinical Biomaterials Centre, University of Turku, Turku, FI, ³ Johan Gadolin Process Chemistry Centre, Åbo

Akademi, Turku, FI

INTRODUCTION: Bioactive glass (BG) is clinically used for bone regeneration. A hydroxyapatite (HA) layer, to which living tissue can bond, forms on the surface of the BG in a physiological environment. Many BG compositions have antibacterial properties due to ion release and pH increase. A drawback of three-dimensional BG scaffolds is their mechanical brittleness, and one way to overcome this is to coat the scaffolds with polymers. However, a polymeric coating may diminish the biological benefits of the glass. The aim of this study was to investigate, whether incorporation of BG granules in polylactide (PLA) coating could improve degradation properties of BG scaffolds in vitro.

METHODS: Cylindrical-shaped scaffolds with an average mass of 748mg and an average porosity of 71% were produced with the foam replication technique from BG 13-93. The scaffolds were dip-coated in a solution containing equal amounts of poly(L-lactide) (PLLA) and poly(D-lactide) (PDLA) with 20, 40 or 60wt.% added BG S53P4 granules of size fraction 32–45µm (PLA-BG coating) or without BG granules in the coating (PLA coating) or left uncoated. The scaffolds were subsequently heat-treated for increased stereocomplex formation of the PLA polymers. The scaffolds were immersed in simulated body fluid (SBF) solution for 0, 2, 4, 6 or 10 weeks. SBF was changed and pH was measured weekly. The scaffolds were analysed with compression testing, SEM and DSC after immersion.

RESULTS: The mass of the coating was 3–5% of the mass of the glass scaffold. BG granules were well dispersed within the stereocomplex PLA coating, and the coating covered the pore walls inside of the scaffold to a large extent (Fig. 1). Si-rich and HA reaction layers could be identified on all scaffolds after immersion in SBF. On coated scaffolds, much of the HA formation had occurred on the surface of the PLA coating. During the first 6 weeks of immersion in SBF, pH for the scaffolds with

PLA-BG coating was significantly higher than for the scaffolds with PLA coating. The peak pH for scaffolds with PLA-BG coating occurred later than for uncoated scaffolds, and the cumulative pH increase over the first 6 weeks was higher for PLA-BG scaffolds compared to uncoated scaffolds. The compressive strength of the scaffolds with PLA-BG coating was higher than for uncoated scaffolds, but lower than for scaffolds with PLA coating.

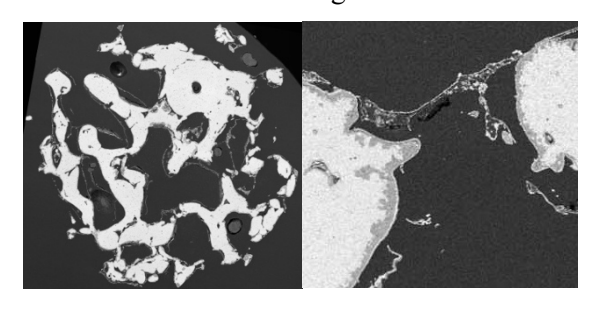


Fig. 1: Cross-sectional panoramic SEM image of a porous BG scaffold with 60% BG granules within the stereocomplex PLA coating after 10 weeks in SBF (left), and a detail showing unreacted glass, Si-rich layer, HA layer and the PLA-BG coating (right).

DISCUSSION & CONCLUSIONS: The results show that inclusion of BG particles in a PLA coating significantly affects the degradation characteristics of BG scaffolds. A prolonged increase in pH could affect bone regeneration positively. PLA-BG scaffolds also showed improved compressive strength compared to uncoated scaffolds. Cell tests and animal models in further studies could prove the biological benefits of adding BG granules into polymeric coatings.

ACKNOWLEDGEMENTS: PU is grateful for financial support from the Finnish Foundation of Technology Promotion and the Åbo Akademi Foundation.

Integration of Functional Proteins into a Membrane for Nanofiltration

M. Schwieters^{1,2}, M. Mathieu¹, U. Glebe¹, A. Böker¹

¹Fraunhofer Institute for Applied Polymer Research IAP, Potsdam, DE, ²Technical University of Berlin, Institute of Materials Science & Technology, Berlin, DE

INTRODUCTION: For the production of safe pharmaceuticals and nourishments, source materials have to comply with enhanced purity specifications. Purification of source materials can be achieved in various ways such as chromatographic and membrane processes. Particularly membrane processes purification are of special industrial interest as they are considered to be cost efficient and easy to scale up [1]. A new generation of ultrathin membranes for nanofiltration is currently being investigated at Fraunhofer IAP. These new membranes consist of functionally tailored transmembrane proteins acting as filter pores. Tailored variants of the \(\beta\)-barrel-shaped transmembrane protein ferric hydroxamate uptake protein component A (FhuA), occurring in Escherichia coli bacteria in nature, are provided by the Department of Biotechnology at RWTH Aachen. Integration of FhuA into a robust membrane [2] while preserving its βbarrel structure is challenging since proteins are particularly sensitive to changing environmental conditions. To further ensure membrane selectivity, feed leakage through intermolecular pores has to be reduced by arranging the proteins as dense as possible.

METHODS: Amphiphilic FhuA-variants were spread at the air-water interface of a Langmuir trough and compressed until a dense monolayer had formed. The protein crosslinker glutaraldehyde was then injected to the subphase. After crosslinking, the protein-monolayer was transferred to a silica substrate and AFM analysis was performed.

RESULTS: The AFM image in Fig. 1 shows a dense and homogenous FhuA-membrane on top of the silica substrate. Analysis of multiple height profiles indicates a consistent membrane thickness of approximately 5 nm.

DISCUSSION & CONCLUSIONS:

Comparing the structure of FhuA-membranes prepared with and without injecting glutaraldehyde to the Langmuir trough subphase demonstrates that crosslinking of FhuA was achieved. The measured membrane thickness of 5 nm closely matches the

dimensions of FhuA, suggesting that a functional FhuA-monolayer membrane was produced.

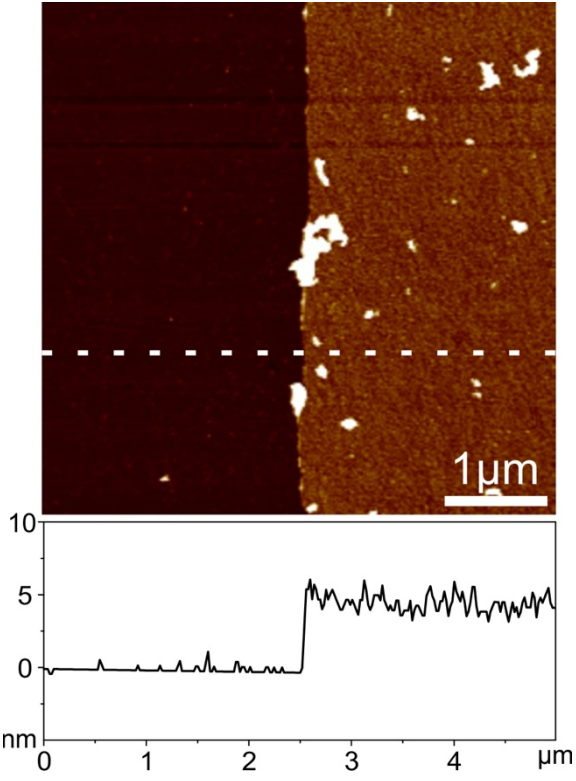


Fig. 1: AFM image of a crosslinked FhuA-membrane (right) on top of a silica substrate (left, after scratching away the membrane). The representative height profile belongs to the dashed line in the image and indicates a membrane thickness of 5 nm.

ACKNOWLEDGEMENTS: The Bundesministerium für Bildung und Forschung (BMBF) is kindly acknowledged for financial support in the framework of the BMBF-Forschertandem "Chiral Membranes" (Förderkennzeichen: 031B0559B).

REFERENCES: [1] Xie et al.: Membranes and membrane processes for chiral resolution. Chemical Society reviews 37 (2008) 6, p. 1243–1263. [2] Charan et al.: Nano-thin walled micro-compartments from transmembrane protein–polymer conjugates. Soft Matter 13 (2017), p. 2866-2875.

Properties of Extracellular Particles & Vesicles Derived from Mesenchymal Stromal Cells & Endothelial Cells in a Fibrin 3D Co-Culture Model for Angiogenesis

M. Pultar^{1,4}, J. Schneider*^{1,4}, M. R. Bobbili^{2,3,4}, S. Mühleder^{1,4}, E. Priglinger^{1,4}, H. Redl^{1,4}, J. Grillari^{2,3,4}, W. Holnthoner^{1,4} (*equal contributions)

¹Ludwig Boltzmann Institute for Experimental & Clinical Traumatology, Vienna, AT, ²Department of Biotechnology, BOKU University of Natural Resources & Life Sciences Vienna, Vienna, AT, ³ Christian Doppler Laboratory on Biotechnology of Skin Aging, Department of Biotechnology, BOKU University of Natural Resources & Life Sciences Vienna, Vienna, AT, ⁴ Austrian Cluster for Tissue Regeneration, AT

INTRODUCTION: Various approaches and applications in regenerative medicine use hydrogels due to its unique properties, among them its biocompatibility. Previously, we showed that endothelial cells form a vascularlike structure when embedded and co-cultured with mesenchymal stromal cells (MSC) in the hydrogel fibrin. biological proangiogenic effect is assumed not only to be derived from direct cell-to-cell contact but also from MSC-secreted extracellular vesicles (EVs) the aim of this study is to investigate if there is any effect of fibrin on the extracellular particle (EP) release of the cells and if the hydrogel could be used as a delivery platform for EVs.

METHODS: Adipose derived stromal cells (ASC) and GFP-expressing human umbilical vein endothelial cells (GFP-HUVEC) were cultured either individually or in co-culture (ratio ASC:HUVEC 1:1) for 7 days. For 3D cultivation, fibrin matrices with 2.5 mg/mL fibrinogen and 0.2 U/mL thrombin were prepared. EPs were collected for 48h in EBM-2 (without serum). The size and number of EPs was measured by nanoparticle tracking analysis and Annexin V+ EVs were detected by flow cytometry.

RESULTS: Differences in particle size and amount were detected when measuring supernatants derived from 2D or 3D cocultures. Further, more particles were detected for ASC cultured in fibrin then for HUVEC, whereas only small differences in sizes were observed.

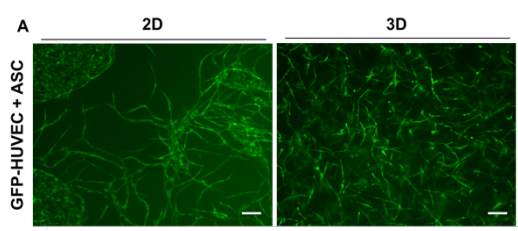


Fig. 1: A)Fluorescent microscopy images of the network formation of ASC and GFP-HUVEC co-cultures after 9 days in a 2D monolayer or in fibrin hydrogel. (Scale bars: 100 um)

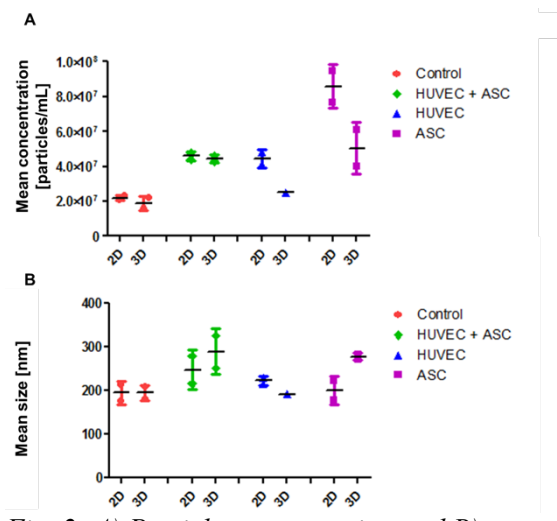


Fig. 2: A) Particle concentration and B) mean size of the particles measured by NTA from medium only, the co-culture and the individual cell supernatants.

DISCUSSION & CONCLUSIONS: The data indicate, that either a difference in the adsorption of the different cell-derived particles by the hydrogel or the release of EPs itself could lead to the differences between the properties of EPs derived from ASC, HUVEC or the co-culture. In further studies the capabilities of fibrin as a delivery platform for MSC derived EVs should be investigated to achieve a supporting 3D environment for the network formation of EC.

Characterization of the Printability of Alginate-Gelatin Bioink Blended with Nanocellulose

J. Paulamäki¹, A. Rashad¹, J. Karvinen², J. T. Koivisto², M. Kellomäki², K. Syverud³, S. Miettinen², K. Mustafa¹

¹Department of Clinical Dentistry, University of Bergen, Bergen, NO, ²BioMediTech, Faculty of Medicine & Health Technology, Tampere University, FI, ³RISE PFI, Trondheim, NO

INTRODUCTION: Alginate is a highly favoured biomaterial in bioprinting because of the instant gelation in divalent ionic solutions. However, in order to hold the integrity of a printed structure until the cross-linking of alginate, gelatin is commonly used as a sacrificial material due to its thermos-sensitive properties: gelation at lower temperatures. It is suggested that cellulosic nanofibers (CNF), a biopolymer extracted from plants could influence the rheological properties of the alginate-gelatin system due to their favourable shear-thinning properties¹. The aim of this study was to investigate the influence of addition of CNF to alginate-gelatin gel in terms of rheology, printability and the cell viability.

METHODS: Different concentrations of CNFs (0, 0.25, 0.5, 0.75 and 1% w/v) were suspended in cell culture medium and mixed with alginate (2%)and gelatin (4%).Rheological measurements of the cell-free gels were performed using a Discovery HR-2 (TA Instruments) rheometer to evaluate the viscosity as function of shear rate and temperature. To evaluate the cellular compatibility before the printing, osteoblast-like cells (Saos-2) were mixed with prepared gels, pipetted into 48-wellplate and cross-linked with CaCl₂ for 10 min. The viability of 3D encapsulated cells was then evaluated using Live/Dead assay. printability of the gels was assessed using a 3D-Bioplotter (EnvisionTEC), with a 500 nm metal needle. The printing parameters were optimized for each hydrogel.

RESULTS: All prepared hydrogels demonstrated shear-thinning properties as the viscosity decreases with the increase of the shear rate. The CNF-containing hydrogels had more stable rheological behavior compared to the pure alginate-gelatin hydrogel. Live/Dead viability staining demonstrated that the gels had no toxic effect and maintained cell viability after 1 and 3 days.

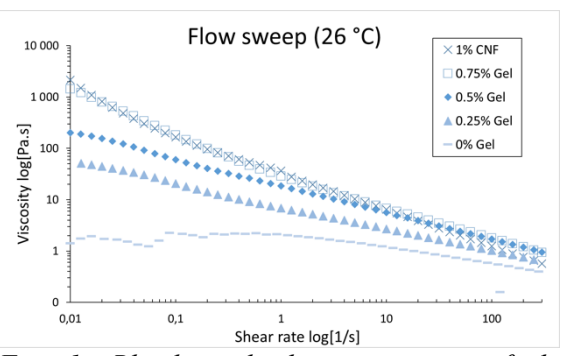


Fig. 1: Rheological characterization of the prepared gels.

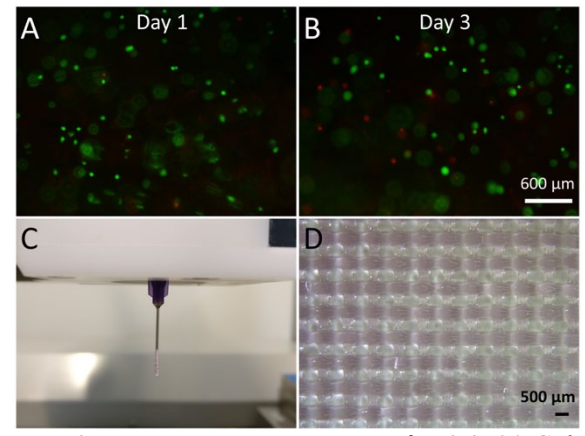


Fig. 2: Representative images of a 0.25% Gel: Live/Dead staining after 1 (A) and 3 (B) days, evaluation of printability (C) and the printed structure (D).

DISCUSSION & CONCLUSIONS: The results of the current study show that CNF influenced the rheological properties of the alginate-gelatin gel without compromising the viability of embedded cells. Thus, the alginate-gelatin-CNF system has a promising potential in bioprinting applications.

ACKNOWLEDGEMENTS: This work has been funded by Bergen Research Foundation (project no. BFS2018TMT10).

REFERENCES: [1] Markstedt, K., et al., Biomacromolecules, 2015. 16(5): p. 1489-1496.

Novel Biomicroconcretes Based on the Hybrid HAp/CTS Granules, αTCP & Pectins

M. Dziadek¹, E. Cichoń¹, A. Zima¹, A. Ślósarczyk¹

¹AGH University of Science & Technology, Faculty of Materials Science & Ceramics, Department of Ceramics & Refractories, Krakow, PL

INTRODUCTION: An increasing number of surgeries performed on young people, as well as an aging society force scientists to develop new bone substitutes with superior properties, enhancing the bone healing process. In this work, the new type of bone substitute biomicroconcretes was proposed. Materials composed of hybrid hydroxyapatite/chitosan (HAp/CTS) granules as aggregate, αTCP as a setting phase, and pectin solutions as a liquid phase, were developed. Materials combine advantages of each components: calcium phosphate biocompatibility, phase (i.a. bioactivity, osteogenic potential, and osteoconductivity) **CTS** (i.a. rapid biodegradation, high biocompatibility, haemostatic and antibacterial properties), and pectins (i.a. crosslinking ability upon divalent ions, biocompatibility, biodegradability), as well as the advantages of hybrid character (i.a. improved mechanical properties).

METHODS: HAp/CTS hybrid granules and highly reactive α TCP powder were synthetized using wet chemical methods. Two types of low esterified amidated pectins from citrus peels (CP) and apple pomace (AP) were used. The microconcretes were prepared by mixing the HAp/CTS granules, α TCP powder and pectin solutions. Phase composition was examined by XRD and FTIR methods. Furthermore, materials were subjected to a compression test.

RESULTS: The results showed that the incorporation of pectins did not influence the setting reaction based on the hydrolysis of αTCP to calcium-deficient hydroxyapatite. Furthermore, fast internal crosslinking of low esterified pectins, induced by Ca2+ released from αTCP, resulted in good cohesion, while setting reaction of aTCP allowed to obtain satisfactory mechanical strength of final materials. **FTIR** spectrum of studied biomicroconcrete was dominated by bands characteristic for CaP phase (HAp/αTCP), but weak bands derived from organic compounds (CTS/pectins) were also visible (Fig. 1).

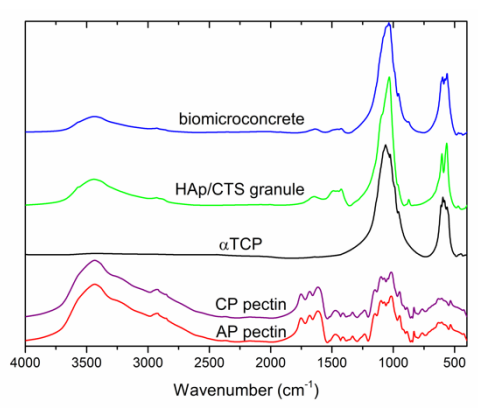


Fig. 1: FTIR spectra of biomicroconcrete and its individual components.

DISCUSSION & **CONCLUSIONS:** Rashidova et al. [1] have shown that electrostatic interactions between the positively charged amino groups of the chitosan and the negatively charged carboxyl groups of the pectin may occur. These interactions may improve adhesion of the cement phase to the surface of the hybrid HAp/CTS granules. As it was shown in our previous work, electrostatic complexes between positively charged. protonated amine groups of chitosan and the negative phosphate species were created [2]. Because of differences in resorption time between the individual components, biomicroconcretes may show multistep degradation process in vivo, fostering porosity development and therefore promoting cell migration. Furthermore, the presence of pectins improved significantly surgical handiness of resulting materials.

ACKNOWLEDGEMENTS: Supported by the National Science Centre, Poland Grant No. 2017/27/B/ST8/01173. MD acknowledges financial support from the Foundation for Polish Science (FNP) - START stipend.

REFERENCES: [1] S. Sh. Rashidova et al., Chromatographia 2004, 59(11/12):779-782. [2] A. Zima, Spectrochim Acta A 2018, 193: 175-184.

Antibacterial Selenium Nanoparticles & their Effect on Properties of Polymer-Phosphate Bone Cement

V. Grézlová¹, L. Michlovská¹, K. Šmerková², P. Kopel², V. Adam², S. Kočiová², P. Bábor³, P. Diviš⁴, L. Vojtová¹

¹Advanced Biomaterials, CEITEC-Brno University of Technology, Brno, CZ, ²Department of Chemistry & Biochemistry, Faculty of AgriScience, Mendel University in Brno, Brno, CZ, ³Preparation & Characterization of Nanostructures, CEITEC-Brno University of Technology, Brno, CZ, ⁴Materials Research Centre, Faculty of Chemistry, Brno University of Technology, Brno, CZ

INTRODUCTION: Each application of bone cement disrupted the body balance by the outside. By the influence of diverse pathogens, around infection bone implants (osteomyelitis) may arise. One possible solution, how to avoid antibiotics, is to add some antibacterial element directly into the bone cement. Selenium nanoparticles (SeNPs) are antibacterial, biogenic, non-metallic with particles with size about 100 nm¹. Selenium is a trace element naturally presented in the human body. That is the reason, why SeNPs can potentially be a unique material for the use in biomedical applications.

phosphate **METHODS:** Polymer-calcium cement (pCPC)² was modified by 20-170 ppm selenium nanoparticles (SeNPs). Antibacterial properties were evaluated by disk method, mechanical properties, injectability, flowability, and setting reaction time via rheology and tensile machine. Crystalline structure was verified by XRD analysis. Scanning electron microscopy figured transformation of amorphous phosphate to flower-like calcium-deficient hydroxyapatite crystals. Distribution of SeNPs in the material was visualized by secondary ion mass spectrometry imaging and SeNPs release from pCPCs at physiological conditions was detected by ICP-OES.

RESULTS: SeNPs improved injectability of bone cement and increased setting reaction rate with the positive effect on mechanical properties of pCPCs. Addition of SeNPs made the bone cement more thixotropic more flowable but cohesive. This is important for mini-invasive surgery. Furthermore, SeNPs had a positive effect on the mechanical strength of the samples of bone cement. Prepared antibacterial cement was very effective on a gram-positive *Staphylococcus aureus* (SA) bacterial strain and even its methicillin-resistant

form MRSA proved by disc diffusion method. The release of SeNPs from bone cement during first two days shows that almost all SeNPs released within 8 hours (96.5 %) in comparison to general polymeric PMMA bone cements releasing only 2% of antibiotics.

DISCUSSION & CONCLUSIONS: Due to the positive effect of SeNPs on rheological, mechanical and antibacterial properties, the novel polymer-phosphate bone cement can be possibly applied in mini-invasive surgery as bone filler for the treatment of osteomyelitis.

ACKNOWLEDGEMENTS: This work was supported by the CEITEC 2020 (LQ1601) with financial support from the MEYS of the Czech Republic under the National Sustainability Programme II, by the Ministry of Health (NV18-05-00379) and CEITEC VUT/FCH-J-19-5927.

REFERENCES: [1] Chudobova D. et al.: FEMS Microbiology Letters 351, 195-201 (2014). [2] Vojtová, L. et al.: International Journal of Molecular Sciences, 20(2), 1-21 (2019).

Design & Macromechanical Analysis of Trabecular Structures Produced by SLM

P. Hájková¹, A. Jíra¹

¹Department of Mechanics, Faculty of Civil Engineering, Czech Technical University in Prague, CZ

INTRODUCTION: In the last years a lot of focus has been put on trabecular structures which are designed for an implantation into bones [1]. The reason is that the structures offer many advantages compared to compact implants. One of the main advantages is a possibility to influence mechanical properties of the structures by changing its morphology. The aim is to converge towards mechanical properties of bones and to prevent an unwanted stress shielding. The other advantage is that the structures enable ingrowth of bone issue which provides better fixation bone-implant. The aim of this study is to design several trabecular structures with different morphology (a shape and size of pores, width of trabeculas) and to test the structures macromechanically.

METHODS: Six types of trabecular structures were designed in total. The structures were composed of three basic units – Diamond 30%, Dode Thick a Rhombic dodecahedron 30%. The models were generated in Magics software (Materialize NV, Leuven, BEL). The method of SLM – M2 Cusing machine (Concept Laser, DE) was used for the fabrication. A material of the structures was titanium alloy Ti6Al4V in the form of powder.

The compression tests were performed on MTS Alliance RT-30 (MTS, USA) machine in accordance with international standard ISO 13314 Mechanical testing – Ductility testing – Compression test for porous and cellular metals [2]. To consider a quality of the fabrication, a microscopic analysis was also performed.

RESULTS: The results show that a global elastic modulus (E) of all tested trabecular structures is significantly lower (2.6–3.8 GPa) than an elastic modulus of the structure material which is 110 GPa according to product lists. In addition, the elastic modulus of the structures is close to the modulus of human bones (3–17 GPa, spongeous – compact part).

Compressive offset stress $(\sigma_{0,2})$ of the structures is 78–142 MPa. The structure with the greatest porosity (0.408), Dode Thick – unit cell

1.25 mm, shows the lowest strength. Conversely, the greater strength shows the structure with the lowest porosity (0.261), Rhombic dodecahedron – unit cell 1.25 mm.

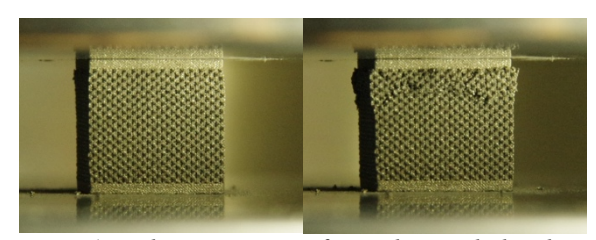


Fig. 1: The process of mechanical loading in a press machine: a nonloaded structure (on the left), a deformed structure in the testing process (on the right).

DISCUSSION & CONCLUSIONS:

According to the compression tests results, the global elastic modulus of all tested trabecular structures is close to the elastic modulus of bones. This is one of the main aims of research focused on porous structures for implantation into bones. However, the microscopic analysis showed discontinuities in the trabeculas and a sinter in the structures which can loose in a patient body and cause a necrosis and an aseptic loss of implant.

ACKNOWLEDGEMENTS: The financial support provided by the Technology Agency of the Czech Republic, project n. TJ01000328 is gratefully acknowledged.

REFERENCES: [1] Mullen, Lewis, et al. "SLM: A regular unit cell approach for the manufacture of porous, titanium, bone ingrowth constructs, suitable for orthopedic applications." *Wiley InterScience* (2008): 325-334. [2] Standard, I. "ISO 13314: 2011 (E) (2011) Mechanical testing of metals—ductility testing—compression test for porous and cellular metals." *Ref Number* ISO 13314.13314: 1-7.

Multifunctional Anodic Oxide Layers on Titanium-Based Biomaterials

M. Jarosz¹, W. Simka², G. D. Sulka¹

¹Jagiellonian University, Faculty of Chemistry, Department of Physical Chemistry & Electrochemistry, Krakow, PL, ²Faculty of Chemistry, Silesian University of Technology, Gliwice, PL

INTRODUCTION: Titanium-based materials are commonly used for bone implants due to their favorable properties, such as good biocompatibility, corrosion resistance acceptable mechanical properties [1]. Despite that, the osseointegration between the implant and the surrounding tissue, which occurs via the natural oxide (TiO₂) needs to be improved. Therefore, scientists are using various surface modifications, among which, anodization seems to be the most favorable [2]. The method is simple and cost-effective, and what is more important, allows for precise control over the nanostructured geometry. Moreover, nanostructured surface enables for incorporation of different compounds, e.g., drugs or antibacterial agents, providing multifunctional properties of scaffolds [3,4].

METHODS: Anodic titanium oxide (ATO) layers on Ti foil and Ti-based alloys (Ti13Nb13Zr and Ti15Mo) were prepared via the anodization process conducted in the ethylene glycol-based electrolyte with the addition of NH₄F and H₂O, under a constant voltage in the range between 40 and 100 V at 20 °C. The obtained anodic layers were characterized in terms of their physicochemical properties by using different methods, e.g., SEM, EDS, XRD, XPS, and contact angle measurements. Moreover, corrosion resistance properties were also investigated. ATO layers were modified with Ag nanoparticles, and their antibacterial activity was tested. Finally, the biocompatibility of such layers was also examined.

RESULTS: Depending on the used substrate (Ti foil or Ti-based alloy), nanostructural oxide layers with different surface morphologies were obtained. Received ATO layers differed in the pore diameter and oxide thickness, which then had an impact on their properties, both physicochemical and biological. All anodized samples showed better wettability and enhanced corrosion resistance when compared with bulk substrates. What is more, the successful deposition of silver nanoparticles on ATO layers was performed. Such modified materials

were characterized by slightly better antibacterial activity towards Gram-positive and Gram-negative bacteria. ATO layers presented also enhanced osteoblast-like cells growth when compared to bare substrates.

DISCUSSION & CONCLUSIONS: By using the anodization process at different conditions, nanostructural TiO2 layers with various morphologies may be obtained on Ti-based materials. Most importantly, such layers provide better biocompatibility than bare substrates. Furthermore, nanoscale structures allow for further modifications depending on the use of the scaffold. Antibacterial properties may be adjusted by deposition of e.g., Ag nanoparticles or by loading antibiotics inside the other hand, pores. On enhanced osseointegration may be provided by adjusting pore size or by modifying surface with hydroxyapatite. Such scaffolds give scientists a vast spectrum of possibilities to create improved and multifunctional materials for bone implants.

ACKNOWLEDGEMENTS: Magdalena Jarosz would like to acknowledge financial support from the National Science Center (no. UMO-2017/25/B/ST8/01599).

REFERENCES: [1] N.K. Awad, S.L. Edwards, Y.S. Morsi, Mat. Sci. Eng. C, 76 (2017) 1401–1412. [2] J.M. Macak, H. Tsuchiya, P. Schmuki, Angew. Chem. 44 (2005) 2100–2102. [3] Q. Ma, S. Mei. K. Ji, Y. Zhang, P.K. Chu, J. Biomed. Mater. Res. A, 98A (2011) 274–286. [4] N. Caliskan, C. Bayram, E. Erdal, Z. Karahaliloglu, E.B. Denkbaş, Mater. Sci. Eng. C 35 (2014) 100–105.

Astrocyte Reactivity in Impacted 3D Tethered Gels

J. Smith¹, R. M. Hall², J. B. Philips³, J. L. Tipper^{1,2}

¹Faculty of Biological Sciences, University of Leeds, Leeds, UK, ² School of Mechanical Engineering, University of Leeds, Leeds, UK, ³ UCL Centre for Nerve Engineering, University College London, London, UK

INTRODUCTION: Spinal cord injury (SCI) can cause paralysis, loss of sensation, and respiratory dependency, which has a significant impact on the quality of life of patients, their life expectancy and is also a significant economic burden due to the high costs associated with primary care and loss of income. The glial scar is considered a physiological and physical barrier regeneration of the injured spinal cord (Kimelberg and Norenberg, 1989). Astrocytes are the principal cells responsible for mediating glial scar formation (Fawcett and Asher, 1999). The aim was to investigate the effect of impaction on 3D constructs containing primary rat astrocytes on reactive gliosis and the formation the glial of scar using immunocytochemistry and imaging techniques to detect glial fibrillary acidic protein (GFAP).

METHODS: Neonatal rat cortical astrocytes were cultured in anisotropic 2mg/ml type 1 collagen hydrogels, which have a lower elastic modulus in comparison to spinal cord tissue, and which maintain astrocytes in a non-reactive state, as determined by the expression of markers for reactive astrogliosis. Contusion models of SCI are thought to generate the most relevant animal models of SCI, therefore their suitability as an injury mechanism within a 3D cellular model was investigated. The study utilised the Infinite Horizons (IH) in vivo impactor, which is a force-controlled contusion device. The experimental parameters utilised with the IH impactor within an in vivo setting were investigated as to their suitability for in vitro collagen gel impactions. Following a detailed investigation, the in vivo parameters of an impact force of 200 kdyn and a dwell time of 0 ms, using a 2.5 mm diameter impaction tip were adopted. The images that were used for the analysis of astrocyte reactivity were tiled images from across the entire impact site where filaments where recorded to be from 0° to 90° relative to the impact zone edge. The marker, GFAP, was used as a method of quantifying the degree of astrocyte reactivity as a function of distance from the impact zone.

RESULTS: Astrocyte cell alignment appeared more constrained (less variable) and more aligned with the impaction zone edge than those areas away from the contusion. This effect appeared to become more prominent with time. The interrogation of the astrocyte response using GFAP immunoreactivity noted two important results (Figure 1); (1) that the cells nearest the impact zone were the first to show elevated levels of GFAP and (2) that this effect appeared to extend to the other areas as time progressed. GFAP expression was higher following impact than in the control samples.

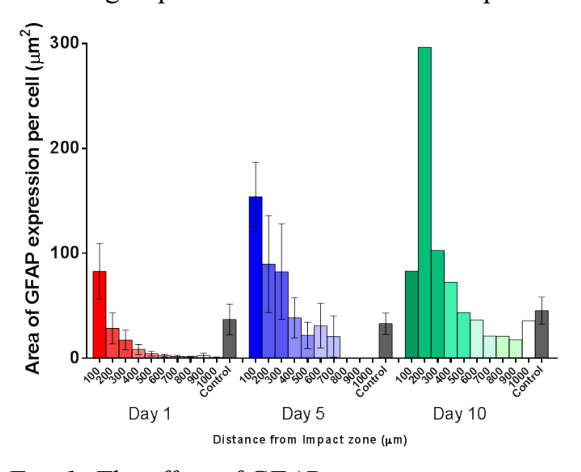


Fig. 1: The effect of GFAP expression as a function of distance from the impact zone at days 1, 5 and 10.

DISCUSSION & CONCLUSIONS: The use of a 3D hydrogel culture model demonstrated features observed clinically i.e. the development of glial scar features. Such models have the advantage of possible adaptability over *in vivo* or *ex vivo* models.

ACKNOWLEDGEMENTS: JS was supported by The EPSRC CDT in Medical & Biological Engineering.

REFERENCES: [1] Fawcett, J.W., and Asher, R.A. (1999). The glial scar and central nervous system repair. Brain Res. Bull. 49, 377–391. [2] Kimelberg, H.K., and Norenberg, M.D. (1989). Astrocytes. Sci. Am. 260, 66–72, 74, 76.

A Non-Linear Relationship between Contusion Velocity & Displacement Depth & Astrocyte Reactivity in an *in vitro* Model of Spinal Cord Injury

T. K. Nguyen¹, J. L. Tipper², J. B. Phillips³, R. M. Hall⁴, J. C. F. Kwok^{5,6}

¹Institute of Medical & Biological Engineering, University of Leeds, Leeds, UK, ²School of Biomedical Engineering, University Technology Sydney, Sydney, AU, ³UCL Centre for Nerve Engineering, University College London, London, UK, ⁴Institute of Thermofluids, University of Leeds, Leeds, UK, ⁵School of Biomedical Sciences, University of Leeds, Leeds, UK, ⁶Institute for Clinical & Experimental Medicine, Prague, CZ

INTRODUCTION: Traumatic injuries to the spinal cord lead to a microenvironment where regeneration is poor. Replicating the biomechanics of injury has been shown to be important in understanding the heterogeneity of pathophysiological events¹. The aim of this work was to investigate the interactions between injury biomechanics and astrocyte responses in a 3D hydrogel model.

METHODS: P2-3 primary Wistar rat astrocyte-seeded collagen gels were prepared in 48-well plates at 1x10⁵ cells p.ml⁻¹ of gel². A contusion regime was implemented after 24 hours: contusion (100 or 1000 mm.s⁻¹) to 25, 50, or 75% gel height, 100 ms dwell, and return to 0%. Astrocyte metabolic activity and reactivity was measured over a 14-day period using an ATPlite assay, and glial fibrillary acidic protein (GFAP) immunostaining.

RESULTS: Cellular ATP levels rose between Days 1 and 14 with an increase in both displacement and velocity. Astrocyte morphologies ranged from small and rounded, in control gels, to progressively more ramified as displacement was increased to 75% (Fig. 1). Quantification of GFAP expression also suggests increased reactivity at 100 mm.s⁻¹ (Fig. 2A). Interestingly, at 1000 mm.s⁻¹ a similar level of reactivity was observed across all displacement depths over time (Fig 2B).

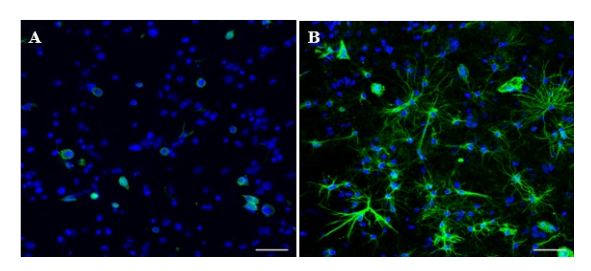


Fig. 1: Simulated contusion results in increased GFAP expression and morphological changes characteristic of astrogliosis. Control (A), and 1000 mm.s⁻¹ 75% displacement at Day 14 (B). 36 μm z-stacks. Scale bar 50 μm.

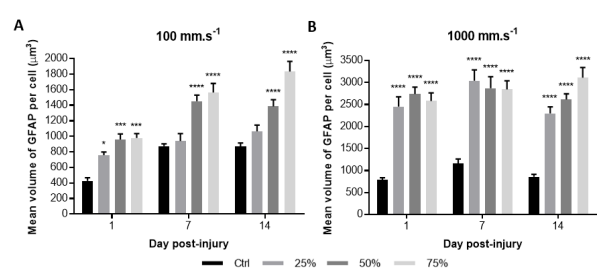


Fig. 2: Effect of contusion velocity and displacement depth on GFAP expression at 100 (A) and 1000 mm.s⁻¹ (B). Mean \pm SEM (n=4). ****p<0.0001.

DISCUSSION & CONCLUSIONS: There is no consensus yet on whether displacement or velocity is the dominant factor affecting neurological outcomes in vivo. Results here suggest interaction between the two, in agreement with Lam et al who used a rat SCI model³. Between 100 and 1000 mm.s⁻¹ lies a threshold where, below this, injury depth defines astrocyte reactivity. This contrasts Lam et al, however, who suggest a depth threshold speed becomes which important. Astrogliosis is a complex process, involving cell death, proliferation, hypertrophy and ramification, all of which are ATP-intensive. At 1000 mm.s⁻¹, increased metabolic activity, together with similar GFAP expression at increasing displacement depth, proliferation is taking place. This work provides a solid basis for the development of additional injury mechanisms, such as distraction and dislocation, which are commonly observed in humans⁴.

ACKNOWLEDGEMENTS: This research was funded by the EPSRC CDT in TERM. Grant number EP/L014823/1.

REFERENCES: [1] S. Mattuci., et al. 2018. *Clin Biomech*. 18: 30262. [2] E. East., et al. 2009. *J Tissue Eng Regen Med*. 3(8): 634-46. [3] C.J. Lam., et al. 2014. *J Neurotrauma*. 31(24):1985-97. [4] Chen. K., et al. 2016. *J Neurotrauma*. 33(18):1667-84.

Hydrogel Variants with Tunable Mechanical Properties & Constant Microarchitecture for the Direction of Neural Stem Cell Differentiation

P. Clarkson¹, J. L. Tipper², G. Tronci³, **R. M. Hall**¹

¹Institute of Medical & Biological Engineering, University of Leeds, UK. ²School of Biomedical Engineering, University of Technology Sydney, AU, ³Centre for Textile Materials Innovation for Healthcare, University of Leeds, UK

INTRODUCTION: Hydrogels have been popular in the development of 3D cell cultures as they can provide a biomimetic matrix and can hold a high aqueous content. The ability of mesenchymal stem cells to sense and respond to the elastic moduli of their environment has been widely reported [1,2]. It is known that the microarchitecture can also affect neural stem cell activities including proliferation rates and differentiation [2]. Increasing the concentration of reagents or crosslinking densities, has been found to reduce the pore size of the hydrogels [1]. The present study aimed to develop a method for changing hydrogel elastic modulus while maintaining a similar architecture.

METHODS: Type I collagen from rat tails was purified and hydrogels were crosslinked using an EDC-NHS reaction [3] for a final collagen concentration of 0.8% (w/v). To create hydrogels with similar microarchitecture, the crosslinker type was changed. Concentrations of 1.3-Phenylenediacetic acid (Ph) and Tartaric acid (Ta) crosslinkers were varied to maintain the number of free carboxyl groups for comparable degrees of lysine functionalisation. Mechanical properties were measured using oscillatory shear frequency sweeps within the linear viscoelastic region, and the hydrogels were compared at 1Hz. The degree of crosslinking was measured using the TNBS assay [3]. Pore diameter was measured using SEM imaging and the BoneJ plugin [4] which was validated before analysis of the hydrogels by comparison with manual measurements. Pore volume was measured using NMR T2 logging. Porosity was measured by wet and dry weight comparison.

RESULTS: The BoneJ plugin [4] was confirmed to measure the pore diameters of the hydrogels from SEM images as effectively as manual measurements, finding no significant difference between the two techniques (n=3). The elastic modulus at 1Hz was found to be significantly different (p<0.05, n=4) between the two hydrogels, at 74.0±6.63 Pa for Ph and

99.6 \pm 6.65 Pa for Ta hydrogels (Fig 1). There was no significant difference in the crosslink density (n=3), pore diameter (n=4) or pore volume (n=3) of the hydrogels. The degree of crosslinking was 45.4 \pm 0.79% on average for the hydrogels and pore diameter was 21.2 \pm 0.92 μ m. Porosity was found to be significantly different (p<0.01 n=3).

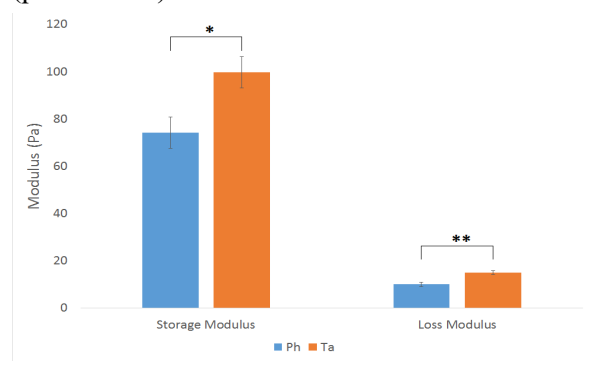


Fig. 1: Storage and loss moduli of hydrogels with Ph or Ta crosslinker at 0.4% strain and 1Hz. Error bars represent standard error, n=4. * signifies p<0.05, ** signifies p<0.01.

DISCUSSION & CONCLUSIONS: The elastic moduli were varied between the two hydrogel types, while the microarchitecture was preserved. Variation of the crosslinker generated hydrogels with tuneable elastic properties but constant microarchitecture and therefore are a useful tool to further interrogate the relationship of neural stem cells with their physical environment.

ACKNOWLEDGEMENTS: This work was funded by the EPSRC and was conducted within the DTC TERM.

REFERENCES: [1] Her (2013) Acta Biomater 9.2, pp.5170-5180. [2] Christopherson (2009) Biomaterials 30.4, pp.556-564. [3] Tronci (2013) J Mater Chem B Mater Biol Med 1.40, pp.5478–5488. [4] Doube (2010) Bone 47, pp.1076-9.

Effect of Deposition Parameters on the Tribocorrosive Performance of Silicon Nitride-Based Coatings

L. Correa Filho¹, S. Schmidt^{2,3}, A. López¹, C. Goyenola³, H. Engqvist¹, M. Tobler², C. **Persson**¹

¹ Division of Applied Materials Science, Department of Engineering Sciences, Uppsala University, SE, ² Ionbond AG, Industriestrasse 211, Olten, CH, ³Thin Film Physics Division, Department of Physics, Chemistry & Biology (IFM), Linköping University, SE

INTRODUCTION: Ceramic coatings could be an alternative to obtain high wear resistance also reducing metal ion release. Silicon nitride based coatings have shown promise for use in joint implants, a decreased chemical reactivity may be required. The aim was to evaluate the effect of adding alloying elements C, and Cr as well as different deposition energies on the tribocorrosive performance of silicon nitride based (SiN_x) coatings sliding against Ultra High Molecular Weight Polyethylene (UHMWPE) pins.

METHODS:

Coatings were deposited by high power impulse magnetron sputtering (HiPIMS) onto CoCrMo discs. Coating composition was evaluated by xray photoelectron spectroscopy (XPS) and the surface roughness by vertical scanning interferometry (VSI). Mechanical properties were investigated by nanoindentation. Multidirectional wear tests against UHMWPE pins were carried out for 2 million cycles in bovine serum solution (25%) at 37°C, at an estimated contact pressure of 2.1MPa (1).

RESULTS: XPS revealed a Si content of 33.8 - 46.5 at%, Ni of 49.7 - 55.5 at%. Surface roughness fulfilled the standard requirements (2). Figure 1 shows the Hardness and Young's Modulus, where coatings with a higher bias voltage (SiN_350V) and higher target power (SiN_HE_150V) had higher values (25.4 and 28.4 GPa, respectively). Volumetric wear rate for UHMWPE resulted in a range 0.7 - 4.0 mm³/MC except for coating SiN_150V, which showed 100 mm³/MC, possibly related to the lower content of N₂ and lower bias voltage resulting in a less dense, and more reactive coating.

DISCUSSION & CONCLUSIONS: Lowdensity coatings gave a lower hardness and failed earlier in the wear test, due to chemical reactions, accelerated by the tribological contact. Coatings with higher energy deposition fulfilled the target profile for surface roughness (Ra<20nm), chemical stability over time, as well as low polymer wear, showing promise for joint bearings. It was found that high density coatings were needed to prevent coating and/or counter surface wear or failure.

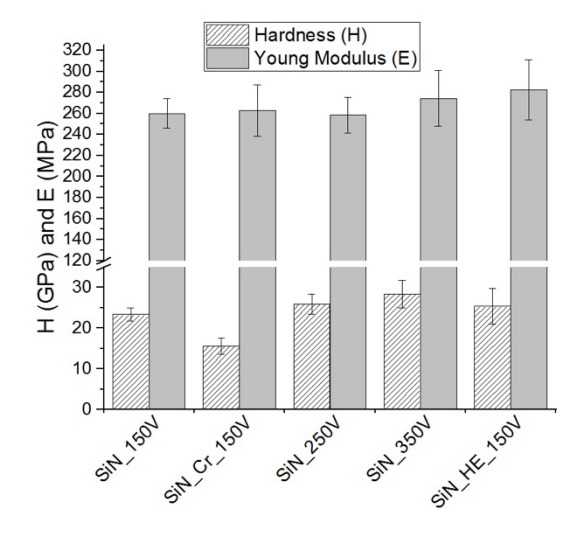


Fig. 1: Hardness and Young's Modulus results for all coatings. Samples were divided by bias voltage, Cr content and higher energy target power (HE).

ACKNOWLEDGEMENTS: Susan Peacock is gratefully acknowledged for proof-reading.

REFERENCES:

[1] ASTM F732-17 Standard Test Method for Wear Testing of Polymeric Materials Used in Total Joint Prostheses; ASTM International: West Conshohocken, PA, USA, 2017. [2] ASTM F2033-12 Standard Specification for Total Hip Joint Prosthesis and Hip Endoprosthesis Bearing Surfaces Made of Metallic, Ceramic, and Polymeric Materials; ASTM International: West Conshohocken, PA, USA, 2012.

Alginate Hydrogels seen with Atomic Force Microscopy

A. Akbarzadeh¹, B. L. Strand ¹

¹NOBIPOL, Department of Biotechnology & Food Sciences, NTNU, Trondheim, NO

INTRODUCTION: Alginates are popular materials in cell encapsulation and tissue engineering due to the hydrogel formation with divalent ions at physiological conditions. Although alginate gels are well studied in general. little known about is their microstructure. Atomic force microscopy (AFM) allows the visualization of the hydrogels in their natural hydrated state. In this work, the effects of alginate concentration, oxidizing alginate and grafting with GRGDSP peptide on the surface structure of alginate hydrogels was studied by AFM. RGD ligands are used to increase cell attachment to alginate hydrogels.¹

METHODS: Laminaria hyperborea stipe alginate (M_w =237000 g/mol, F_G =0.68) was oxidized to 8% degree of oxidation. Oxidized alginate was further grafted with GRGDSP peptide by reductive amination² Alginate hydrogels (Ca-Alg) were made by internal gelation with CaCO₃ and glucono-δ-lactone. The hydrogels were casted in petri dishes and kept humid until measurements. A few droplets of HEPES buffer were added on the surface before imaging. Images were acquired using quantitative imaging (QI) mode AFM (JPK Instruments).

RESULTS: Alginate gels with different concentrations of alginate showed differences both regarding topography and density of the structures (Fig 1). 0.5 % (w/v) alginate gel presented a rougher surface compared to the 2.0 % (w/v) alginate gel with peak height of 561 and 388 nm, respectively.

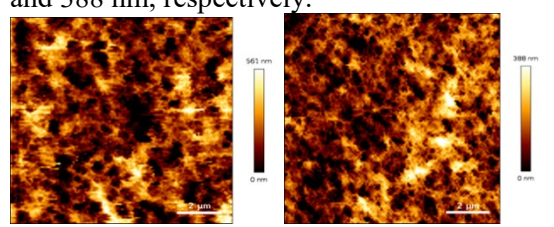


Fig 1. AFM images of (left) 0.5% (w/v) Ca-Alg gel and (right) 2% (w/v) Ca-Alg gel.

The black areas in the AFM images were defined as pores and pore size distributions were determined from the AFM images (Fig 2). Pore sizes shifted towards larger values and the distributions got broader by reducing the alginate concentration, increasing the content of

oxidized alginate, and by grafting the alginate with GRGDSP peptide.

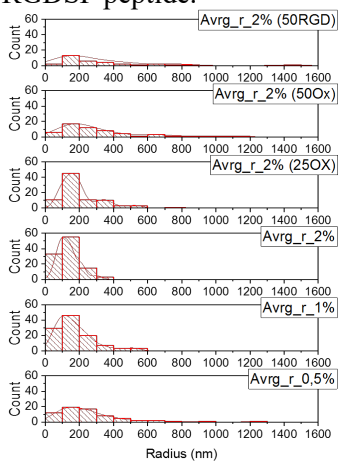


Fig 2. Ca-Alg pore size distribution. From bottom: 0.5%, 1%, 2%(w/v) Ca-alg, 2%(w/v) Ca-alg with 3:1 ratio unmodified alginate:oxidized alginate [2%(25OX)], 2% (w/v) Ca-Alg with 1:1 ratio unmodified alginate:oxidized alginate [2%(50OX)], and 2%(w/v) Ca-Alg with 1:1 ratio unmodified alginate:alginate grafted with GRGDSP peptide [2%(50RGD)].

DISCUSSION & CONCLUSIONS: AFM has previously been reported to study microstructure of alginate gel beads saturated with gelling ions.³ Alginate hydrogels made with limited calcium have relevant mechanical properties for soft tissue engineering, however these have been tough to characterise by AFM due to the soft structures. In this work we characterise soft alginate gels both regarding topography and pore structures using AFM.

ACKNOWLEDGEMENTS: This work has been supported by NTNU and the Research Council of Norway (269273/O70, "3DLife"). AFM images were recorded at JPK BioAFM center Bruker Nano GmbH with the help of Andre Koernig.

REFERENCES: [1] J. A. Rowley, G. Madlambayan, D. J. Mooney, *Biomaterials*, 1999, vol. 20, P. 45-53. [2] M. Ø. Dalheim, J. Vanacker, M. A. Najmi, F. L. Aachmann, B. L. Strand, B. E. Christensen, *Biomaterials*, 2016, vol. 80, P. 146-156. [3] C. Wandrey et al., *Langmuir*, 2004, vol.20, P. 9968-9977.

Decellularized Cornea Constructs Incorporating Gelatin Methacrylate

M. Uyanıklar¹, G. Günal¹, A. Tevlek¹, P. Hosseinian², **H. M. Aydin**^{1,3}

¹ Bioengineering Division, Institute of Science, Hacettepe University, Ankara, TR, ²Nanotechnology & Nanomedicine Division, Institute of Science, Hacettepe University, Ankara, TR, ³ Centre for Bioengineering, Hacettepe University, TR

INTRODUCTION: In recent years, corneal tissue engineering (TE) has been an emerging field to overcome the main problem of limited availability of allografts. Researchers have been suggesting either synthetic TE constructs or native matrices obtained via decellularization protocols. In this study, we proposed for the first time a combinational approach in order to benefit both. Gelatin methacrylate (GelMA) was impregnated in decellularized bovine cornea samples and crosslinked in situ to obtain hvbrid constructs with optimal transparency.

METHODS: Corneas were dissected from Bovine eveballs and treated with a modified SDS-based (1% SDS (w/v)) decellularization process. GelMA was synthesized by the direct reaction of gelatin with methacrylic anhydride (MA) in phosphate buffer (pH=7.4) at 50 °C Decellularized corneas were impregnated with GelMA and crosslinked in situ by using varying UV irradiation (3200, 6210 and 6900 µJ/cm²). Fourier Transform Infrared Spectroscopy (FTIR) and Differencial Scanning Calorimetry (DSC) analyses were performed to investigate chemical and thermal properties. Histological analyses conducted by using Hematoxylin and Eosin 4',6-diamidino-2-phenylindole (H&E) and (DAPI) staining in order to reveal the success of decellularization. Hydroxyproline, dimethylmethylene Blue (DMMB), PicoGreen ds-DNA assays were performed to evaluate sulfated glycosaminoglycan (s-GAG), collagen and residual DNA content. Hydration degradation characteristics investigated. Mechanical properties of native tissues and hybrid constructs incorporating GelMA were studied. Acquired transmittance features evaluated. Cell viability and cytotoxicity characteristics were also evaluated by using related techniques.

RESULTS: Histological studies were revealed the success of chosen decellularization protocol. PicoGreen analysis showed a residual DNA

content of 24.3 \pm 2.5 ng. FTIR and DSC confirmed *in situ* crosslinking of GelMA within decellularized cornea extracellular matrix. The optimal light transmittance values were achieved by using 6210 μ J/cm² UV radiation (Figure 1B). Hybrid cornea constructs showed 50% weight reduction in phosphate buffered saline (PBS) after 28 days. Alamar Blue analysis revealed that hybrid constructs prepared in this study support cell proliferation.

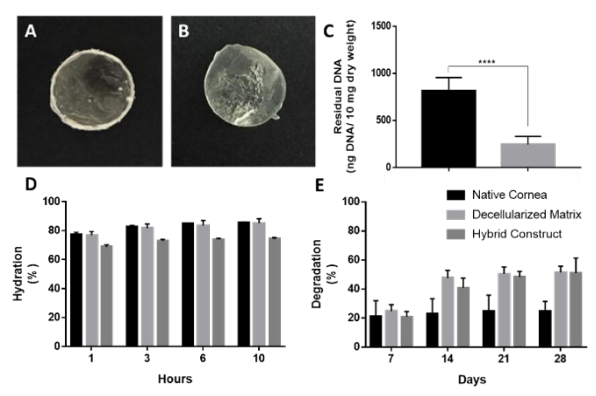


Figure 1. (A) Native cornea, (B) Cross-linked hybrid construct, (C) Residual DNA content of native and decellularized matrix, (D) Hydration and degradation percentages of native cornea, (D, E) decellularized matrix and hybrid constructs.

DISCUSSION & CONCLUSIONS: This study suggest for the first time a hybrid cornea construct obtainable by combining a native ECM and a polymer. The proposed approach can benefit from nanoarchitecture of the decellularized tissue and handling and light transmission properties of a synthetic material and can be utilized in another TE applications.

ACKNOWLEDGMENTS: The authors would like to thank BMT Calsis Co. and Hacettepe University (Grant No: FBB-2018-16688).

REFERENCES

[1] Khademhosseini A et. al., Biomaterials. 73: 254-271, 2015. [2] Aslan B et. al., Journal of Biomedical Materials Research Part B:Applied Biomaterials. 106(6): 2157-2168, 2018.

Influence of Selected Surfactants on α-TCP Hydrolysis: XRD Studies

E. Cichoń¹, A. Zima¹, A. Ślósarczyk¹

¹Faculty of Materials Science & Ceramics, AGH University of Science & Technology, Krakow, PL

INTRODUCTION: Recently, foamed calcium phosphate bone cements (fCPCs) as the novel bone tissue substitutes with developed porosity strongly attract the attention of scientists and clinicians[1,2]. Surfactants, as air-entraining agents are suitable compounds that make it possible to create pores during the preparation of cement paste[3]. It should be highlighted that the addition of surface active agent not only exerts influence on the porosity of the prepared material, but also on its other properties such as alpha tricalcium phosphate (α-TCP) hydroxyapatite (HAp) conversion rate. In this study the influence of selected surfactants addition on the α-TCP hydrolysis and phase composition offinal materials investigated.

METHODS: The powder phase of the studied cements consisted of the highly reactive α-TCP (specific surface area = $7.25 \pm 0.01 \text{ m}^2/\text{g}$). Initial powder was synthesized by the wet chemical method. For the synthesis, CaOH and 85% phosphoric(V) acid were used. As the liquid phase served 2 wt% Na₂HPO₄ solutions with 10 wt% surfactant addition. In our study the following surfactants were applied: Tween 20 (TW20), Tween 80 (TW80) and Tetronic 90R4 (90R4). Liquid to powder ratio was 0,42 g/g. α-TCP cement without any surfactant was used as reference sample (TCP). The XRD studies of the examined cements were performed three times: 7 days and 4 months after setting in the air at room temperature as well as after one week of incubation in simulated body fluid (SBF) at 37 °C.

RESULTS: X-ray diffractograms of the examined materials are presented in Fig. 1. The diffractograms of all prepared cements after setting revealed the presence of reflections from crystalline α TCP and hydroxyapatite (HAp). The diffractograms after 7-day incubation in SBF revealed the presence of only one crystalline phase – HAp.

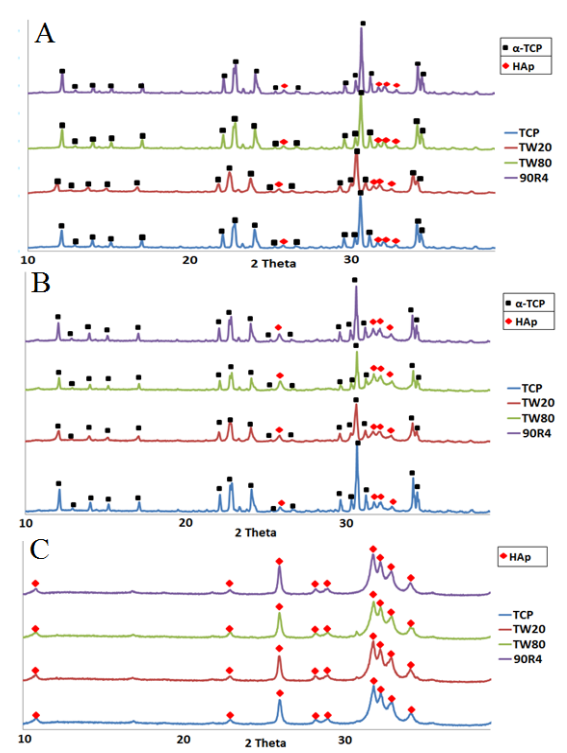


Fig. 1: X-ray diffractograms of materials after A) 7 days from setting, B) 4 months from setting, C) 7-day incubation in SBF.

DISCUSSION & **CONCLUSIONS:** obtained results indicate that the addition of all selected surfactants accelerated α-TCP hydrolysis during setting in the air of the prepared cements. The effect of surface active agents on phase composition was negligible after 7 days but after 4 months was clearly visible. In the case of TW80 nearly 60% of HAp was present (only 22% for reference material). After 7-day incubation in SBF α-TCP hydrolyzed completely to HAp in all materials.

ACKNOWLEDGEMENTS: The study was funded by the National Science Centre, Poland within the project no. 2017/27/N/ST8/00913.

REFERENCES: [1] Ginebra MP (et al.) Acta Biomater. 2010; 6(8):2863-2873. [2] Zhang J (et al.) Acta Biomater. 2016; 31:326-338. [3] Montufar EB (et al.) Acta Biomater. 2010; 6(3):876-885.

Elucidating Host Responses towards Alginate Microspheres using Proteomics

A. E. Coron^{1,2,3}, D. M. Fonseca², A. Sharma², G. Slupphaug², A. M. Rokstad³, B. L. Strand¹ Deptartment of Biotechnology & Food Science, NTNU, Trondheim, NO, ² Deptartment of Clinical & Molecular Medicine, NTNU, Trondheim, NO, ³Centre of Molecular Inflammation Research, NTNU, Trondheim, NO

INTRODUCTION: The biocompatibility of biomaterials in general is a major challenge in biomedical applications. Hydrogel biomaterials, such as alginate, are relevant for both tissue engineering and immunoisolation (cell therapy) purposes. Utilisation of alginate microspheres for cellular therapy has shown to be limited in terms of long-term graft survival, due to pericapsular fibrotic overgrowth. Fibrotic overgrowth is a complex process that involves several factors, including protein adsorption. This work investigates the protein adsorption profiles of alginate microspheres incubated in human plasma, to identify central proteins that may play a role in the fibrotic responses observed on alginate microspheres in vivo.

METHODS: Various alginate microspheres were prepared under sterile conditions: (A) UP-LVG alginate, (AP) UP-LVG alginate with poly-L-lysine coating, and (SA) sulphated UP-MVG alginate mixed with UP-LVG alginate. The alginate microspheres were incubated in human plasma for 24h at 37°C. Plasma proteins adsorbing to the microspheres were collected for mass spectrometry analysis and separated into two fractions: eluted proteins (E) and proteins directly digested from the alginate microsphere surface (T). Peptides analysed on a LC-MS platform consisting of an Easy-nLC 1000 UHPLC system interfaced with LTQ-Orbitrap Elite hybrid spectrometer via a nanospray ESI ion source. Raw files were analysed with MaxQuant v 1.5.8.3 and searched against the March 2017 v of Human proteome set with isoforms from Uniprot. The mass spectrometry proteomics data was deposited to the ProteomeXchange Consortium via the PRIDE partner repository dataset identifier PXD009135. with the Notur/NorStore Project NS9036K.

RESULTS: Identification and quantification of adsorbed human plasma proteins to the surface of alginate based microspheres by LC-MS revealed distinctive protein adsorption profiles (*Fig. 1*). Key proteins involved in inflammatory

responses, such as complement and coagulation cascades, were identified for the alginate microspheres. E.g. the highest protein abundancies of pro-inflammatory complement C3 and anti-inflammatory factor H were found on AP and SA-microspheres, respectively. The protein adsorption profiles of the biomaterials in question may give insight into the performance *in vivo*. The adsorption of selected human plasma proteins to alginate microspheres was studied by confocal laser scanning microscopy and the results were in accordance with the protemics analysis.

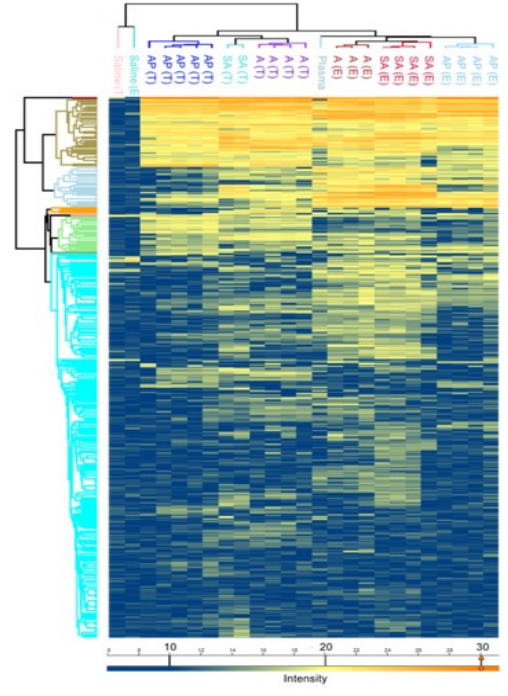


Fig. 1: Protein adsorption profiles of plasma incubated alginate microspheres: A, AP and SA (E-and T-peptide fractions), including saline and plasma controls. The heat map shows log2 label free quantification values of 479 identified proteins.

DISCUSSION & CONCLUSIONS: In this study MS-based proteomics was used to identify key proteins adsorbed to alginate microsphere surfaces exposed to human plasma. These results are important to understand host responses towards alginate microspheres and alginate hydrogels, and to guide alginate based biomaterial design.

Nanohydroxyapatite Synthesized by Hydrothermal Microwave Synthesis for Medical Applications

S. Dąbrowska 1,2* , A. Chodara 1,2 , U. Szałaj 1,2 , J. Rogowska-Tylman 1,2 , T. Chudoba 1 , W. Łojkowski 1

¹Institute of High Pressure Physics, Sokolowska 29/37, 01-142 Warsaw, PL, ²Warsaw University of Technology, Faculty of Materials Science and Engineering, Warsaw, PL

INTRODUCTION: Bioactive materials which can support bone ingrowth and osseointegration are common used in orthopedic and dental applications. Hydroxyapatite (HAP) is a phosphate compound having calcium chemical formula Ca₁₀(PO₄)₆(OH)₂. Bioactive hydroxyapatite is one of the inorganic components of hard tissues, which is manufactured in The Institute of High Pressure Physics (IHPP PAS) and it is called GoHAPTM. Microwave solvothermal synthesis (MSS) is an example of microwave assisted wet chemical synthesis process and nowadays it is counted as one of the most popular chemical methods of obtaining nanomaterials, like HAP, ZnO, ZrO₂ and others.

METHODS: Microwave hydrothermal heating enables a better control of the reaction time, fast heating and reducing the thermal gradients. This results in a better crystallinity of the nanoparticles comparing to the precipitation process. An additional advantage is a reduced synthesis temperature, so no powder calcination is needed. The morphology, grain size and specific surface area of the nanopowder can be controlled by the microwave reactor [1][2].

At our laboratory, we have been developing new type microwave reactors for nanomaterials synthesis for more than 10 years. The use of the microwave radiation and the unique design of the reactor permits precise pressure control which allows for an automatic operation in the stop-flow or use batch (closed vessel) mode. GoHAPTM is synthesized by hydrothermal synthesis using microwave reactor MSS2 made by cooperation IHPP PAS and The Institute for Sustainable Technologies NRI.

RESULTS: Nanohydroxyapatite was synthesized by precipitation method in room temperature and after heated by hydrothermal synthesis using microwave reactor MSS2. In the IHPP PAS we are able to synthesize and obtain six types of hydroxyapatite with different crystallinity degree and grain size. Obtained nanoparticles were in the range of 8-45 nm

grain size. Phase purity was measured using X-ray diffraction. Thanks to scanning electron microscopy (SEM) the morphology of produced hydroxyapatite was characterized. The density and specific surface area were determined using helium pycnometry and BET method. Our GoHAPTM has a high similarity to the natural mineral bone and we are using this material in the various projects in the Laboratory, as the scaffold layers, ligament layers, dental materials and bone implants.

ACKNOWLEDGEMENTS:

The MSS2 reactor was constructed as a part of the CePT project, reference: POIG.02.02.00-14-024/08, financed by the European Regional Development Fund. Research was supported by the polish National Centre for Research and Development (NCBR) project: NANOLIGABOND (POIR.04.01.02-00-0016/16) "Artificial tendons and ligaments fixation to bone tissue using nanotechnological approach".

REFERENCES: [1] Patent application P-369906, Lojkowski et al, The method of nanoplates and method of nanopowder with nanoplates obtaining from synthetic hydroxyapatite. [2] S. Kuśnieruk, "Influence of hydrothermal synthesis parameters on the properties of hydroxyapatite nanoparticles", Beilstein Journal of Nanotechnology 7:1586-1601, November 2016.

Porcine Pericardium Re-cellularized with Adipose Tissue-Derived Stem Cells & Endothelial Cells for Heart Valve Prostheses

E. Filova¹, R. Matejka^{1,2}, M. Travnickova¹, J. Knitlova¹, J. Musilkova¹, S. Prazak¹, M. Konarik³, J. Pirk³, A. Lodererova³, E. Honsova³, T. Riedel⁴, J. Kucerova⁴, E. Brynda⁴, L. Bacakova¹

¹Institute of Physiology, Czech Academy of Sciences, Prague, CR, ² Faculty of Biomedical Engineering, Czech Technical University in Prague, Kladno, CR, ³Institute for Clinical & Experimental Medicine, Prague, CR, ⁴Institute of Macromolecular Chemistry, Czech Academy of Sciences, Prague, CR

INTRODUCTION: Human bovine pericardium are currently used in a form of patches or heart valve prostheses after their decellularization or crosslinking glutaraldehyde. Fifteen years after implantation these grafts undergo degeneration and must be replaced. Re-cellularization of de-cellularized tissue should prolong their functionality, reduce immune response or even support graft growth in children. Adipose tissue-derived stem cells (ASCs) are able to differentiation towards smooth muscle cells and produce extracellular matrix: endothelial cells create an antithrombogenic layer. These cell types are therefore suitable for re-cellularization.

METHODS: Porcine pericardium was decellularized using 1% sodium dodecvl sulfate and DNase solution, washed with distilled water, sterilized in 70% ethanol, and washed in PBS. Pericardium was then coated with a fibrin mesh (Fb) or with the mesh containing immobilized heparin and VEGF165 (Fb+VEGF, GenScript). Human ASCs were seeded on pericardium samples (55,000 cells/cm², passages 3-4) and cultured in DMEM medium supplemented with TGF-\(\beta\)1 and BMP-4 (both 2.5 ng/ml) for 16 days or for 5 weeks. After 16 days of colonization with ASCs, the samples were seeded with human umbilical vein endothelial cells (HUVECs, 100,000 cells/cm²) and cultured for 5 days in EGM-2 medium (PromoCell GmbH, Germany) with TGF-β1 and BMP-4. The samples were then fixed and immunohistologically stained for von Willebrand factor, calponin, vimentin, and with phalloidin-TRIC for F-actin.

RESULTS: The Fb+VEGF coating accelerated both ingrowth of ASCs into pericardium and ASCs differentiation into smooth muscle cells (calponin staining) (Fig. 1) in comparison with Fb-coated samples. In addition, this

modification supported HUVECs attachment and proliferation.

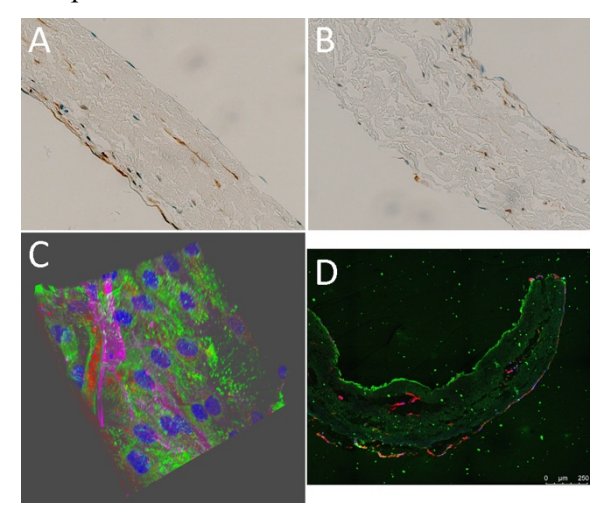


Fig. 1: Immunohistological staining of calponin (A, B) in ASCs on pericardium coated with Fb (A) and with Fb+VEGF (B). The 3D projection of Fb-coated sample (C) and tile scan of Fb+VEGF (D) stained for von Willebrand factor (green, C, D), for calponin (C, red) and F-actin (C, purple, D, red). Olympus IX51 microscope, obj. \times 20 (A, B), Leica SP8 confocal microscope, obj. \times 20, zoom \times 0.75 (C), scale bar = 250 µm (D).

DISCUSSION & CONCLUSIONS: Growth factors TGF-β1 and BMP-4 have been used to differentiate mesenchymal stem cells into smooth muscle cells. In this study we proved a positive effect of Fb+VEGF coating on both differentiation of ASCs towards smooth muscle cells and on endothelialization of pericardium graft.

ACKNOWLEDGEMENTS: Supported by the Czech Health Research Council, project No. 15-29153A, and by the Czech Science Foundation, project No. 18-01163S.

Effect of PVA Nanofibers Releasing Platelet Lysate Components on Growth & Differentiation of Keratinocytes, Fibroblasts & Endothelial Cells in vitro

E. Filová¹, M. Plencner¹, M. Andělová¹, B. Kopřivová², R. Procházková³, V. Jenčová², L. Bačáková¹

¹Institute of Physiology of Czech Academy of Sciences, Prague, CR, ²Technical University in Liberec, Liberec, CR, ³Regional Hospital Liberec, Liberec, CR

INTRODUCTION: Upon injury, platelets are incorporated into fibrin clot and release many chemical compounds and growth factors, which attract cell migration, proliferation, and differentiation during wound healing. In this study, potentially favourable effects of platelet lysate (PL), either added into medium or incorporated in polyvinyl alcohol nanofibers (PVA_PL), were assessed on keratinocytes, fibroblasts and endothelial cells.

METHODS: Platelet suspension was prepared in the Transfusional Department. of Regional Hospital Liberec, Liberec, CR from buffy coat from 4 patients; the platelet concentration was in the range from 793×10^6 to 845×10^6 cells/ml. PL was made by freezing/thawing method, centrifuged at 2830 x g, 5°C, 30 min. Both PVA nanofibers and PVA/PL nanofibers were prepared by electrospinning NanospiderTM NS 1WS500U (Elmarco, Czech Republic); PVA/PL solution contained 10% of PL. Human keratinocyte cell line HaCaT, human saphenous endothelial cells (HSVEC) and murine fibroblast cell line (3T3) were seeded at the concentrations of 4,000 cells/well, 20,000 cells/well, and 5,000 cells/ well, respectively, onto 24-well glass bottom plate (Cellvis, U.S.A.) and cultured in a medium supplemented with 1, 2.5, and 5% PL or with PVA or PVA/PL (1cm²) nanofibers for 7 days. On days 1, 3, and 7, an MTS assay was HaCaT performed. For and 3T3. DMEM+2%FBS (positive control with 10% FBS) and for HSVEC, ECGM-2 medium (Promocell, Germany) without (a positive control with) growth factors supplemented with 2% FBS, heparin, ascorbic acid, hydrocortison and 1% antibiotic-antimycotic solution (Sigma, were used. Immunofluorescence U.S.A.) staining of cytokeratins 5, 14, 1 and 10 in HaCat keratinocytes was performed.

RESULTS: The highest metabolic activity of 3T3 fibroblasts was found in the medium containing 1% PL or PVA_PL on days 3 and 7, the lowest in the medium with 2% FBS. HaCaT

reached the highest value in the medium with 2.5% PL, the lowest in the medium with 10% FBS. Surprisingly, the cell metabolic activity did not differ between the samples PVA and PVA PL, although this activity was higher than in control samples. The metabolic activity of HSVEC rose with increasing PL concentration up to 5%. On the other hand, it was lower on PVA PL compared to pure PVA on days 3 and 7. Basal cytokeratin 5 was developed in HaCaT cells on all samples, cytokeratin 14 fibres in samples with higher appeared concentrations in medium and in medium with 10% FBS. Filaments of cytokeratin 10 were best developed in the medium with added PVA PL nanofibers (Fig.1). Only diffuse staining of cytokeratin 1 was observed.

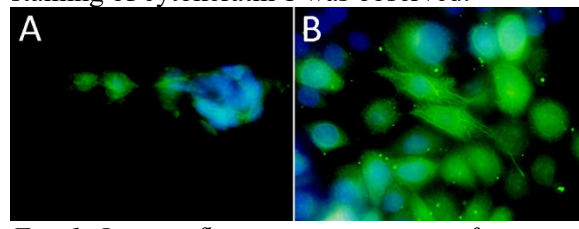


Fig. 1: Immunofluorescence staining of cytokeratin 10 in HaCat cells on glass cultured in DMEM + 2% FBS (A) and in DMEM +2% FBS + PVA_PL (B) on day 7. Olympus IX71, obj.×40.

DISCUSSION & CONCLUSIONS: HaCaT, 3T3 and HUVEC cells had different sensitivity to PL and PVA_PL. PL added into medium supported the cell metabolic activity more intensively than PVA_PL nanofibers. On the other hand, PVA_PL nanofibers improved formation of cytokeratin 10 fibres in HaCaT cells, probably due to prolonged delivery of growth factors from PVA_PL nanofibres.

ACKNOWLEDGEMENTS: Supported by the Czech Research Health Council, project No NV18-01-00332. We thank Ivana Zajanova for help with immunofluorescence staining.

Composite Bilayer Scaffold for the Regeneration of Osteochondral Defects in Rabbits

<u>E. Filova^{1,2}</u>, Y. Kolinko³, A. Litvinec¹, V. Blahnova^{1,2}, V. Pavlinakova⁴, V. Sovkova^{1,5}, V. Lukasova^{1,5}, K. Vocetkova^{1,5}, M. Rampichova¹, R. Divin^{1,2,5}, E. Amler^{2,5}, M. Kralickova³, Z. Tonar³, <u>L. Vojtová</u>⁴

¹Institute of Experimental Medicine of Czech Academy of Scinces, Prague, CR, ²Second Faculty of Medicine, Charles University in Prague, Prague, CR, ³Faculty of Medicine in Pilsen, Charles University in Prague, Pilsen, CR, ⁴Central European Institute of Technology, Brno University of Technology, Brno, CR, ⁵University Centre for Energy Efficient Buildings, Czech Technical University in Prague, Buštěhrad, CR

INTRODUCTION: Three-dimensional scaffolds containing bioactive molecules should support cell homing, proliferation, and differentiation. We have developed a bi-layered scaffolds from type I collagen foam, tricalcium phosphate (TCP), nanofibers with different growth factors, and hyaluronan sodium (HYA). The scaffolds were tested in rabbits.

METHODS: Polycaprolactone-hyaluronic acid nanofibres (nf), either pure or with BMP-2 or TGFbeta2-bFGF-IGF-I were electrospun using Nanospider™ NS 1S500U (Elmarco). Then three scaffold types based on type I collagen foam were prepared (Table 1) and analyzed by SEM. We tested biomechanical properties of dry scaffolds in compression.

Table 1. Composition of scaffolds

| Group | Bone layer | Cartilage layer |
|-------|----------------|-----------------------|
| I. | Col | ColHYA |
| II. | ColTCP-nf pure | ColHYA –nf pure |
| III | CoTCP-nf | ColHYA-nf (TGF-beta1, |
| | (BMP-2) | bFGF, IGF-I) |

Each scaffold type without cells was implanted into osteochondral defect of 8 rabbits. After 12 weeks, the animals were euthanized; knees were fixed in 10% buffered formalin. Samples were decalcified, embedded in paraffin, cut, and stained with hematoxylin-eosin and green trichrome with Verhoeff's hematoxylin, Alcian blue/PAS at pH 2.5, immunohistochemically for type II collagen, and osteocalcin. The microphotographs were quantified stereological software newCASTTM6.1 (VisioPharm, Denmark) in three circular compartments. Statistical analysis performed using Statistica Base 10.

RESULTS: The defects were filled mainly by fibrous tissue with islands of granulation. In group III, higher amount of nonspecific granulated tissue was observed in defects. The

amount of cartilage in the central compartment of defects was similar, however, in group III, the scattering of values was very low compared to other groups. Hyaline cartilage was observed mainly at the edges and at the bottom of the defects. In groups II and III, the connective tissue was covered by islands of hyaline cartilage at the surface of the defect. Bone formation was significantly higher in outer compartments compared to other ones in all groups, no other differences were observed. The higher amount of osteocalcin was found in group I in regions adjacent to bone. Scaffold II showed the lowest plateau stress in compression than other scaffolds.

DISCUSSION & CONCLUSIONS: Cell migration into defects is influenced by scaffold porosity, pore size, growth factors, etc. Growth factors increased maturation of macrophages that might negatively influence defect healing. Cartilage in islet on the surface in groups II and III and more homogeneous cartilage formation in group III were observed.

ACKNOWLEDGEMENTS: The work was supported by Czech Science Foundation 18-09306S, by Charles University Grant Agency Nos. 448218, 512216, by the project CEITEC 2020 (LQ1601) and Ministry of Education, Youth and Sports of the Czech Republic under the National Sustainability Programme II, EFRR No. CZ.02.1.01/0.0/0.0/6_019/0000787, NPU I: LO1309, LO1508, MZVES 16-28637A.

Comparison of Properties of Conventional & 3D-printed Titanium & Their Mechano-Regulative Potential

M. Gasik¹, A. Zühlke¹, N. E. Vrana², J. Barthes²

¹Aalto University Foundation, Espoo, FI, ²Protip Medical SAS, Strasbourg, FR

INTRODUCTION: There is a growing trend of use of 3D-printed implants made of titanium alloys. It is also known that the microstructure and topology of porous layers are different from similar conventional materials made by sintering or powder spraying technology. In this way local fluid permeability and respectively nutrients transport are also varied. Here we are analysing elastic properties and respective mechano-regulative index (MRIX) variations for different titanium specimens during representative loading scenarios.

METHODS: Strips of titanium of 10 x 40 mm were made from a rolled metal sheet (conventional) and by 3D-printing with electron beam melting. Mechanical properties were measured with DMA 242E "Artemis" (Netzsch Gerätebau GmbH, DE) in 0.1-20 Hz and 1-30 um flexion amplitude range. Surface topology digitizing was performed from µCT scans to create a 3D micromodel, Fig. 1. Modelling of deformation and associated generated fluid flow (COMSOL Multiphysics 5.3a) was made with HP Apollo 6000 XL230a supercluster (CSC -IT Center for Science, FI). Mechano-regulative index (MRIX) as by [1] was compared for different titanium specimens during typical loading scenarios.

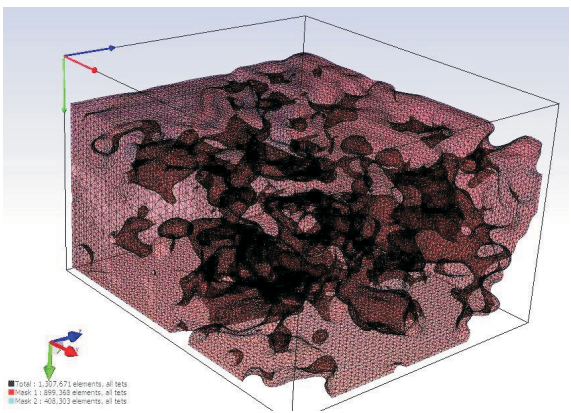


Fig. 1: Micro-model of surface layer of 3D printed titanium (100x100x20 µm).

RESULTS: There are identified differences in mechanical properties of titanium made by different methods. 3D-printed specimen having higher bending modulus than conventional one

(~61 GPa vs. ~47 GPa at 1 Hz), meaning 3D printed titanium will deform less at the same applied load.

Dynamic deformation of conventional titanium specimen will respectively generate higher adjacent fluid velocities, Fig. 2, than for surface of 3D printed specimen. This results in a higher fluid velocity share contribution for more "smooth" surface to MRIX than for "rough" (3D-printed).

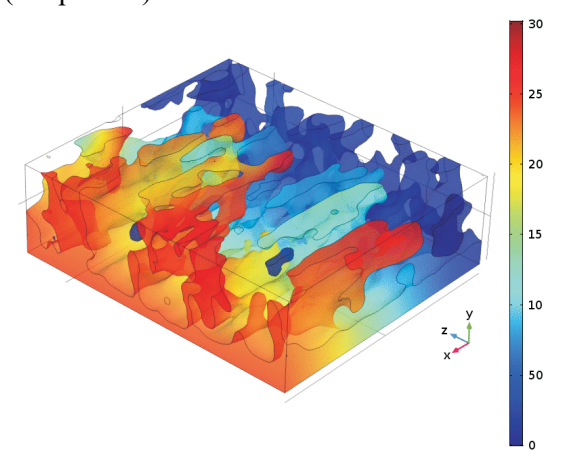


Fig. 2. Fluid velocity magnitude (µm/s) at micro level domain (Fig. 1) at 1 Hz for deformation on x-axis for 3D printed titanium.

DISCUSSION & CONCLUSIONS: At micro level, for 3D printed titanium there is expected a wide dispersion of generated fluid velocities, and cells attached to this surface will also have more dispersion of the biomechanical cues these cells will be sensing. There could be also noticeable differences in mechanical properties of conventional and 3D printed Ti, needed an assessment for correct design of implants.

ACKNOWLEDGEMENTS: This project has received funding from the European Union's Horizon 2020 research and innovation programme under grant agreement No 760921 "PANBioRA".

REFERENCES: [1] J. Biomech. 30 (1997), 539-548.

Miniaturizing High Frequency Mechanical Vibrator for Live Cell Microscopy

H. Halonen¹, J. A. K. Hyttinen¹, T. O. Ihalainen¹

¹Faculty of Medicine & Health Technology, Tampere University, Tampere, FI

INTRODUCTION: Mechanical environment has important role in directing cellular processes, and thus tissue homeostasis [1]. We directed differentiation of mesenchymal stem cells to bone cells with high frequency (HF) mechanical vibration in combination with osteogenic supplements [2]. However, a deeper understanding of the mechanocoupling of the stimulus is needed to utilize the method more efficiently. Therefore, we have developed for the purpose a miniaturized stimulator, which combines the mechanical vibration and live cell imaging [3].

METHODS: We designed the stimulator to be commercial microscope unit -compatible (ZEISS LSM 780 LSCM). A commercial speaker (Partco) was utilized as the linear actuator of the 3D printed stimulator (Fig. 1). (i.materialise) We measured accelerations (3-axis, ADXL325) of the sample vehicle to test device performance in 37 °C at 30-200 Hz frequencies (n=2). Accuracy and precision of the HF vibration (0.5 G_{peak} , 30/60 Hz) were tested by measuring accelerations (n=6). Effects to sample (Au-printed line, Frame rate: 265 FPS; living epithelial cells, 2.1 FPS) locations were tested with imaging time lapses (25x/0.8Im Korr DIC UV M27, Carl Zeiss AG) [3].

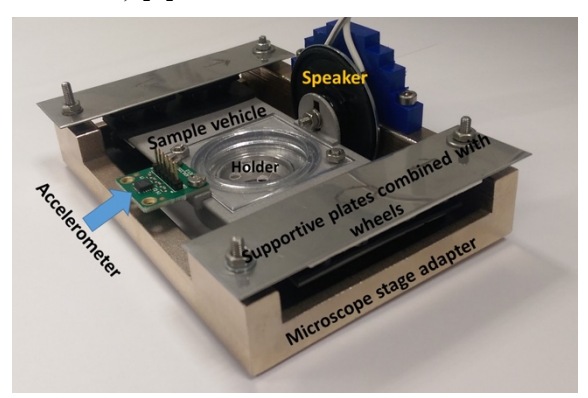


Fig. 1: Sample vehicle moves according to speaker on the microscope stage adapter. Holder accepts commercial cell chambers.

RESULTS: The stimulator performance range was 30-70 Hz, on which even high magnitudes $(G_{\text{peak}} \ge 1 G_{\text{peak}})$ horizontal stimulation could be reached (30-50 Hz). The HF vibration was

accurately and precisely produced, as demonstrated both by the acceleration measurement and the real-time imaging. The image field was adequately maintained during the stimulation bouts (Fig. 2). [3]

Real-time imaging of sample movement Observing live cell responses Omin HF (0.5 Gpeak, 30 Hz) vibration of Au-line Of epithelial cells (MDCKII)

Fig. 2: Representative light microscopy images of sample movement (left) and imaging of fast cellular responses to the stimulus (right).

DISCUSSION & CONCLUSIONS: Our miniaturized stimulator is user-friendly and easily transportable. It is applicable for studying varying mechanobiology -related research questions. The current design enables us to observe chronic cellular responses (e.g. Ca²⁺ responses, morphological and localization changes of cellular structures). In order to observe immediate cellular responses we will replace the linear actuator and design the vehicle to enable even higher magnitudes. In the future, gas exchange of the sample will be controlled with a portable cell incubation chamber, enabling to observe stimulation responses more reliably [4].

ACKNOWLEDGEMENTS: Financial support from City of Tampere, Instrumentariumin tiedesäätiö s.r. foundation, Finnish Cultural Foundation (The Kainuu Regional Fund), and the Finnish Academy of Science and Letters (Väisälä Foundation), and the Central Finland Regional Fund are acknowledged.

REFERENCES: [1] Paluch et al. 2015. BMC Biol. 13:47. [2] Tirkkonen et al. 2011. J. R. Soc. Interface. 8:736-47. [3] Halonen et al. 2019. Proc. IFMBE (accepted), Springer Nature. [4] Kreutzer et al. 2017. J. Neurosci. Methods. 280:27-35.

Polycaprolactone Nanofibres as a Novel Drug Delivery System for Osteogenic/Chondrogenic Differentiation of Human MSCs

J. Hlinkova¹, V. Blahnova¹, R. Divin^{1,2}, S. Burysova¹, K. Vocetkova¹, E. Filova^{1,2}

¹Department of Tissue Engineering, Institute of Experimental Medicine of Czech Academy of Sciences, Prague, CZ, ²Second Faculty of Medicine, Charles University in Prague, Prague,

INTRODUCTION: Bone and cartilage formation occur through transforming growth factor beta (TGF- β) and bone morphogenetic protein (BMP) signalling pathway (1). The work presented here compares development of human mesenchymal stem cells (hMSCs) to cartilage promoted by TGB- β and basic fibroblast growth factor (bFGF), and to bone promoted by bone morphogenetic protein 2 (BMP-2).

METHODS: hMSCs were cultured poly-ε-caprolactone (PCL) nanofibrous scaffolds for 28 days. Each scaffold was prepared by the method of electrospinning from 24% PCL 45 kDa, 0.2 mg/ml hyaluronic acid 500-750 kDa and 1% Synperonic® PE. 3.5 mg/ml Insulin Actrapid was added in chondrogenic group. Growth factors (GF) were added in concentrations as follows: 0.4 µg/ml bFGF, 0.04 μg/ml TGF-β1, 2 μg/ml BMP-2. αMEM (10% fetal bovine serum, 1% penicillinstreptomycin and 50 µg/ml ascorbate-2phosphate) was used as cultivation medium while 10 mM glycerol-2-phosphate was added for promotion of osteogenic differentiation. Scaffolds without growth factors were used as control groups with respective cultivating medium. Analysis of hMSCs cultures included measurement of the metabolic activity (MTS), DiOC staining for cell visualization, Alizarin Red S staining (ARS) for calcium deposit detection and type II collagen staining.

RESULTS: hMSCs proliferated well in all types of scaffolds with used media according to both MTS and DiOC staining methods. Cell metabolic activity was comparable with tissue culture polystyrene and was highest on day 21. Cell density was growing and spreading evenly from day 7. Calcium deposits were intense in a group with PCL - BMP-2 osteogenic medium, and in PCL with osteogenic medium compared to negative chondrogenic and both control groups on day 7.

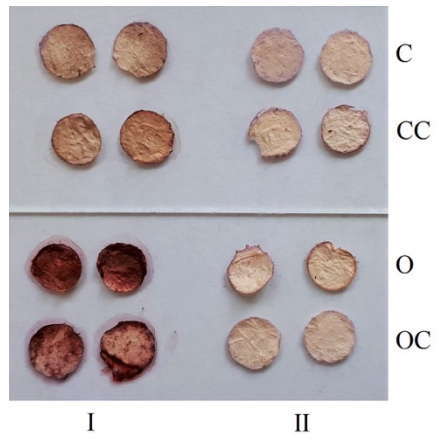


Fig. 1: Calcium deposits in hMSCs stained by ARS method on day 7. I C – chondrogenic medium with TGF- β /bFGF, CC – chondrogenic medium, O – osteogenic medium with BMP-2, OC – osteogenic medium. II cell- free control groups in corresponding media

DISCUSSION & CONCLUSIONS: growth factors were successfully encapsulated in PCL nanofibers. Our results indicate that BMP-2 protein bound to 24% PCL promotes bone differentiation of hMSCs if cultivated in αMEM enriched by ascorbate-2-phosphate and glycerol-2-phosphate, while chondrogenic medium combination in with TGFβ/bFGF/insulin encapsulated in PCL does not lead to calcium incorporation but is positive for type II collagen.

ACKNOWLEDGEMENTS: This project was funded by Ministry of Education, Youth and Sports of the Czech Republic, project NPU I: LO1309 and LO1508, by Charles University Grant Agency No. 448218, and 512216.

REFERENCES: [1] Li X., Su G., Wang J., Zhou Z., Li L., Liu L., Guan M., Zhang Q., Wang H. (2013): Exogenous bFGF promotes articular cartilage repair via up-regulation of multiple growth factors. Osteoarthritis Cartilage, 21(10):1567-75. doi: 10.1016/j.joca.2013.06.006.

3D Layered Fibre-Hydrogel Composite Scaffold for *in vitro* Neural Applications

L. Honkamäki¹, T. Joki¹, L. Ylä-Outinen¹, S. Narkilahti¹

¹ NeuroGroup, BioMediTech, Faculty of Medicine & Health Technology, Tampere University, Tampere, FI

INTRODUCTION: Neural tissue engineering aims to development of functional substitutes that mimic neuron's natural microenvironment and offers physical support for the cells. Ability to control neuronal growth into the certain direction opens new possibilities to treat defected tissue in central nervous system in the future. Especially in 3D systems this has turned out to be challenging. Here, we describe a method to create three-dimensional (3D), layered fiber-hydrogel scaffold for in vitro cell culture by combining electrospun, aligned oriented poly (D,L-lactide) (PLA) fibers (Grigoryev and Levon 2018) and collagen hydrogel. The aim of the work is to study alignment of neuronal cells in 3D hydrogel.

METHODS: In this work 3D composite scaffold was created by novel method of alternating in situ electrospinning of aligned oriented PLA fibers and cell laden collagen hydrogel gelation (Figure 1A). Cultured cells were human pluripotent stem cell (hPSC) neurons. Diameter and derived surface topography of the fibers were studied using microscope scanning electron (SEM). Expression of neuron specific marker were immunocytochemical investigated using staining. Scaffolds were imaged using confocal microscope.

RESULTS: Optimization of the electrospinning process has been successfully performed. We have cultured hPSC derived neurons on aligned oriented fiber layer for two weeks. Our results indicate the ability to guide neuronal orientation in relation to fiber orientation (Figure 1B and 1C).



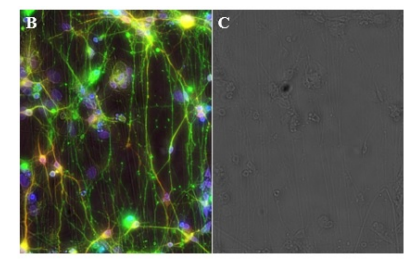


Fig. 1: A) Schematic image of layered fibre-hydrogel composite scaffold. B) hPSC derived neurons cultures on 2D fiber layer. C) Phase contrast image of fiber layer presented in image B).

We have managed to construct layered structures of two fiber layers and two hydrogel layers. We have also managed to produce fluorescent PLA fibers in order to help analysing 3D layered structure of the scaffold.

DISCUSSION & CONCLUSIONS: We successfully prepared 3D layered fiber-hydrogel scaffold for neural cell orientation. *In situ* electrospinning enables us to spin fibers on freshly gelated, cell laden collagen hydrogel, therefore bringing fibers and cells to closer contact to each other.

ACKNOWLEDGEMENTS: This work was funded by Academy of Finland Center of Excellence in Body-on-Chip research 312409 and 312414.

REFERENCES: [1] N. A. Grigoryev and K. Levon (2018). Novel Method of Electrospinning; Rotating Dual Electrode Collector Design. Journal of Microelectrochemical Systems, Vol. 27, No. 2.

Gamma-Irradiation of Decellularized Porcine Corneas Reduced the Proinflammatory Response in Human Whole Blood

R. Islam¹, M. M. Islam², P. H. Nilsson^{1,3}, K. Thorvaldsen Hagen⁴, M. Gonzalez-Andrades^{2,5}, T. E. Mollnes^{1,6,7,8,9}

¹Department of Immunology, Oslo University Hospital/University of Oslo, Oslo, NO,

²Massachusetts Eye & Ear & Schepens Eye Research Institute, Department of
Ophthalmology, Harvard Medical School, Boston, MA, USA; ³Linnaeus Centre for
Biomaterials Chemistry, Linnaeus University, Kalmar, SE, ⁴Department of Pathology, Oslo
University Hospital/University of Oslo, Oslo, NO, ⁵Maimonides Biomedical Research
Institute of Cordoba (IMIBIC), Department of Ophthalmology, Reina Sofia University
Hospital & University of Cordoba, Cordoba, ES, ⁶K. G. Jebsen Inflammatory Research
Center, University of Oslo, Oslo, NO, ⁷Research Laboratory, Nordland Hospital, Bodo, NO,
⁸Centre of Molecular Inflammation Research, Norwegian University of Science &
Technology, Trondheim, NO, ⁹Faculty of Health Sciences, K. G. Jebsen Thrombosis Research
& Expertise Center, University of Tromsø, Tromso, NO

INTRODUCTION: To meet the increasing demand of donor corneas to treat blindness, xenotransplantation of porcine corneas to human recipients appeals as a promising procedure. The innate immune system is a substantial barrier for graft acceptance in the xenotransplantation situation. Data from non-human primates showed that rejection of xenotransplanted cornea was mediated by the complement system¹. Here, we assessed acute host inflammatory response in human whole blood to native, decellularized and gamma-irradiated decellularized porcine cornea.

METHODS: Human whole blood, anticoagulated with the thrombin inhibitor lepirudin, was incubated at 37°C with three groups of differently treated corneas: A) native porcine cornea (NPC); B) decellularized porcine cornea (DPC); C) gamma irradiated decellularized porcine cornea (g-DPC). Complement activation was evaluated after incubation for one hour and cytokine levels after four hours. Complement activation was assessed by measuring soluble plasma C4b/c and C3b/c fragments, and the soluble terminal C5b-9 complement complex (sC5b-9) using ELISA. Cytokines were measured in plasma using a multiplex based 27-plex assay.

RESULTS: All the corneas activated complement and induced cytokine release. Proinflammatory cytokines including IL-1 β , IL-6, IL-8, MIP-1 α and MIP-1 β were elevated in response to all three cornea groups. The elevated release of all aforementioned cytokines was significantly higher by DPC compared to NPC. Among these g-DPC-induced release of

IL-1 β and MIP-1 β were significantly lower than the release induced by DPC. For IL-8, and MIP-1 α , g-DPC and NPC groups were comparable. Only IL-6-release by g-DPC were significantly higher than the release by NPC.

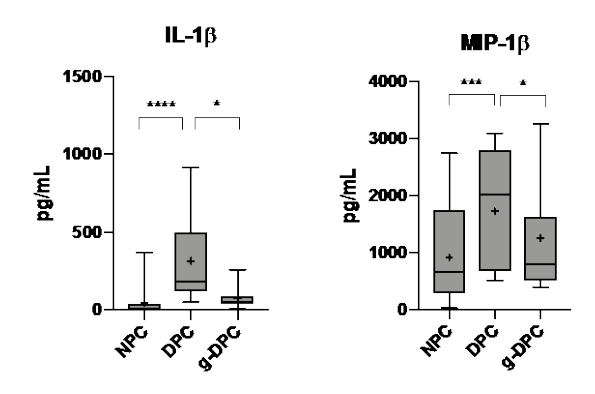


Figure: Effect of differently treated porcine corneas (NPC, DPC, g-DPC) on the IL-1 β and MIP-1 β release in human whole blood.

DISCUSSION & CONCLUSIONS: Porcine cornea led to increased release of proinflammatory cytokines when in contact with human whole blood. The magnitude of cytokines overall suggests that the gamma irradiation renders the decellularized cornea from pro-inflammatory to less proinflammatory implants.

REFERENCES: [1] Oh, J. Y. *et al.* Complement depletion with cobra venom factor delays acute cell-mediated rejection in pig-to-mouse corneal xenotransplantation. *Xenotransplantation* 17, 140-146, doi:10.1111/j.1399-3089.2010.00574.x (2010).

Platelet Derived Growth Factors Incorporation into Nanofibers for Skin Tissue Engineering

V. Jencova¹, B. Koprivova¹, K. Solarska-Sciuk⁴, K. Strnadova¹, R. Prochazkova³

¹Technical University of Liberec, Liberec, CR, ²Wroclaw University of Environmental and Life Sciences, Wroclaw, PL, ³Regional Hospital in Liberec, Liberec, CR

INTRODUCTION: As polymeric fibrous scaffold fabrication techniques strive to create structures that more closely replicate tentative extracellular matrix form and function, the need for increased scaffold bioactivity becomes more pronounced. The fibrous structure made from biocompatible and nontoxic polymers ensures mechanical stability, however cell proliferation requires further stimulation. Platelet-rich plasma, which has been shown to contain over 300 bioactive molecules, has the potential to deliver a combination of growth factors (GFs) and cytokines capable of stimulating cellular activity. The presented work deals with the preparation of nanofibrous materials with platelet growth factors incorporated into the internal fiber structure. Polyvinyl alcohol (PVA) was used for the preparation a material providing a progressive release of native GFs without need of subsequent crosslinking.

METHODS: Materials were prepared from PVA (Mw 125 000, 98% of hydrolysis) using electrospinning technology (NanospiderTM 1WS500U). Platelet lysate (PL) was prepared from thrombocyte rich solution (obtained from regional hospital in Liberec, the concentration of 700-900 x106 PLT/ml, freeze-thaw method with subsequent centrifugation). Nanofibers were electropsun from 10% PVA solution using water: ethanol (8:2) solvent system. Materials with proteins were electrospun from solution containing 10% of PVA and 10% of PL. Morphological analysis was performed by scanning electron microscopy. Protein release was monitored using spectrophotometry method) and chromatography. (Bradford Nativity of incorporated proteins was measured using enzyme model - horse radish peroxidase (HRP).

RESULTS: The prepared fibrous materials consisted of random oriented end-less fiber with smooth surface with minimal defects in structure (Fig. 1). The morphology of materials was not altered by the addition of proteins. The average fiber diameter was: 340 ± 120 nm for pristine PVA fibers and 350 ± 148 nm for PVA

with incorporated proteins (PVA/PL). PVA/PL layers contain 5-10 mg of protein per gram of PVA. 60% of the proteins are released during the first day (burst release) followed by a gradual release of up to 2 weeks. The HRP enzyme assay confirmed that there was no loss of protein activity.

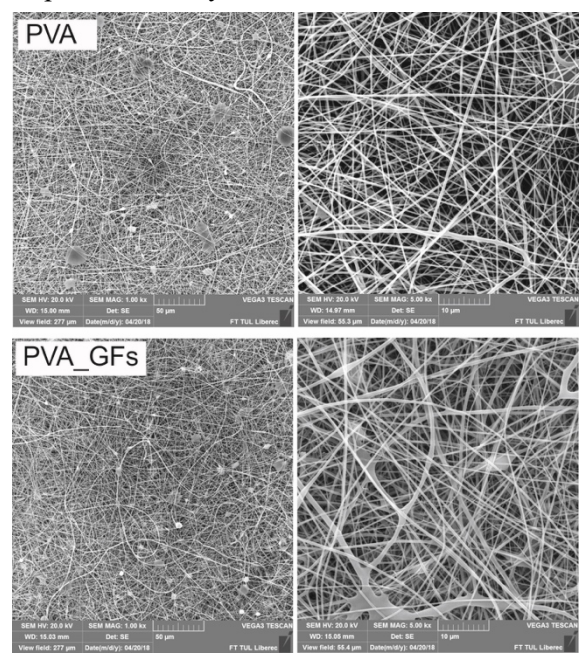


Fig. 1: SEM pictures of nanofibrous materials: pristine PVA (PVA) and PVA with incorporated proteins (PVA_GFs). Magnification 1000x and 5000x.

DISCUSSION & CONCLUSIONS:

Nanofibrous PVA-based nanofiber materials were prepared with native growth factors. The process used for the preparation of solutions and subsequent spinning does not affect the activity of the incorporated proteins, which are being gradually released. Therefore, we believe that the developed material has great potential for use in tissue engineering e.g. to promote healing of chronic wounds.

ACKNOWLEDGEMENTS: Supported by the Czech Health Research Council, project No NV18-01-00332.

Human Pluripotent Stem Cell Derived Neural 3D Cultures: Building Neural Tissue Block for Body-on-a-Chip Platform

T. Joki¹, V. Harju¹, L. Ylä-Outinen¹, J. Koivisto², J. Karvinen², M. Kellomäki², S. Narkilahti¹ NeuroGroup, BioMediTech, Faculty of Medicine & Health Technology, Tampere University, Tampere, FI, ² Biomaterials & Tissue Engineering Group, BioMediTech, Faculty of Medicine & Health Technology, Tampere University, Tampere, FI

INTRODUCTION: The brain tissue, like many other tissues, is highly organized 3D structure with specific functionality (Murphy et al., 2017). Sophisticated 3D models (organ-on-chip -models) utilize native extracellular matrix (ECM) –mimicking biomaterials as scaffold to support tissue specific functionality *in vitro* (Murphy et al., 2017). Hydrogels as biomaterials are soft tissue ECM mimicking (Koivisto et al., 2017) and thus prominent scaffold material for brain organ-on-chip – models.

METHODS: Human neural cells used in this study were in-house differentiated from either human embryonic stem cells (hESCs) or human induced pluripotent stem cells (iPSCs). Cells were maintained and cultured in hydrogels according to previously published protocol (Ylä-Outinen et al., 2014). Hydrogels used were either commercial; PuraMatrix (Corning), Rattail collagen 1 (A1048301, GIBCO) and GrowDex (UPM) or hydrogels obtained from Prof. Kellomäki; Gellan gum and hyaluronic acid - poly(vinyl)alcohol. Hydrogels and neuronal cultures were evaluated using four different indexes: Gel performance index, Gel mechanical properties index, Neurite spreading index and Cell adhesion index (NCAM, Integrin, vinculin).

RESULTS: We found that the mechanical properties of the scaffold material did not always correlate with neural cell growth and network formation indexes inside the scaffold. We found that HA-PVA and collagen 1 both have good properties as a scaffold material and that composite hydrogel from those two (HA-PVA-collagen 1) was able to combine those good properties in one hydrogel (Fig.1).

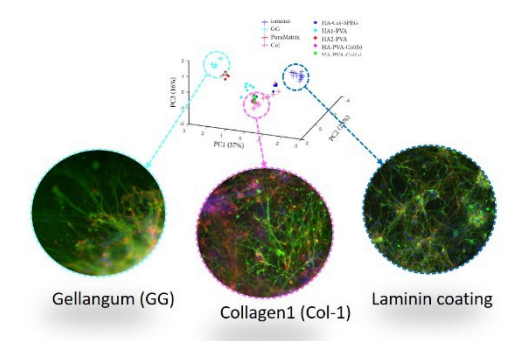


Fig. 1: PCA results from different scaffold materials.

DISCUSSION & CONCLUSIONS: Our results suggest that both the choice of cells and the choice of analysis methods have effect on which material has the best performance. Also, the usability of the biomaterial and reproducibility of the cultures are important aspects to take into account when building brain organ-on-chip—models.

ACKNOWLEDGEMENTS: This work was funded by TEKES (the Finnish Funding Agency for Innovation) Human Spare Parts project, the Finnish Cultural Foundation grant numbers 00140325 and 00150312, the Academy of Finland grant number 286990, and Academy of Finland Center of Excellence in Body-on-Chip research 312409 and 312414.

REFERENCES: [1] Murphy, A. R. et al. (2017) 'Scaffolds for 3D in vitro culture of neural lineage cells', Acta Biomaterialia. Acta Inc., pp. 1–20. Materialia 54, 10.1016/j.actbio.2017.02.046. [2] Koivisto, J. T. et al. (2017) 'Bioamine-crosslinked gellan gum hydrogel for neural tissue engineering', Biomedical Materials, 12(2), pp. 1–38. doi: 10.1088/1748-605X/aa62b0. [3] Ylä-Outinen, L. et al. (2014) 'Three-dimensional growth matrix for human embryonic stem cell-derived neuronal cells.', Journal of tissue engineering and regenerative medicine, 8(3), pp. 186-94. doi: 10.1002/term.1512.

Bacterial Attachment to Nanostructured Surfaces

P. Kallas¹, H. Valen², M. Andersson³, H. J. Haugen¹, M. Hulander³

¹Department of Biomaterials, Institute of Clinical Dentistry, University of Oslo, Oslo, NO, ² Nordic Institute of Dental Materials, Oslo, NO, ³ Department of Chemistry & Chemical Engineering, Chalmers University of Technology, Gothenburg, SE

INTRODUCTION: Oral cavity is populated by more than 700 prokarvote species. Some of them play no significant role in our daily life, but presence of the others may lead to gum disease, such as periodontitis, or tooth decay, which could result in tooth replacement with implant1. That gives bacteria opportunities to colonize new areas (surface of the implant) and as a result - infect host's body2,3. Nowadays, many implants are coated with nanoparticles, which might present different properties, such as antimicrobial activity. The influence of distance between nanoparticles on bacteria adhesion is not well known yet.

METHODS: Our experiments aim at characterizing attachment of bacteria present in oral cavity (Streptococcus mitis) and those that are prevalent species associated with infections of medical devices (Staphylococcus aureus and Staphylococcus epidermidis) to surfaces coated with nanoparticles and observing whether the distance between the nanoparticles has any significant influence on bacterial adhesion. Nanostructured surfaces were fabricated by functionalizing substrates. so negatively charged nanoparticles could attach to them. To perform bacterial studies within a single experiment, nanoparticle gradients formed. The gradients have been characterized by using scanning electron microscopy (SEM). Bacteria were injected on the nanostructured surfaces with dynamic flow. Number of bacteria attached to the surface was calculated using ImageJ.

RESULTS: The nanoparticle gradients were obtained. The change of density and distribution of nanoparticles is presented on *Fig. 1*. We could observe that the density of nanoparticles is gradually changing over a given distance. Adhesion time was set for 5 minutes, and during attachment to the gradients different behaviour was observed between tested bacteria species.

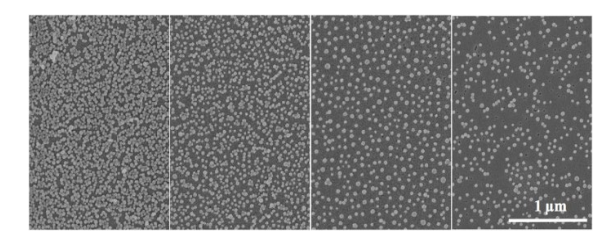


Fig. 1: SEM images of nanoparticle gradient.

DISCUSSION & CONCLUSIONS: Three different types of bacteria were tested towards their ability to attach to nanostructured surfaces. The differences observed between their attachments could lead us to the conclusion that distribution of nanoparticles has influence on bacterial adhesion to nanocoated surfaces. Future tests will be focused on ability to form biofilms on presented surfaces.

REFERENCES: [1] Aas JA, Paster BJ, Stokes LN, Olsen I, Dewhirst FE. Defining the Normal Bacterial Flora of the Oral Cavity. J Clin Microbiol, Nov 2005, 43(11): 5721–5732. [2] Buddula A. Bacteria and dental implants: A review. Journal of Dental Implants, Jan-Jun 2013, Vol 3, Issue 1. [3] Shahabouee M, Rismanchian M, Yaghini J, Babashahi A, Badrian H, Goroohi H. Microflora around teeth and dental implants. Dental Research Journal, Mar 2012, Vol 9, Issue 2.

Mechanical Studies of Hydrazone Crosslinked Hyaluronan-Polyvinyl Alcohol-Based Hydrogels intended for 3D Neuronal *in vitro* Applications

J. Karvinen¹, L. Ylä-Outinen², V. Harju², T. Joki², J. T. Koivisto¹, S. Narkilahti², M. Kellomäki¹

¹Biomaterials & Tissue Engineering Group, BioMediTech, Faculty of Medicine & Health Technology, Tampere University, Tampere, FI, ²NeuroGroup, BioMediTech, Faculty of Medicine & Health Technology, Tampere University, Tampere, FI

INTRODUCTION: The mechanical properties and structural parameters of hydrogels have shown to play important roles when designing hydrogel-based materials for different cell applications. In this work, the mechanical properties and structural parameters (the average mesh size, the average molecular weight of the polymer chain between neighboring crosslinks, and the crosslinking density) were determined for hydrazone crosslinked hyaluronan (HA)-polyvinyl alcohol (PVA)-based hydrogels (with or without collagen I) intended for 3D neuronal in vitro applications. These HA-PVA hydrogels have already shown their potential as 3D scaffolds for human pluripotent stem cell-derived neuronal cells [1].

METHODS: Hydrazone crosslinked HA-PVA hydrogels were fabricated from aldehyde- and hydrazide-modified polymer components [1]. Collagen I was added as a physical mixture. Compression tests were performed using a BOSE Electroforce Biodynamic 5100 machine equipped with a 225 N load sensor and Wintest 4.1 software (Bose Corporation, Eden Prairie, Minnesota, USA). Results were compared with previously measured brain tissue data [1,2]. Rheological measurements were conducted using a Discovery Hybrid Rheometer 2 equipped with a TRIOS software (TA Instruments, New Castle, DE, USA). The structural parameters of hydrogels were calculated according to [3].

RESULTS: Since the elastic portion of the stress-strain curve of hydrogels and tissues is non-linear, linear fit cannot be used. Instead, polynomial fit-based method [2] was used, and the stiffness-strain curves (Fig. 1) were shown for the hydrogels instead of giving only one value. The stiffness of hydrogels was close to that of brain tissue at small strains, but was different at higher strains. The rheological tests (amplitude, frequency and time sweeps, and repeated creep) were conducted in DMEM at

37°C in order to mimic the cell culture environment. Hydrogels showed typical gel behaviour. The time dependent behaviour showed some small changes in the storage and loss moduli. The structural parameters showed typical values compared with similar hydrogels. The addition of collagen was shown to affect to the mechanical properties of hydrogels.

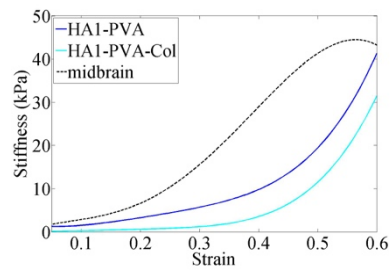


Fig. 1: Stiffness-strain curves of HA-PVA-based hydrogels and midbrain tissue.

DISCUSSION & CONCLUSIONS: The mechanical properties and structural parameters of HA-PVA-based hydrogels were affected by the addition of collagen. A difference seen in the cell test results of these hydrogels can be explained with the cell favourable properties of collagen, but also partly with the differences seen in the mechanical properties and porosity.

ACKNOWLEDGEMENTS: This work was funded by Business Finland (Human Spare Parts project), the Finnish Cultural Foundation grant numbers 00140325 and 00150312, the Academy of Finland grant number 286990 and Academy of Finland Center of excellence grant 312409.

REFERENCES: [1] J. Karvinen, et al., React. Funct. Polym. 124, 29–39, (2018). [2] J. Karvinen, et al., J. Mech. Beh. Biomed. Mat. 71, 383-391, (2017). [3] J. Karvinen, et al., Mater. Sci. Eng. C 94, 1056-1066 (2019).

Gellan Gum Hydrogel Compression Testing Combined with Digital Image Correlation

J. T. Koivisto^{1*}, J. Nafar Dastgerdi^{2*}, O. Orell³, M. Kanerva³, M. Kellomäki¹

¹Biomaterials & Tissue Engineering Group, BioMediTech, Faculty of Medicine & Health Technology, Tampere University, Tampere, FI, ²Department of Mechanical Engineering, School of Engineering, Aalto University, Espoo, FI, ³ Laboratory of Materials Science, Faculty of Engineering & Natural Sciences, Tampere University, Tampere, FI

INTRODUCTION: When developing scaffold materials for tissue engineering (TE), one important aspect is producing mechanically biomimicking materials. The stiffness affects cell response via mechanotransduction and can, for example, enhance stem cell differentiation into wanted lineage. However, the current field of hydrogel design and production is lacking standardized methods to reproducibly test the materials. To study in detail the response of a hydrogel to compression, we combined threedimensional digital image correlation (3D-DIC) technique [1] with compression testing to describe the true stress-strain curve. We used bioamine crosslinked gellan gum (GG) as model hydrogel in the study [2].

METHODS: All materials acquired from Sigma Aldrich. GG hydrogels crosslinked with 1.1 wt-% spermine were prepared according to a previously published protocol [2]. Compression testing was done using Bose Electroforce BioDynamic 5100 machine (TA Instruments, MN, USA). 3D-DIC [1] was used with two simultaneously recording cameras (5Mpix Imager E-Lite, LaVision, Germany) to obtain surface deformation map of the sample (Fig.1).

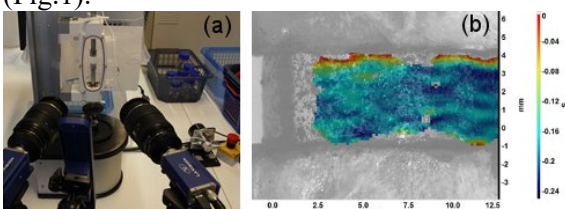


Fig 1. (a) The 3D-DIC test set up, (b) strain field on hydrogel surface measured with the 3D-DIC.

The sample deformation is analysed as Cauchy stress and logarithmic (or Hencky) strain obtained from the engineering stress and strain according to the following equations, respectively [3]:

$$\sigma^{c} = \sigma^{eng}(1 + \varepsilon^{eng})$$
 and
$$\varepsilon^{n} = \ln(1 + \varepsilon^{eng})$$

RESULTS: The 3D-DIC data shows real deformation of the hydrogel during testing (Fig. 2.). Based on the observed bilinear elastic deformation, we defined two elastic moduli for the hydrogel, initial 'toe-region' modulus E_1 and second elastic modulus E_2 .

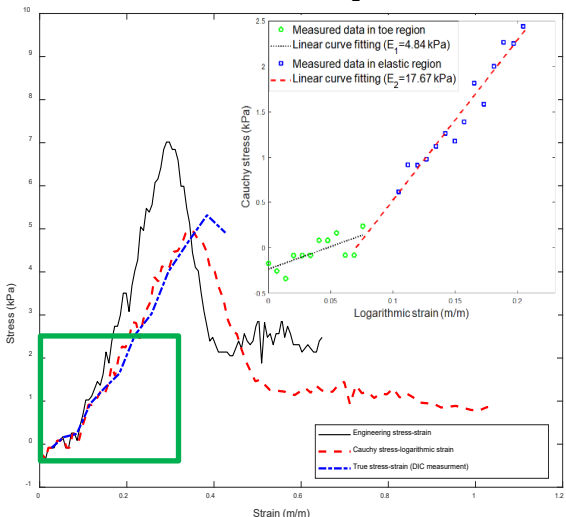


Fig. 2: Comparison of Cauchy stress—Hencky strain curve with engineering stress-strain curve & 3D-DIC measured true stress-strain. Magnified green rectangle depicts determination of first & second elastic modulus.

DISCUSSION & CONCLUSIONS: We propose hydrogel compression characterization in two-phase format for more accurate determination of the elastic moduli and representation of stiffness. This is more similar to real tissue, which has two-phase elastic response as well, and the method also clarifies the determination of elastic region.

ACKNOWLEDGEMENTS: The authors would like to thank Business Finland projects 'Human Spare Parts' & 'LuxTurrim 5G' and the Finnish Cultural Foundation Pirkanmaa Regional Fund for funding this research.

REFERENCES: [1] Palanca,M., et al, Int. (1) Biomech. **3**: 1-21 2016. [2] 2. Koivisto,J.T., et al, Biomed. Mater. **12**: 025014 2017. [3] 3. (2) Xiao,H., et al, Acta Mech. **168**: 21-33 2004.

Solid-State NMR Spectroscopy as a Tool for the Analysis of Calcium Phosphate Biomaterials

J. Kolmas¹, K. Pajor¹, Ł. Pajchel¹

¹Department of Analytical Chemistry & Biomaterials, Analytical Group, Faculty of Pharmacy with Laboratory Medicine Division, Medical University of Warsaw, Warsaw, PL

INTRODUCTION: Characterization modern biomaterials requires the use of various analytical methods, such as powder X-ray diffractometry, electron microscopy, infrared and Raman spectroscopy, atomic absorption spectrometry or inductively coupled plasma – spectrometry. Solid-state magnetic resonance (ssNMR) is a powerful spectroscopic tool for structural analysis of crystalline and amorphous materials [1]. In this project we used ssNMR spectroscopy for physicochemical analysis of calcium phosphatebased materials (CaPs). CaPs with the main representative hydroxyapatite commonly used as bone substitutes, bone cements and implant coatings [2]. In our research, we were focused on synthetic CaPs modified with various ions as well as commercial CaP biomaterials of porcine origin.

METHODS: "Pure" and substituted synthetic CaPs were prepared using two different ways: standard precipitation and solid-state methods. Various materials enriched in manganese (Mn²⁺), selenium (SeO₃²⁻ and SeO₄²⁻), silicon (SiO₄⁴⁻), zinc (Zn²⁺), carbonates (CO₃²⁻) or silver (Ag⁺) were obtained. Commercial samples were purchased from Tecnoss® Dental. The materials were investigated using several NMR techniques: Bloch-decay (BD), conventional cross polarization (CP – 1 H \rightarrow ^XY), inverse CP (X Y \rightarrow ¹H) and CP kinetics.

RESULTS: ¹H MAS NMR studies of selenium enriched HA shown significant dehydroxylation of HA during the selenites or selenates substitution (Fig.1). For biological samples containing organic matrix, the calculation of structural OH groups content was possible by using inverse ³¹P \rightarrow ¹H technique [3]. For Zn²⁺ containing HA and brushite, the crystallinity was study by using ³¹P BD and CP experiments. Silicates and carbonates in HA were located in the crystal interior and on the crystal surface (hydrated surface layer). For Mn-HA the location of Mn in Ca(I) and Ca(II) sites was detected by ¹H \rightarrow ³¹P CP MAS kinetics [4].

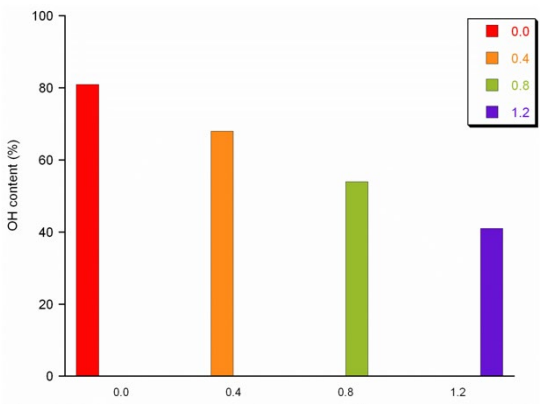


Fig. 1: Structural hydroxyl group content in Sesubstituted HAs x_{Se} =0.0-1.2).

DISCUSSION & CONCLUSIONS: In this study, we have presented the possibility of use ssNMR spectroscopy for CaPs structural analysis. Our results shown that ssNMR is a powerful method for both synthetic and biological samples. Moreover, it may be useful in testing samples without need for samples pretreatment. ssNMR spectroscopy provide information about concentration of structural hydroxyl groups, location "foreign" ions or presence of different types of water. It may be a complementary tool for powder X-ray diffractometry.

ACKNOWLEDGEMENTS: This work was supported by the research program (Project UMO-2016/22/E/ST5/00564) of the National Science Center, Poland).

REFERENCES: [1] F. Pourpoint et al., J. Mater. Res. 26(18) 2355-2368 (2011). [2] A. Haider et al., RSC Adv. 7 7442–7458 (2017). [3] J. Kolmas et al., J. Pharm. Biomed. Anal. 61 136-141 (2012). [4] J. Kolmas et al., J. Am. Ceram. Soc. 98 (4) 1265–1274 (2015).

Hydroxyapatite Modified with Zn²⁺ & SeO₃²⁻ Ions: A Promising Material for Bone Tissue Engineering

A. Laskus¹, A. Zgadzaj², J. Kolmas¹

¹Department of Analytical Chemistry & Biomaterials, Analytical Group, Medical University of Warsaw, Warsaw, PL, ² Department of Environmental Health Sciences, Medical University of Warsaw, Warsaw, PL

INTRODUCTION: During the last few decades calcium phosphates (CaPs) have become one of the most frequently used biomaterials in bone tissue engineering. Their excellent biocompatibility and handiness let them be applied as bone fillers and coating materials. Among them, synthetic hydroxyapatite (HA) with the general formula Ca₁₀(PO₄)₆(OH)₂ most strongly resembles a natural, biological apatite, which builds mammalian hard tissues. There are several trends concerning CaPs-based current bioengineering. One of them is substituting CaPs with foreign ions, which could give them additional, unique properties. In this study a similar approach was made. Due to their wellconfirmed osteogenic, antibacterial anticancer activity, Zn²⁺ and SeO₃²⁻ ions were chosen to modify the crystal lattice of HA [1,2].

METHODS: In this study zinc and selenite cosubstituted HA was synthesized via a standard, wet precipitation method [3]. Different amounts of both ionic modifiers were applied. The obtained powders were diligently examined, using the following, physicochemical methods: FTIR, ssNMR, PXRD, TEM and ICP-OES. Additionally, the release kinetics tests and cytotoxicity evaluation were conducted.

RESULTS: ssNMR, PXRD and FTIR studies confirmed that the synthesized powders were homogenous HAs and did not contained other crystalline phases. What is more, the outcomes of ICP-OES analysis proved the effective incorporation of both ionic modifiers. Also, the FTIR spectrum confirmed the presence of SeO₃²- ions in the material (the band ca. 769 cm⁻¹). Both PXRD patterns and FTIR spectra showed also that the increasing content of Zn²⁺ lowers the crystallinity of synthesized material. In turn, TEM studies provided information of the morphology of the crystals (Figure 1). Crystals of all the samples were of both platelike and needle-like shape and performed strong tendency to agglomerate.

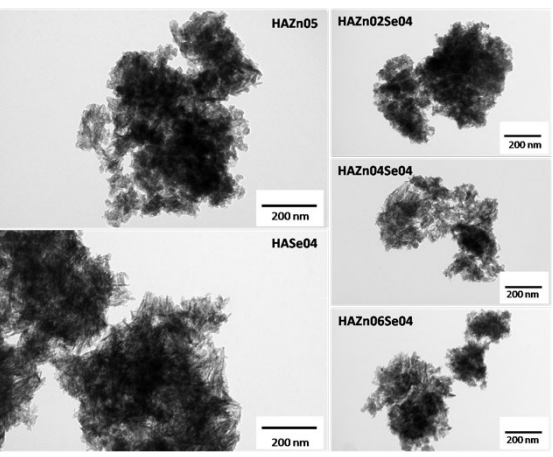


Fig. 1: TEM microphotographs of the samples.

The release kinetics tests revealed that the selenite ions were adsorbed partially on the surface of the material, which in turn affected substantially the cytotoxicity of the samples containing SeO_3^{2-} .

DISCUSSION & CONCLUSIONS:

In this study hydroxyapatite containing Zn²⁺ and SeO₃²⁻ was obtained. The physicochemical analysis proved the identity of the material and the effective incorporation of both types of ions. Studies of the release kinetics and cytotoxicity tests might be a starting point to create osteogenic and non-toxic material for future bone engineering.

ACKNOWLEDGEMENTS: This work was supported by the research program UMO-2016/22/E/ST5/00564 of the National Science Center, Poland and FW23/PM2/18 of Warsaw Medical University.

REFERENCES: [1] E. Boanini, M. Ganzano, A. Bigi., *Acta Biomater.*, 2010, 6, 1882-94. [2] M. P. Rayman, *Lancet*, 2000, 356, 233-41. [3] J. Kolmas, E. Oledzka, M. Sobczak et al., *Mat. Sci. Eng C*, 2014, 39, 134-42.

Development of Synthesis of Amorphous Calcium Phosphate With Biomimetic Chemical Composition

J. Vecstaudza¹, J. Locs¹

¹Rudolfs Cimdins Riga Biomaterials Innovations & Development Centre of RTU, Institute of General Chemical Engineering, Faculty of Materials Science & Applied Chemistry, Riga Technical University, Riga, LV

INTRODUCTION: Despite the intense efforts put towards the biomaterial design in the last decades, there still is a need for more effective bone grafts that mimic both composition and structure of human bone tissue. Up to now there are no studies about synthetic amorphous precursor phase with biomimetic elemental composition available for bone tissue engineering. Generally, amorphous structures are more susceptible to inclusion of large quantities of various ions than crystalline ones. Current work presents development of synthesis of novel amorphous calcium phosphate (ACP) nanoparticles with biomimetic bone-like chemical composition. The elemental composition of the biomimetic ACP will be composed of Ca2+, PO43-, OH-, CO32-, Mg2+, Sr²⁺, Na⁺, K⁺, Cl⁻, F⁻, Zn²⁺ and citrate ion building blocks.

METHODS: Current synthesis of biomimetic ACP is based on recently developed wet chemistry method [1]. To incorporate necessary biomimetic elements into ACP various watersoluble salts were used additionally, e.g., MgCl₂, SrCl₂, sodium citrate etc. As a reference material ACP without another ion presence was used.

Quantitatively chemical composition was determined with atomic absorption spectroscopy and titration analysis, chemical group information was obtained with FT-IR spectrometry, phase composition was determined by XRD. In addition, specific surface area, particle size and porosity were determined from BET surface area analyser.

RESULTS: It was possible to obtain nanostructured ACP with biomimetic bone-like chemical composition with specific surface area over 50 m²/g. Previous studies [1] of the reference ACP have shown that it is possible to synthesize nanosized (<20 nm) ACP with specific surface area over 150 m²/g that is stable in air for at least one year.

DISCUSSION & CONCLUSIONS:

Precipitation of ACP from ionically enriched solutions ensured obtaining of ACP with biomimetic bone-like composition. Possible crystallization of metastable ACP was hindered by the complex interplay of the many trace ions. Calcium phosphate nanostructures with the biomimetic composition will provide all the necessary preconditions for successful use in bone tissue engineering. It will guide synthesis of biological HAp *in vivo* and ensure superior bone regeneration properties.

ACKNOWLEDGEMENTS: Grant No lzp-2018/1-0238: Future of synthetic bone graft materials - *in vivo* guided biosynthesis of biomimetic hydroxyapatite, 2018-2021.

REFERENCES: [1] J. Vecstaudza, J. Locs, J. Alloy. Compd., 700 (2016), 215-222.

Hydrolytic Degradation of Polylactide/Polybutylene Succinate Blends with Bioactive Glass

I. Lyyra¹, J. Massera¹, M. Kellomäki¹

¹BioMediTech, Faculty of Medicine & Health Technology, Tampere University, Tampere, FI

INTRODUCTION: Polylactides (PLA) is an attractive polymer group for biomedical applications because they are biodegradable and can be derived from renewable resources. They are also available as purified, medical grade raw material, which shortens the time span from research to products, if such approach is desired. However, relative stiffness and slow degradation rate limit the applications. Blending with polymers with a higher degradation rate and ductility, e.g. polybutylene succinate (PBSU), the properties of PLAs can be altered.¹ One characteristic of PLA degradation is the decrease in the local pH accelerating the autocatalytic reactions. To buffer these effects, biodegradable materials with basic degradation products, like bioactive glass, can be added.² In this study, PLA and PBSU were blended and mixed with bioactive glass and characterized for their in vitro degradation properties.

METHODS: High purity, medical grade PLDLA (L/DL ratio 70/30, Evonik Nutrition and Care GmbH) and commercial grade PBSU (Showa Denko) were dried and extruded into rods (diameter approximately 2 mm). Four different types of plain polymer rods were manufactured: plain PLA, plain PBSU and two blends, one with 75 wt-% of PLA and 25 wt-% of PBSU (75/25 blend) and one with 50 wt-% PLA and 50 wt-% of PBSU (50/50 blend). In addition to these, composites with the same plain polymers and blends with 30 wt-% (15 vol-%) of bioactive glass 13-93 as 125-250 um particles were processed. In total, the current study consisted of eight different materials. The extruded rods were cut to 70 mm length samples and were immersed in phosphate buffered saline (37 °C) for 0, 3, 6, 12 and 24 weeks. Over the immersion time, changes in water absorption, mass loss and mechanical properties, as well as the pH and the ion release in the buffer solution were studied.

RESULTS: The more there was PBSU in the polymer blends, the more they absorbed water until 12 weeks. For the composites it was the opposite, the plain PLA composite absorbed more water than the blend or PBSU composites.

In general, the composites absorbed much more water than the plain polymers and blends. There was no significant change in the mass of the plain polymers and blends over 12 weeks, but the blend composites lost more mass compared to the other materials. There were no significant differences in the dimensions of the samples over 12 weeks. The mechanical properties (bending and shear stress, Young's modulus) decreased with an increase in PBSU content. Upon immersion, the plain polymers and blends exhibited no change in the mechanical properties for up to 12 weeks. The composites were more brittle compared to the plain polymers and the mechanical properties deteriorated already before 12 weeks.

DISCUSSION & CONCLUSIONS: The hydrolytic degradation properties of PLA, PBSU and their blends with and without bioactive glass were measured. As expected, adding the more hydrophilic PBSU in the hydrophobic PLA seemed to increase the hydrophilicity of the blends. The blends and the plain PBSU absorbed more water compared to the plain PLA. Introducing the bioactive glass into the material made it more brittle, accelerated its degradation and greatly increased the water absorption. Tailoring the properties of these new composite materials by changing their compositions makes them versatile materials for both soft and hard tissue engineering.

ACKNOWLEDGEMENTS: The authors would like to thank TUT Foundation and Business Finland (Human Spare Parts project) for financial support and Ms. Nina Sandberg for conducting the hydrolysis study.

REFERENCES: [1] Wang et al. Polym. Bull. (2016) 73:1067-1083. [2] Lu et al. J Biomed Mater Res A. (2003) 64:465-474.

Electroconductive Silk-Based Fibres for Peripheral Nerve Regeneration

A. Magaz^{1,2}, C. Phamornnak¹, X. Li^{2*}, S. H. Cartmell¹, J. J. Blaker¹

¹School of Materials, University of Manchester, Manchester, UK, ²Institue of Materials Research & Engineering, A*STAR, SG

INTRODUCTION: Peripheral nerve injury (PNI) alone is a cause of medical consultation in more than 1 million patients worldwide, of which around 40% cases occur in Europe. Electroconductive biohybrids based on natural proteins are emerging as functional materials to be used as scaffolds to regenerate stimuli responsive tissues [1]. They have great potential to allow direct delivery of electrical signals, being stimulatory to the tissues as well as triggering a controlled/responsive release of therapeutics [2]. Carbon based nanomaterials can provide conductive properties and may be an effective scavenger of reactive oxygen species for further neuroprotection. Herein, we assess the influence of reduced graphene oxide (rGO)-filled micro/nano- fibrous silk fibroin (SF) scaffolds for nerve regeneration.

METHODS: Nano- fibres were produced by electrospinning a 10% w/v regenerated SF solution in formic acid (FA) with incorporation of hydrazine-reduced GO at increasing concentrations (1%, 5% and 10% w/w rGO/SF). In parallel, micro- fibres were produced by spinning the silk solution in hexafluoro-2propanol (HFIP), with incorporation of GO (same amounts as above), and later reduced in L-ascorbic acid. Fibres were insolubilized in 80% v/v ethanol. Fibre morphology and structure were characterized using field electron microscopy emission scanning (FESEM), Fourier-transform infrared (FTIR) and Raman spectroscopy. Electrical properties were characterized in both dry and hydrated states using a 4-point probe. Antioxidant activity was assessed with a 2,2-diphenyl-1picryl-hydrazyl (DPPH) assay. NG108-15 neuroblastoma/glioma hybrid cells (5,000 cells/cm²) at passage number P20 – P24 were seeded onto laminin-coated fibres. Laminin adsorption, metabolic activity, cell proliferation and viability were quantified; immunofluorescence against neuronal investigated markers was via confocal microscopy.

RESULTS: Mean fibre diameter could be controlled by the choice of solvent (150 nm or 1.2 μm for FA and HFIP fibres respectively).

Fibre morphology was smoother and more consistent for those produced using HFIP with increasing (r)GO content. The overall chemical structure of the silk remained unchanged as determined by FTIR, and Raman spectroscopy presence of confirmed the the Conductivity of the membranes fibrous increased with the presence of rGO, up to 2x10⁻¹ ⁶ S/cm for FA fibres and 4x10⁻⁵ S/cm for HFIP fibres in dry state. Hydration resulted in an increase in conductivity to 1x10⁻³ S/cm and 3x10⁻⁴ S/cm, respectively. Laminin adsorption decreased (p<0.01) with incorporation of rGO in the fibres. Silk loaded rGO fibres exhibited antioxidant properties as a function incubation time. In vitro analysis showed that the presence of rGO could maintain the overall biological response of the scaffolds.

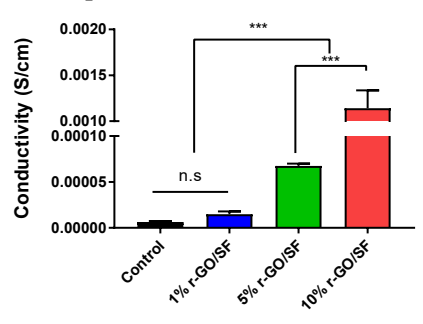


Figure 1. Conductivity of rGO/SF fibres (FA), measured in hydrated state (*** p<0.001).

DISCUSSION & CONCLUSIONS: This data illustrates the beneficial effects of developing conductive silk-based scaffolds, which could enhance electrical signal propagation in nerve tissue engineering applications.

ACKNOWLEDGEMENTS: The University of Manchester EPSRC DTP, A*STAR, and the Royal Thai Government. A. Magaz and C. Phamornnak contributed equally to this work.

REFERENCES: [1] Magaz A. et al. Adv Healthc Mater. 2018; 7, 1800308 (pp1-20). [2] Tandon B. et al. Adv Drug Deliver Rev. 2017; 129 (pp148-168).

Role of Material Characteristics in Regulating Bone Cell Differentiation

M. Nakamura¹, T. Hentunen¹, J. Salonen¹, K. Yamashita²

¹Institute of Biomedicine, University of Turku, Turku, FI, ² Institute of Biomaterials & Bioengineering, Tokyo Medical & Dental University, Tokyo, JP

INTRODUCTION: Understanding of the interaction between biomaterials and osteogenic cells may help to clarify physiologic cellular reactions between biomaterials and interface. We recently demonstrated that compared with conventional hydroxyapatite (HA), HA with charged surfaces induced by polarization treatment has enhanced osteoconductivity, protein early stage adsorption after implantation in vivo, and initial cell adhesion and migration of osteoblast-like cells. The aim of this study is to investigate a mechanism through which the wettability of biomaterials can be improved and determine the effects of biomaterial surface characteristics on cellular behaviours.

METHODS: Synthesis and characterization of biomaterials: HA and carbonate-substituted HA (CA) powders synthesized by the wet method were pressed in a mold and sintered for 2h at 1250°C and 800°C, in a saturated water vapour and carbon dioxide atmosphere, respectively. The highly crystalline HA and CA were electrically polarized with a pair of Pt electrodes in dc electric fields at 400°C. The surface characteristics, including roughness, ion content, zeta potential, surface free energy, and wettability were investigated. Cell culture: Human osteoclast progenitors isolated from peripheral blood were seeded onto the samples and cultured in osteoclast-inductive medium. The cells were fixed, and stained with tartrateresistant acid phosphate (TRAP), rhodamine phalloidin and Hoechst. Mesenchymal stem cells isolated from mouse bone marrow were seeded onto the samples and cultured in osteoblast-inductive medium. The cells were fixed and stained with alkaline phosphatase and examined by RT-PCR.

RESULTS: The surface free energy of HA and CA with electrical polarization treatment were approximately 6 and 10 times higher than that of conventional one, respectively. The contact angles of water significantly decreased on electrically polarized HA. These changes in the contact angles indicated that the wettability of the polarized surfaces was improved by the

increase in surface free energy on polarized surfaces. Osteoblast analyses revealed that osteoblast differentiation on the polarized HA was accelerated compared with that on conventional HA. Osteoclast analyses revealed that osteoclast resorption on the polarized CA was accelerated compared with that on conventional CA.

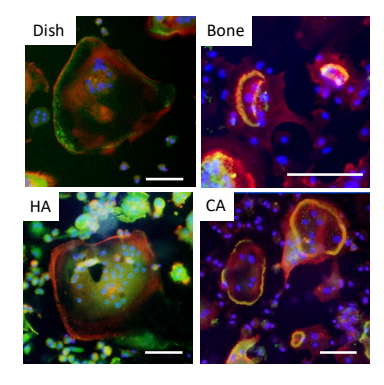


Fig. 1: Osteoclast morphologies on plastic cell culture dish, bone slices, HA and CA. Bar=100µm.

DISCUSSION & CONCLUSIONS: HA and CA have polarization capacity that increased surface free energy and improved wettability, which in turn accelerated differentiation of osteoblasts and osteoclasts.

ACKNOWLEDGEMENTS: This study was financially supported by Grants-in-Aid for the Promotion of Joint International Research (Fostering Joint International Research) (15KK0299).

REFERENCES: [1] Nakamura M, et al. Mater Sci Eng C 2016: 62, 283-292. [2] Nakamura M, et al. ACS Biomater Sci Eng 2016: 2 (2), 259-267. [3] Nakamura M, et al. Biomed. Mater 2015: 10, 011001. [4] Nakamura M, et al. J Biomed Mater Res A, 2013: 101A (11), 3141-3151.

MAS NMR Characterisation of Drug Delivery System Nano-Composite MCM-48/Hydroxyapatite Loaded with Ibuprofen

L. Pajchel¹, W. Kolodziejski¹

¹Medical University of Warsaw, Faculty of Pharmacy with Laboratory Medicine Division, Chair of Analytical Chemistry and Biomaterials, Warsaw, PL

INTRODUCTION: Sparse papers reported on composites of mesoporous molecular sieves and HAs, which combine the characteristics of both components and thus enhance usefulness of such new materials. Generally, the porous structure of silica and the biocompatibility of HA confer on their composite excellent properties for implantation and DDS [1]. It has also been suggested that the silica component plays an important role in biological mineralization processes. Additionally, the presence of silica in the HA matrix increases the bioactivity of this material. In this work, we confirmed incorporation of ibuprofen into mesopores of the HA coated molecular sieve MCM-48.

METHODS: The MCM-48/HA composite was obtained by the wet synthesis method. The MCM-48/HA/Ibu composites were prepared by soaking the MCM-48/HA powder in the different solvent solution of Ibu. The obtained composites were analysed by ¹H and ¹³C MAS NMR spectroscopy [1].

RESULTS: The comparison of the ¹H MAS NMR spectra (Fig. 1) clearly reveals specificity of Ibu introduced into the MCM-48/HA host. The spectrum of bulk, crystalline Ibu contains very broad, overlapped lines, typical of a rigid solid. In contrast, the spectra of the drug containing composites show sharp, "liquid-like" peaks of Ibu, so its molecules are very mobile inside the MCM-48/HA host matrix [1,2,3]. This in turn indicates that a considerable fraction of the adsorbed Ibu molecules resides inside the mesopores, having there enough room for dynamic motions. The ¹³C CP/MAS NMR spectra of the drug containing composites are dominated by the Ibu peaks. Especially indicative are signals at 17 and 30 ppm from the C11 and C8 carbons, respectively. Their positions are particularly dependent on the drug location in the MCM-48/HA matrix.

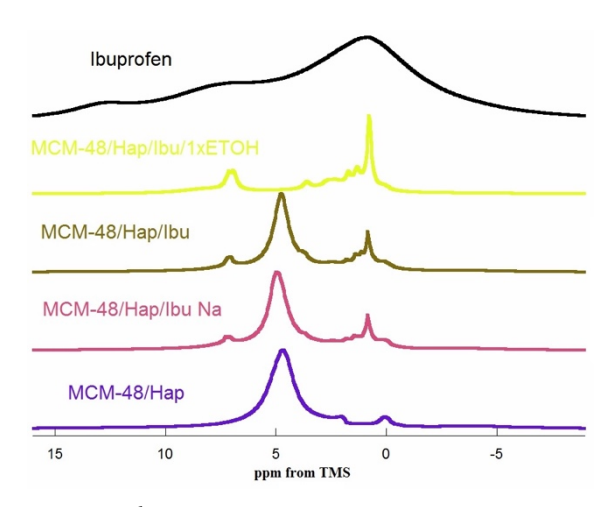


Fig. 1: ¹H MAS NMR spectra of pure Ibu, MCM-48/HA/Ibu/IxETOH, MCM-48/HA/IbuNa(H2O) and MCM-48/HA.

DISCUSSION & CONCLUSIONS: The 1H and ¹³C CP/MAS spectra of the drug loaded samples clearly confirmed the incorporation of Ibu into mesopores when compared to the bulk Ibu spectra. The Ibu deposition on the external surface was best achieved from NMP. The highest Ibu concentration in the MCM-48/HA/Ibu conjugate was obtained from NMP, in which the Ibu solubility is the best. Further studies, involving blocking of mesopores entrances by HA and unblocking them with various agents to release drug molecules are necessary to explore full pharmaceutical potential of the MCM-48/HA/drug conjugates. In our opinion, the MCM-48/HA composite offers a significant potential for controlled drug delivery systems involving small molecules.

REFERENCES: Pajchel, W. [1] L. Kolodziejski, Science Materials and Engineering: C, 91 (2018) 734-742. [2] T. Azaïs, C. Tourné-Péteilh, F. Aussenac, N. Baccile, C. Coelho, J.-M. Devoisselle, F. Babonneau, Chemistry of Materials, 18 (2006) 6382-6390. [3] E. Skorupska, A. Jeziorna, P. Paluch, M.J. Potrzebowski, Molecular Pharmaceutics, 11 (2014) 1512-1519.

Fabrication & Characterization of Doxycycline-Coated Nanoporous TiO₂ Layers

A. Pawlik^{1,2}, G. D. Sulka¹, H. J. Haugen²

¹Jagiellonian University, Faculty of Chemistry, Department of Physical Chemistry & Electrochemistry, Krakow, PL, ² Department of Biomaterials, Institute of Clinical Dentistry, Faculty of Dentistry, University of Oslo, Oslo, NO

INTRODUCTION: Nanoporous anodic titanium oxide (TiO₂) (ATO) layers have shown as a promising implantable materials [1]. Cellular behavior on such surface can be modified by the incorporation with drugs. One of the antibiotics which is used to treat infections is doxycycline, has also shown positive effect on osteoblasts [2].

METHODS: Nanoporous TiO₂ layers were prepared via a three-step anodization process in an ethylene glycol-based electrolyte containing NH₄F and H₂O. The coating process was performed at constant current density (1 or 3 mA cm⁻²) for 60 min in doxycycline solution (1 or 5 mg mL⁻¹) in an acetate buffer (2 M, pH = 3.8) or water. The morphology and structure of the obtained coatings were examined by field emission scanning electron microscopy (FE-SEM) and compositional analysis energy-dispersive performed by spectroscopy (EDX). Fourier transform infrared spectroscopy (FTIR) spectra in transmittance mode were collected. In addition, ATO layers were examined as potential drug delivery systems for doxycycline.

RESULTS: The morphology of the nanoporous TiO₂ layer after the coating process was characterized with SEM (Fig. 1).

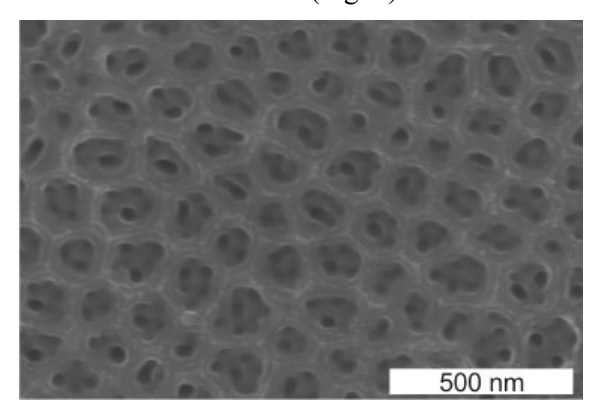


Fig. 1: SEM image of the nanoporous TiO_2 layer after the coating process at the current density of 3 mA cm⁻² for 60 min in a doxycycline solution (1 mg mL⁻¹) in the acetate buffer.

The doxycycline release process from ATO layers was examined (Fig. 2).

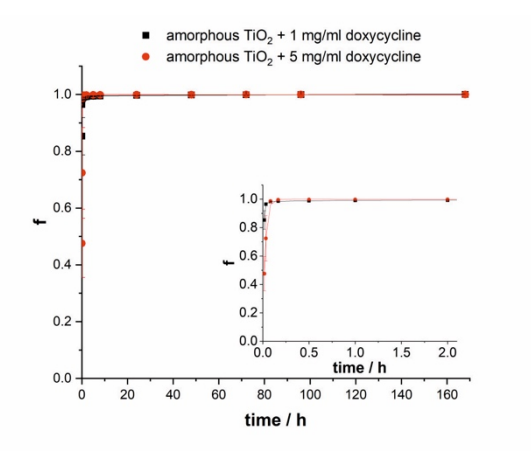


Fig. 2: Doxycycline release profiles from amorphous TiO_2 layers for two different concentrations of the loaded solution (1 and 5 mg mL⁻¹).

DISCUSSION & CONCLUSIONS: SEM images confirmed the coating process in doxycycline solutions (in both, the acetate buffer and water) did not cause the changes in the morphology of nanoporous TiO₂ samples. FTIR spectra showed the characteristic peaks of doxycycline. Therefore ATO layers can be used as potential delivery systems for doxycycline.

ACKNOWLEDGEMENTS: Anna Pawlik acknowledges the support from the National Science Centre, Poland (Grant number 2018/28/T/ST5/00413).

REFERENCES: [1] K.S. Brammer, S. Oh, Ch.J. Cobb, L.M. Bjursten, H. van der Heyde, S. Jin, *Acta Biomater*. 5 (2009) 3215–3223. [2] M.S. Walter, M.J. Frank, M. Satué, M. Monjo, H.J. Ronold, S.P. Lyngstadaas, H.J. Haugen, *Dent. Mater.* 30 (2014) 200-214.

Densitometry-Based FEM Simulations of Novel Trabecular Implants & Corresponding Stress Distribution at the Peri-Implant Area

L. Řehounek¹, A. Jíra¹

¹Department of Mechanics, Faculty of Civil Engineering, Czech Technical University in Prague, CZ

INTRODUCTION: The dental implants market seems to be one of the most rapidly developing markets in the field of biomaterials [1] and recently, inhomogeneous structures started to emerge as a viable alternative to conventional implants. The goal of this research is to compare different geometrical solutions of a novel trabecular dental implant with the aid of FEM. The main quantitative measure of this computation is the stress distribution in the surrounding bone and in the body of the implant. The research also aims to evaluate the viability of FEM in regard to simulation of small-scale biomechanical models, such as the human mandible, dentition and dental implants.

METHODS: A numerical analysis simulating the conditions of chewing food has been performed on a FEM model. This model has been created using anonymized real patient CT data and a dental implant model. The CT data served as a 3D geometry and also as a way to construct the global matrix of stiffness of the bone material. Bone density was used as the defining parameter in determining the values of Young's moduli of individual finite elements by the computational program. The implant was introduced as a user-created STL file, which was imported to the computational software and situated inside the geometry of the human mandible.

RESULTS: The results show that by incorporating the trabecular structure into the body of the implant, we can improve the uniformity of the stress distribution at the perimplant area along the longitudinal axis of the implant. Another positive effect is also reduction in the global Young's modulus of the outer layer by incorporating the trabeculae. This reduction was significant, as the modulus of the Ti-6Al-4V alloy implant material is $E_a=110\,$ GPa and the global modulus of the trabecular structure is at around $E_t=0.97\,$ GPa.

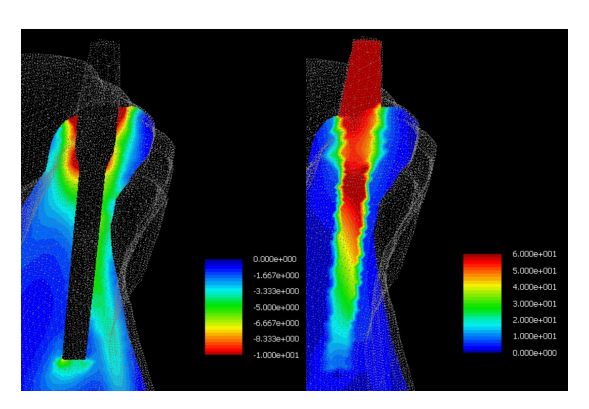


Fig. 1: Two screenshots showing the distribution of different mechanical quantities. Maximum principal stress in bone material (left) and equivalent (von-Mises) stress in the implant. Screenshots show a thin slice of human mandible. Model of mandible obtained from a CT scan. Implant imported as an STL file.

DISCUSSION & CONCLUSIONS: The acquired results show that the trabecular structure can positively affect stress distributions at the peri-implant area. This fact can improve osseointegration and primary stability of the implant, mainly preventing the aseptic loss of stability, which is one of the main causes of failure of dental implants [2].

ACKNOWLEDGEMENTS: The financial support provided by the Ministry of Industry and Trade, project n. CZ.01.1.02/0.0/0.0/17 102/0011518 is gratefully acknowledged.

REFERENCES: [1] Abraham, Celeste M. "Suppl 1: A Brief Historical Perspective on Dental Implants, Their Surface Coatings and Treatments." The open dentistry journal 8 (2014): 50. [2] Osman, Reham, and Michael Swain. "A critical review of dental implant materials with an emphasis on titanium versus zirconia." Materials 8.3 (2015): 932-958.

3D printing of bone-like materials studied by SAXS

A. Rodriguez-Palomo¹, R. Kadar¹, V. Lutz-Bueno², M. Andersson¹, M. Liebi^{1,3}

¹Chalmers University of Technology, Gothenburg, SE, ²Swiss Light Source, Paul Scherrer Institut, Villigen, CH, ³MAX IV Laboratory, Lund University, Lund, SE

INTRODUCTION: Bones are mainly composed of collagen and hydroxyapatite. The microstructure and distribution of these two components define basic physical properties in the macro-scale, such as bone strength and flexibility. A bone-mimetic composite with a hierarchical structure is proposed as a future replacement for bone defects. This composite is made of ordered micellar structures, which are mineralised with hydroxyapatite nanoplatelets. In contrast to casted and mechanised implants, 3D printing can induce anisotropy in the microstructure of the printed objects. Thus, implants with heterogenous and more complex micro-structures can be produced, maximising functionality and adaptability. understanding of the processes occurring during the 3D printing is necessary to set a reliable protocol to fabricate composites which mimic the hierarchical architecture of bone.

METHODS: The composites studied here consist of self-assembled polymeric structures called lyotropic liquid crystals (Pluronic® F-127 and P-123, modified with acrylate groups), which are cross-linked with UV light and then mineralized with nanometric hydroxyapatite. Different liquid-crystalline phases can be tailored by changing the amount of solvent [1,2] and long-range order is controlled by 3D printing, which induced alignment of the nanoentities [3]. A study of the alignment of the polymeric crystals during 3D printing was performed by scanning SAXS to understand the process. In addition, a characterization of the physical properties of the 3D composited was done to set the basic standards for further applications as bone replacements.

RESULTS: The nozzle was reproduced by microfluidics and straight and conic channels were tested. The SAXS pattern analysis gave information of the anisotropy of each pixel as well as the crystalline phase of the printed sample. In both samples (hexagonal and lamellar phase), a straight geometry produced a better alignment and higher degree of orientation. The rheological properties of the material were characterised by cyclic tests and viscosity and shear stress were measured.

Tensile tests were performed in samples printed parallel and perpendicular to the stress direction. This showed the elastic modulus and fracture point of aligned and non-aligned samples.

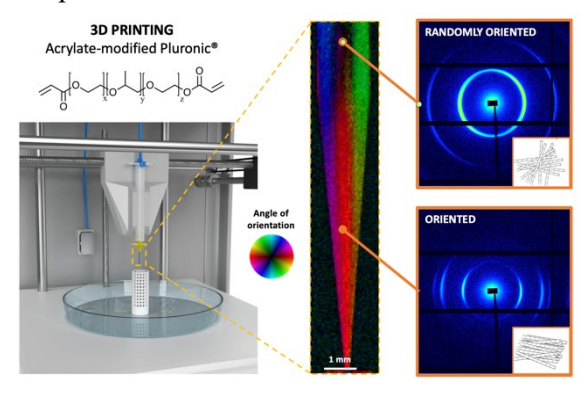


Fig. 1: Effect of extrusion in polymeric liquid crystals. Study of the alignment in the polymeric material in a microfluidic channel [4] by SAXS. The colourful regions show orientation in a specific angle.

of the alignment of the polymeric micelles showed the effect of pressure in the extrusion and the geometry used in the nozzle. A nozzle with sharp angles or straight section reached better alignment and higher pressures increased the degree of orientation. A rheological study of the polymeric ink was also performed, and the main values of viscosity and shear rate were measured. During the tensile test, influence in the geometry of the sample and the crystalline phase was shown and a better design of the process can be done.

ACKNOWLEDGEMENTS: This work has been supported by the Area of Advance Material Science at Chalmers University of Technology. We acknowledge SLS, Paul Scherrer Institute, Switzerland for beamtime.

REFERENCES: [1] W. He *et al.* Adv. Mater. 27, (2015), 2260. [2] A.K. Rajasekharan *et al.* Cryst Groth Des. 15, (2015) 2775. [3] A.K. Rajasekharan *et al.* Small. 13, (2017), 1700550. [4] V. Lutz-Bueno *et al.* Lab Chip, 16, (2016), 4028.

Synthesis of Alpha-TCP for Bone Cement Applications

D. Loca¹, M. Skrinda¹, J. Locs¹, Z. Irbe¹

¹Rudolfs Cimdins Riga Biomaterials Innovations & Development Centre of RTU, Institute of General Chemical Engineering, Faculty of Materials Science & Applied Chemistry, Riga Technical University, Riga, LV

INTRODUCTION: Calcium phosphate bone cements (CPCs) have attracted extended attention because of their ability of self-setting *in vivo*, moldability and injectability, opening new opportunities for minimally invasive surgical procedures [1] and local drug delivery. Cements based on α -TCP set via reaction between aqueous salt solutions and α -TCP solid phase [2]. Within the current research, impact of α -TCP preparation method on α -TCP particle size and specific surface area was evaluated.

METHODS: Two approaches were applied for an α -TCP preparation: high temperature synthesis at 1300 °C and low temperature synthesis <1000°C. The phase composition of prepared powders was analyzed using XRD, the specific surface area of α -TCP was determined using the BET method (ISO 9277:2010). The value of specific surface area found was used to calculate the average α -TCP particle size.

RESULTS: It was determined that high temperature α -TCP particles have irregular morphology, specific surface area of 1.5 m²/g and average particle size (calculated from BET results) of 1.4 μ m, while specific surface area of low temperature α -TCP particles is 7 m²/g and average particle size (calculated from BET results) equals to 0.3 μ m.

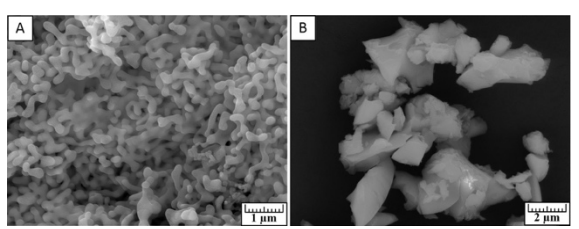


Fig.1. SEM images of α -TCP microstructure: A) low temperature and B) high temperature.

DISCUSSION & CONCLUSIONS: During the research it was established that by low temperature synthesis approach it is possible to obtain α -TCP particles with more than 4 times higher specific surface area and respectively decreased particle size.

ACKNOWLEDGEMENTS: The project "Drug Delivering 3D Printed Scaffold Strategy Brings Human Body Implants to Next Level of

Personalization" (DD-SCAFF) has partly received funding from the European Regional Development Fund under Agreement No.1.1.1.5/ERANET/18/01.

REFERENCES: [1] Loca D et al. Mater. Sci. Eng. C. 2015; 49(1):106-113. [2] Irbe Z et al. Mater. Sci. Eng. C. 2012; 32:1690-1649.

Composite Beads Containing Hydroxyapatite Modified with Mg²⁺ & SiO₄⁴⁻ Ions as Carriers for Antiresorptive Drugs

K. Szurkowska¹, A. Zgadzaj², J. Kolmas¹

¹Department of Analytical Chemistry & Biomaterials, Analytical Group, Medical University of Warsaw, Warsaw, PL, ² Department of Environmental Health Sciences, Medical University of Warsaw, Warsaw, PL

INTRODUCTION: Hydroxyapatite (HA, main $Ca_{10}(PO_4)_6(OH)_2),$ the inorganic component of human mineralized tissue, is considered as one of the most popular biomaterial in implantology, dentistry and bone surgery [1]. Its unique capacity for ionic substitutions allows to obtain material with additional features, such as enhanced biological activity or thermal stability. In the following research, HA was co-substituted magnesium and silicon ions (MgSiHA) to improve its osteogenic potential and bioactivity [2]. In order to improve the mechanical properties and surgical convenience, three types of small composite beads were formed [3]. Granules loaded with raloxifene hydrochloride (RAL) were made of MgSiHA, sodium alginate (SA) and one of the following additives: chondroitin sulfate (CS), keratin (KER) or pullulan (PUL) (Table 1) [4]. Then, the release profiles of ions as well as RAL were tested and compared to choose the optimal composition.

METHODS: MgSiHA sample was synthesized by wet precipitation method and thoroughly physicochemically examined using FT-IR, ssNMR, PXRD, TEM and ICP-OES methods. The preliminary *in vitro* cytocompatibility tests were performed on BALB/c 3T3 mice fibroblasts. Beads were formed by crosslinking the alginate with Mg²⁺ ions. Before the crosslinking, HA, RAL and one of the additives (CS, KER or PUL) were added into the alginate suspension. The release profiles of ions and RAL from various beads were examined in pH 7.4 phosphate buffer at 37°C. Moreover, the density and external surface of samples were characterized.

RESULTS: Multicomponent granules, composed of MgSiHA, SA and CS, KER or PUL were successfully obtained. Crosslinking with Mg²⁺ ions allowed to introduce an additional amount of magnesium into the composite beads. Various beads compositions resulted in differences in the release profile of

the drug substance. Furthermore, SEM images demonstrated variability in the morphology of granules.

Table 1. The chemical composition of beads.

| CS | KER | PUL |
|-------|--------------------|-------|
| beads | beads | beads |
| + | + | + |
| + | + | + |
| + | - | - |
| - | + | - |
| - | - | + |
| + | + | + |
| | CS beads + + + + + | |

DISCUSSION & CONCLUSIONS:

Various additives (CS, KER or PUL) resulted in differences in the release profiles of RAL. The obtained results made it possible to select the appropriate composition of granules taking into account the purpose of the material and the expected release rate. Thus, composite granules could potentially be used for local delivery of ions and drugs into the injured tissue.

ACKNOWLEDGEMENTS: This work was supported by UMO-2016/22/E/STS/00564 grant of the National Science Centre, Poland and FW23/PM1/18 grant from the Medical University of Warsaw.

REFERENCES: [1] M. Vallet-Regi, J.M. Gonzales-Calbet, Prog. Solid State Chem. 32 (2004) 1-31. [2] M. Supova, Ceram. Int. 41 (2015) 9203-9231. [3] J. Venkatesan, S.K. Kim, J. Biomed. Nanotechnol. 10 (2014) 3124-3140. [4] K. Szurkowska, A. Zgadzaj, M. Kuras, J. Kolmas, Ceram. Int. 44 (2018) 18551-18559.

Thermal Stability of BaTiO₃ Functionalised Zirconia

L. Tiainen¹, M. Gasik², J. Pinto¹, O. Carvalho¹, F. Silva¹

¹CMEMS-UMinho, University of Minho, Guimarães, PT, ²Aalto University Foundation, Espoo, FI

INTRODUCTION: The development of this smart ceramic (MEMS) with piezoelectric functionality is inspired by nature for osteoblast stimulation. There is also extended relevance for improving understanding about the immune interface at implanted biomaterials. The possible "Bone-on-Chip" applications could be utilised in studying the responses of biota to different stimuli related to osteointegration and for instance crack-healing process [1].

METHODS: The chosen materials, barium titanate Ba_{0.997}-Sr_{0.003}-TiO₃ (BT) and 3 mol% stabilized zirconia (YSZ)vttria biocompatible [2]. Zirconia is used in implants and studies on barium titanate have evidence for non-toxicity and report potentiality positive immune host response [2]. Dispersions of 5 and 10 wt.% of BT in YSZ were prepared through press and sinter route under atmospheric conditions. XRD, EDS and micro-Raman spectroscopy were utilised phase in identification. Materials' stability was studied with differential scanning calorimetry [3,4].

RESULTS: The distribution of BT inclusions in the matrix was evaluated with SEM in backscattered electron mode. Fig.1 shows the micro structure of YSZ, BT and 5% BT/YSZ composite. The inclusions with white contrast to the matrix were confirmed to be BT with EDS and micro-Raman spectroscopy.

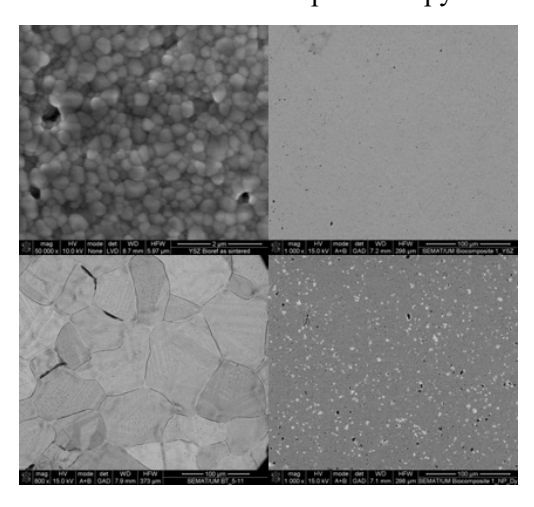


Fig. 1: SEM micrographs of processed materials. YSZ (top), BT (left, bottom) and 5%BT/YSZ composite (right, bottom).

YSZ grain size was $\sim 0.25 \mu m$. BT grains, $\sim 54 \mu m$, have a trace of twin lamella. DSC studies (Fig.2) found the composites very stable. Global piezoelectric response to deflection was measured and the local effect modelled with FEM.

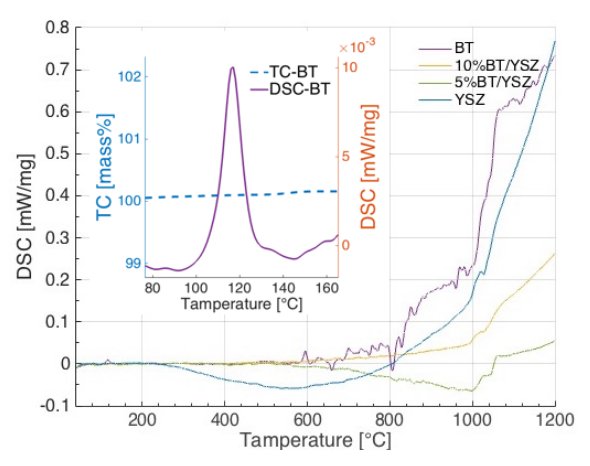


Fig. 2: DSC study on BT, YSZ and their composites. The peak at ~116°C in BT, indicates a ferroelectric transition [3].

DISCUSSION & CONCLUSIONS: In this work we have succeeded in processing BT/YSZ composites with different degree of piezoelectric functionalisation. These materials have potential in investigation of cell stimuli related to osteointegration.

ACKNOWLEDGEMENTS: This work has been supported by FCT (Fundacao para a Ciencia e Tecnologia – Portugal) in the scope of the projects UID/ EEA/ 04436/ 2013 and NORTE-01-0145-FEDER-528 000018-HAMaBICo. For guidance with electrical measurements authors thank Prof. L.Gonçalves and PhD J.Ribeiro from CMEMS, University of Minho.

REFERENCES: [1] Rajabi, A., et al. 2015. doi: 10.1016/j.actbio.2015.07.010. [2] Zhang, Y., et al. 2014. doi: 10.1016/j.msec.2014.02.022. [3] Baeten, F., et al. 2005. doi: 10.1016/j.jeurceramsoc. 2005.06.029. [4] Hedges M., et al. 1991. doi: 10.1111/j.1151-2916.1991.tb08306.x.

Macroporous PEGDA-Hydrogels Reinforced by Brushite as Bone-Substituent Implants

A. Tikhonov¹, **D. Zuev**¹, E. Klimashina^{1,2}, P. Evdokimov^{1,2}, G. Shipunov³, I. Scherbackov³, D. Zyuzin³, V. Putlayev^{1,2}, V. Dubrov³

¹Department of Materials Science, Lomonosov Moscow State University, Moscow, RU, ²Department of Chemistry, Lomonosov Moscow State University, Moscow, RU, ³Department of Fundamental Medicine, Lomonosov Moscow State University, Moscow, RU

INTRODUCTION: Hydrogels represent the materials with viscoelastic properties and an ability to swell in different media which make them perspective for using as the materials for soft tissue replacement. The filling of such matrixes with calcium phosphates, in particular plate-like particles of brushite, allows creating biocomposite with the the composition to the native bone tissue and opportunities to manage the strength, elasticity, swelling and biodegradability. Required for the bone implants osteoconductive modern properties usually are determined by the geometry (specific architecture) and the porosity (in conjunction with pore channel size and their direction) of the material and created by additive manufacturing, i.e. 3D-printing.

This work was aimed at the development of osteoconductive composite materials with viscoelastic properties based on calcium phosphate-filled hydrogels for their use in the reconstruction of bone tissue.

METHODS: Hydrogels based on polyethylene glycol diacrylate (PEGDA), which are mostly used for the regeneration of the soft tissues, were studied. To create the biocomposite, a based on aqueous solution of biocompatible PEGDA (Mw = 700 Da), and containing photoinitiator (PI) Irgacure®819 (phenyl bis (2,4,6-trimethylbenzoyl) phosphine oxide), quinoline yellow dye (maximum extinction at 405 nm), and the filler (either a) synthesized powders of brushite and OCP, or b) salts of CaCl₂ with a mixture of NaH₂PO₄ and Na₂HPO₄), was prepared. The composites were fabricated by means of stereolithography as a result of slurry photopolymerization under the irradiation (ca. at 390-440 nm) by LED source of DLP-projector of the 3D-printer Ember (Autodesk, USA). The characterization of the obtained biocomposites was carried out by means of scanning electron microscopy, X-ray diffraction, FTIR-spectroscopy, rheometry and mechanical tests, toxicity tests (MTT assay). The biocomposite geometry was optimized by

SolidWorks simulation of water flow and uniaxial and unilateral loading.

RESULTS: Study of the suspension optical properties revealed the main problem of stereolithographic printing of hydrogels due to the high photosensitivity of an optically transparent medium. The addition of a dye, a calcium phosphate filler with different size of the particles, as well as variation of the photoinitiator content, allow to reduce the photosensitivity and achieve a high printing resolution along z-axis (up to 100 μm). Uniform filling of the hydrogel (up to 10 wt.%) was realized only by introducing in the initial composition the pre-synthesized crystals of brushite or OCP. After the one-sided diffusion of Ca²⁺ or HPO₄²⁻ ions into the polymerized hydrogel phosphate crystals are formed predominantly on the surface of the hydrogel in contact with the solution. For geometry optimization, it was shown that Kelvin and "gyroid" structures have the greatest flexibility and permeability. The permeability of such implants with 70% porosity are close to that one of cancellous bone tissue (about 1000 darcy, for water flux).

DISCUSSION & CONCLUSIONS: Thus, the biocomposite based on PEGDA-hydrogel/brushite with "gyroid" structure that is similar in chemical composition and structure to native bone tissue has been developed which possesses viscoelastic mechanical properties and reversibly deforms up to 20% and allows full filling of defects of complex shape due to 24% swelling.

ACKNOWLEDGEMENTS: The work was supported by RSF, grant #17-79-20427. The authors acknowledge partial support from Lomonosov Moscow State University Program of Development.

Structural Study & Biocompatibility of Mixed-Cationic Polyphosphates

D. Zuev¹, E. Klimashina^{1,2}, M. Kikuchi³, S. Oshima³, J. Labuta⁴, V. Putlyaev^{1,2}

¹Department of Materials Science, Lomonosov Moscow State University, Moscow, RU, ²Department of Chemistry, Lomonosov Moscow State University, Moscow, RU, ³Bioceramics Group, Research Center for Functional Materials, NIMS, Tsukuba, JP, ⁴International Center for Materials Nanoarchitectonics (WPI-MANA), NIMS, Tsukuba, JP

INTRODUCTION: Polyphosphates (PolyPs) with Ca²⁺/Mg²⁺ or Ca²⁺/Na⁺ cations can be perspective biomaterial for bone grafts with cumulative regeneration effect since linear PolyPs can be cut consequently by ALP enzyme [1] in extracellular medium into orthophosphates (Pi), and statistically into pyrophosphates (PP_i) and metaphosphates. Biomineralization rate of osteoblasts can be regulated by kinetics of PolyPs solubility in aqueous solution in vivo. Structural study of soluble and insoluble mix-cationic PolyPs is necessary for better understanding degradation model in a living organism. Biocompatibility is also required for living interaction. matter/graft interface materials can be used as a cumulative resorbable filler for a 3D (CaP/biopolymer) with a complex macroporous framework providing osteoconductivity [2].

METHODS: Mixed-cationic PolyPs can appear in specific areas of phase diagrams of CaO-Na₂O-P₂O₅ and CaO-MgO-P₂O₅. As a result, Ca(PO₃)₂, CaNa(PO₃)₃, CaNa₄(PO₃)₆, Mg(PO₃)₂, and biphase CaMg(PO₃)₄ (Ca(PO₃)₂ · Mg(PO₃)₂) compounds were synthesized via solid-state reaction through thermal treatment of H₂PO₄ with selected cations. The temperature varied from 400°C to 700°C with treatment time from 2 to 12 hours. The characterisation was done using TG/DTA, XRD, SEM/EDX, ATR FTIR, ICP-OES, ³¹P NMR, ion-exchange chromatography, pH, phase-contrast microscope and equipment for cell culture test (line MG-63).

RESULTS: Soluble and solid mixed-cationic PolyPs were characterized. Ca/P in a solid state was determined from 0.4 to 0.7 by EDX in the most soluble phases. PO₃/POP ratio was calculated from 2 to 28 by FTIR, which can be caused by the presence of PP_i. There are some differences in determination of soluble PolyPs structures, caused by the possible overlapping in ³¹P NMR spectra (see Table 1).

Table 1. Comparison of PolyPs products of hydrolysis as obtained by liquid-state ³¹P NMR and ion-exchange chromatography for CaNa(PO₃)₃ (500°C and 2 hours of treatment).

| | liquid-state | ion-exchange |
|-------------------|---------------------|----------------|
| | ³¹ P NMR | chromatography |
| P_{i} | 20±3% | 25±2% |
| $\mathbf{PP_{i}}$ | possible | - |
| | overlap | |
| $P_3O_9^{3-}$ | possible | 75±2% |
| | overlap | |
| $P_3O_{10}^{5-}$ | 80±3% | - |
| $PolyP_n$ | (n = 20) | |

DISCUSSION & CONCLUSIONS:

Perspective mix-cationic PolyPs were obtained via synthetic optimisation. The solubility ranges from low 1 g/L ($Ca(PO_3)_2$, $Mg(PO_3)_2$) to 10 g/L (Na₄Ca(PO₃)₆) and 50 g/L for fully soluble phase of NaPO₃. The process of aqueous degradation of PolyPs can lead to chain hydrolysis and possible hydroxyapatite (HAp) formation with decreasing pH to 3.5 ± 0.5 . At ^{31}P liquid-state NMR chromatography are necessary for identification of anionic structure of soluble mixed-cationic PolyPs. Human osteosarcoma cells MG-63 showed full biocompatibility for CaMg(PO₃)₄ sample containing P₃O₁₀⁵ anions with around 30% superior cell proliferation over the control HAp.

ACKNOWLEDGEMENTS: The work was funded by RFBR grants №18-08-01473, 18-33-00789 and 18-53-00034. D. Zuev was supported by MSU - NIMS Cooperative Graduate School Program OH-1619-2014-5. Equipment purchased through the Program for Development of MSU was used.

REFERENCES: [1] Müller, W.E., et al., J Cell Sci, 2015. 128(11): p. 2202-2207. [2] Neufurth, M., et al., Acta biomaterialia, 2017. 64: p. 377-388.

Anodization of Tantalum to Enhance Biocompatibility

E. Uslu¹, B. Ercan^{1,2}

¹Department of Metallurgical & Materials Engineering, Middle East Technical University, Ankara, TR, ²BIOMATEN, Middle East Technical University, Center of Excellence in Biomaterials & Tissue Engineering, Ankara, TR

INTRODUCTION: Tantalum is one of the most corrosion resistant materials due to the formation of stable oxide layer in ambient conditions. This layer hinders ion release and protects tantalum from corrosion¹. In addition, tantalum has optimal mechanical properties for orthopaedic applications, i.e. fatigue resistance, wear resistance, etc. Despite its superior properties, tantalum does not possess bioactive properties, leads to suboptimal which osseointegration in clinical applications. To make tantalum surfaces bioactive, surface modification in the nanoscale can be a potential solution. Among various surface modification techniques, anodization has been gaining significant popularity due to its versatility and possibility to control morphology and nanoscale size of the oxide surface layer. In this research tantalum surfaces were anodized to possess nanotubular, nanocoral and nanodimple surface morphologies, followed by assessing biocompatibility.

METHODS: 1x1cm tantalum samples were sonicated by using acetone, ethanol and distilled water consecutively for 15 minutes. Platinum was used as cathode and tantalum was anode during anodization. Concentrated HF:H₂SO₄, DMSO, NH₄F were used as electrolyte. Different voltages (10-60V) and anodization durations (10s-4hr) were applied to obtain nanotubular, nanocoral and nanodimple morphologies on tantalum. To investigate biocompatibility of the samples, osteoblast (ATCC CRL-11372) adhesion and proliferation were investigated up to 5 days of culture.

RESULTS: Nanotubular morphology was obtained by using concentrated HF: H₂SO₄ (1:9 v/v) as electrolyte. Applied potentials were systematically changed from 10V to 20V and anodization durations were varied between 30s to 3 min to increase tubular diameter (20-80nm) and oxide layer thickness (0.8-4.5μm). 3.3 wt% NH₄F in 1M H₂SO₄ were used as electrolyte and nanocoral tantalum surfaces were obtained. Anodization durations were tuned between 60 min to 150 min at 20V to obtain different pore sizes ranging 20 to 120 nm. Small amount of

DMSO were added into concentrated HF: H_2SO_4 (1:9 v/v) solution to obtain nanodimple morphology. Increase in dimple diameter (25-70nm) were observed by changing voltage (10-30V) and duration (10-30min). Moreover, enhanced osteoblast cell adhesion and proliferation on nanotubular, nanocoral and dimple morphologies compared to non-anodized Ta surfaces were observed.

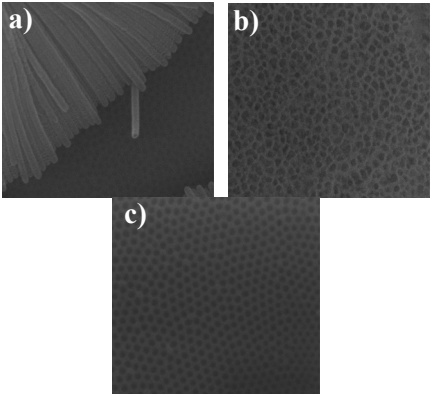


Fig. 1: a) Nanotubular, b) nanocoral and c) nanodimple morphologies obtained by anodization of tantalum.

DISCUSSION & CONCLUSIONS: Different morphologies and feature sizes (20nm to 200nm) on tantalum surfaces (nanotubular, nanocoral, nanodimple) were obtained via altering anodization parameters. Osteoblast functions were improved on anodized tantalum surfaces compared to non-anodized surface, potentially leading to enhanced osseointegration of tantalum upon anodizing its surfaces.

ACKNOWLEDGEMENTS: Authors would like to thank the Scientific and Technological Research Council of Turkey (Grant no: 117M187) for providing financial support.

REFERENCES: [1] Ruckh, T. *et.al.*, (2008). Nanotechnology, 20(4).

Efficient Wet Adhesion through Mussel-Inspired Proto-Coacervates

T. Huynh¹, F. Bach-Gansmo¹, **Y. Chen**¹, J. Dehli¹, V. Ibsen¹, M. Foss¹, H. Birkedal¹

Department of Chemistry & iNANO, Aarhus University, Aarhus, DK

INTRODUCTION: Adhesion underwater is a challenge. Bioinspired coacervates have been proposed to be an excellent approach to underwater adhesion but efficient nontoxic procedures for harnessing them is lacking. Herein, coacervate adhesives were formed underwater by simple injection of acidic proto-coacervate of L-3.4an dihydroxyphenylalanine (L-DOPA) functionalized polyallylamine (DOPA-PAAm) and poly(acrylic acid) (PAA). The adhesive abilities of our mussel-inspired glue were tested on glass substrates, and the cytotoxicity of the mussel-inspired glue was assessed by cell cytotoxicity tests and application on human epidermis in vitro.

METHODS: DOPA-PAAm was synthesized according to previously published procedure. Different solutions and proto-coacervates of $0.25\%C_{3:1}$, $1\%C_{3:1}$, $1\%C_{1:1}$, $1\%C_{1:1,control}$, and $10\%C_{1:1}$ were prepared. Coacervation of $0.25\%C_{3:1}$, $1\%C_{3:1}$, $1\%C_{1:1}$, and 1%C_{1:1.control} was observed by dropwise addition of NaOH solutions. Coacervation of 5%C1:1 and 10%C_{1:1} proto-coacervates was carried out by injection of their solution into demineralized water. Turbidty of coacervation was examined by UV-vis spectrophotometer (Agilent). The rheological properties and adhesive properties of the coacervates were investigated by performing dynamic oscillatory experiments and using overlap shear testing with an Anton Parr MCR 501 Rheometer. Test of in-vitro cytotoxicity of coacervates and cyanoacrylates were performed according to ISO 10993-5 using a conditioned media.

RESULTS: The formation of coacervate adhesives is shown in Figure 1 a-b. We prepared mixtures of DOPA-PAAm and PAA under acidic conditions (pH \sim 1), which resulted in a homogenous non-coacervated solution (Figure 1c-d, stage I). Then base (NaOH) was slowly added to the solution and coacervation happened at pH = 2 to 2.5 as observed from the solution turning highly turbid (Figures 1c-d). DOPA played an important role in the adhesion of the formed coacervates. The coacervates showed good adhesion even on standard microscope glass substrates.

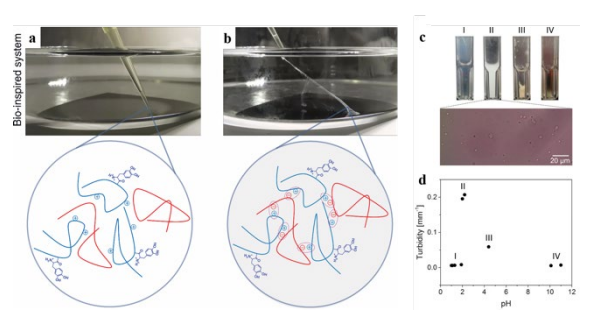


Fig. 1: (a) Mussel-inspired proto-coacervate secreted in a pipette tip and (b) coacervate plaque. (c) Images of the titration stages of a $1\%C_{1:1}$ solution using NaOH. (d) Dependence of turbidity on pH of $1\%C_{1:1}$.

DISCUSSION & CONCLUSIONS: The coacervation is driven by electrostatic complexation between the polycationic DOPA-PAAm and polyanionic PAA resulting in phase separation (Figures 1a-b). This phenomenon depends strongly on the pH of the medium and the pK_a of the polyions. When the concentration of polyions in the proto-coacervate increased to 10%, the lap shear strength on untreated glass of the corresponding coacervates was 2.39 DOPA-containing coacervates MPa. The $10\%C_{1:1}$ obtained from proto-coacervates reached strengths similar to commercially available glues when dry and to mussel glue when wet. Moreover, it is free of organic solvent and has no negative effect on the epidermis at the wound site tested by in vitro cytotoxicity. The simple injection method, mechanical performance and biocompatibility with cells qualify this material with practical application in real-life applications.

ACKNOWLEDGEMENTS: We acknowledge funding from the Danish Council for Independent Research | Technology and Production Sciences (Grant No. 0602-02426B), the Carlsberg Foundation through a Carlsberg Foundation's Distinguished Postdoctoral Fellowship to TPH (Grant No. 21903), and the financial support of China Scholarship Council (CSC).

Biomicroconcretes on the Basis of Hybrid Hydroxyapatite/Chitosan Granules & Highly Reactive αTCP Powder

A. Zima¹, E. Cichoń¹, M. Dziadek¹, A. Ślósarczyk¹

¹Department of Ceramics & Refractories, Faculty of Materials Science & Ceramics, AGH UST University of Science & Technology, Krakow, PL

INTRODUCTION: The new generation of biomaterials should combine bioactive (e.g. phosphates ceramics) calcium bioresorbable (e.g. polymers) materials, in order to accurately reproduce the bone microstructure and activate the mechanisms of bone tissue regeneration. Recently, hybrid materials composed of mixture of inorganic, organic or both types of the above components (usually interpenetrate on a scale of less than 1 µm) are the subject of many studies [1]. The aim of this work was to obtain new surgically handy biomicroconcrete type bone substitutes. We focused on the evaluation of size of hybrid hydroxyapatite-chitosan granules (HA/CTS) on setting time of biomicroconcretes in the system αTCP (matrix) – HA/CTS granules (playing the role of aggregates).

METHODS: The preparation method of hybrid HA/CST granules containing 13, 17 and 20 wt.% of chitosan was described in our previous paper [2]. The highly reactive α -tricalcium phosphate powder (αTCP) was synthesized by the wet chemical method. Solid phase of biomicroconcretes was obtained by mixing of initial aTCP powder with hybrid HA/CTS granules at the 3:2 weight ratio using the ball mill (MM 400 Retsch). For cement pastes preparation as the liquid phase methylcellulose solution was used. The physicochemical properties of the biomicroconcretes such as: setting times (Gillmore Apparatus), phase composition (XRD, D-2 Phaser, Bruker) and compressive strength (Universal machine, Instron) were determined.

RESULTS: The initial compositions as well as setting times of biomicroconcretes are presented in table 1. X-ray diffraction analysis revealed that the prepared materials one week after setting and hardening consisted of: hydroxyapatite and α TCP crystalline phases. The obtained biomicroconcretes possessed compressive strength from 3.1 ± 0.4 MPa to 5.4 ± 0.4 MPa.

Table 1. Initial composition and setting times of studied materials.

| No. of | Composition of materials | Size of granules [µm] | Setting t | Setting time [min] | |
|-----------|--|-----------------------|-----------|-----------------------|--|
| material | | | Initial | Final | |
| | αTCP + granules HA/CTS (13wt% of chitosan) | 300-400 | 4±0.5 | 18±1.0 | |
| M1 | | 400-600 | 4±0.5 | 15±1.0 | |
| | | 600-800 | 3±0.5 | 13±0.5 | |
| | αTCP + granules HA/CTS (17wt% of chitosan) | 300-400 | 6±1.0 | 21±1.0 | |
| M2 | | 400-600 | 7±0.5 | 26±0.5 | |
| | | 600-800 | 7±1.0 | 27±0.5 | |
| | αTCP + granules HA/CTS | 300-400 | 10±0.5 | 32±1.0 | |
| M3 | | 400-600 | 9±0.5 | 30±1.0 | |
| | (20wt% of chitosan) | 600-800 | 9±0.5 | 31±0.5 | |

DISCUSSION & CONCLUSIONS: The obtained biomicroconcretes, composed of highly reactive αTCP powder and hybrid HAp/CTS granules, showed appropriate setting times for medical application (from 3±0.5min.—the shortest initial setting time to 32±0.5min.—the longest final setting time). The mechanical strength depended on the size of HA/CTS granules. All materials possessed compressive strength on the level of cortical bone. These perspective biomicroconcretes require further studies.

ACKNOWLEDGEMENTS: This work was supported by the Polish National Science Centre – project no. 2017/27/B/ST8/01173.

REFERENCES: [1] Aleman J. at al., Pure Appl. Chem. 79 (2007) 1801-1829. [2] Zima A., Spectrochim. Acta A 193 (2018) 175-184.

Dual-Delivery of Hydroxyapatite & Connective Tissue Growth Factor Derived Osteoinductive Peptide Enhanced Bone Healing

R. Xu¹, F. Dagnæs-Hansen², J. S. Thomsen², A. Bruel, M. Chen¹

¹Department of Engineering, Aarhus University, DK-8000 Aarhus C, DK, ² Institute of Biomedicine, Aarhus University, Wilhelm Meyers Allé 4, DK-8000 Aarhus C, DK

INTRODUCTION: In bone tissue engineering, electrospun fibrous scaffolds can provide excellent mechanical support, extracellular matrix mimicking components, such as 3D spacial fibrous environment for cell growth and controlled release of signaling molecules for osteogenesis.

METHODS: Here, a facile strategy comprising the incorporation of an osteogenic inductive peptide H1, derived from the cysteine knot (CT) domain of connective tissue growth factor (CTGF), in the core of Silk Fibroin (SF) was developed for osteogenic induction, synergistically with co-delivering hydroxyapatite (HA) from the shell of poly(Llactic acid-co-ε-caprolactone) (PLCL). The core-shell nanofibrous structure was characterized by scanning and transmission electron microscopy (SEM and TEM). The release profile of H1 together with the effect on proliferation and osteoblastic differentiation of human induced pluripotent stem cells derived mesenchymal stem cells (hiPS-MSCs) was investigated by metabolic activity (MTS), qPCR, Alkaline phosphatase (ALP) analysis, and immunocytochemistry staining. In vivo bone formation using scaffolds was evaluated using critical sized carvarial defects in mice by micro Computed Tomography (µCT).

RESULTS: From the core-shell nanofibers (Fig 1), a burst release of H1 (36 \pm 3.4%) was detected in the first two days, followed by a continuous and slow release ofApproximately $61.3 \pm 6.2\%$ of H1 was released during 40 days. A significantly higher gene expression of ALP was observed in SF-H1/PLCL-HA than that in SF-H1/PLCL at days 21. The ALP enzymatic activity of the SF-H1/PLCL-HA was significantly higher than those in the SF/PLCL at both day 14 and 21. Furthermore, cells on the SF-H1/PLCL-HA scaffolds were found expressed higher amount of Osteopontin than the other groups, which is consistent with the qPCR results. After 8 weeks implantation in mice, this SF-H1/PLCL-HA composite induced bone tissue formation

significantly faster than SF/PLCL as indicated by μ CT (Fig 1).



Fig. 1: SEM image of SF-H1/PLCL-HA coreshell nanofibers and μ CT analysis of the dual-delivery for bone healing in cranial defect.

DISCUSSION & CONCLUSIONS: Bone tissue is a hard tissue, which is composed of an organic part, which is dominated by collagen fibers, and of an inorganic part distributed in the fibrous matrix consisting of mainly hydroxyapatite (HA) but also of carbonate and inorganic salts [1]. The inorganic nanoparticles aid bone formation reconstruction by providing a nucleation center for mineralization. Furthermore, the fibrous network also plays a role in regulating the growth factor delivery. Mimicking ECM of bone, HA loaded nanofibrous scaffolds delivering an osteogenic peptide H1 was designed in the present study [2]. The core-shell structure was confirmed by TEM. A sustained release of H1 was achieved and was found to play an important role in stem cell survival and proliferation. When accompanied with HA, H1 exerted an additive effect on osteogenic induction, which was evidenced by qPCR, immunostaining, and µCT. The work should provide instructive insights towards improvement of small peptide delivery system for bone regeneration.

ACKNOWLEDGEMENTS: We gratefully acknowledge funding from Aarhus University Research foundation and Carlsberg Foundation for the financial support. The μCT scanner was donated by the VELUX Foundation.

REFERENCES: [1] X. Feng, Curr. Chem. Biol. 3 (2009) 189–196; [2] Xu et al, J. Controlled Release, 301 (2019) 129-139.

Composite Silk-Glycolipid Hydrogels: Symbiosis or Simple Coexistence? A. Lassenberger¹, N. Baccile²

¹Institut Laue-Langevin, Soft Matter Science & Support Group, Grenoble, FR, ² Laboratoire de Chimie de la Matière Condensé, Sorbonne Université, Paris, FR

INTRODUCTION: Hybrid hydrogels composed of low natural molecular weight gelators (LMWG) such as sophorolipids (SL) and natural polymers such as silk fibroin mark the future trend in hydrogel research. LMWG are particularly interesting for their stimuli responsiveness and the reversibility of the gelation process. However, their mechanical properties suffer from the weak intermolecular forces that build up the hydrogel. Silk fibroin (SF), a protein with exceptional mechanical properties, forms hydrogels by a conformational change from random coil to β-sheet. However, the process is very slow and irreversible. To overcome these disadvantages, we prepared composite hydrogels of SF and SL to join their properties. Here we aim to study the structure of such natural composite hydrogels.

METHODS: SL were obtained from the yeast of *S. bambicola*.¹ SF solution was prepared as described by A. Martel *et al*.² Composite hydrogels were prepared in 100 % H_2O , 50% H_2O : D_2O and 100 % D_2O . Gelation was characterized by absorption measurements at λ = 595 nm. Protein conformation was examined by ATR FT/IR by analyzing the amide I, II and III regions. Small angle neutron scattering (SANS) experiments for structural analysis were carried out at the Institut Laue-Langevin, Grenoble on the instrument D11 covering a qrange of $0.0005 - 0.5 \, \text{Å}^{-1}$.

RESULTS: D_2O can alter the structure and aggregation state of proteins and speed up the gelation of fibroin. With IR and SANS measurements we could show that the fastened gelation in D_2O is solely of kinetic nature and the resulting fibroin structure is the same as in H_2O . SL forms negatively charged micelles in water³ and has been reported to speed up the gelation of SF,⁴ in agreement with our findings. IR confirmed that the fastened gelation of silk was a still conformational change from random coil to β -sheet. SANS data of silk hydrogels were fitted with a model for an elliptical cylinder from which the length and thickness of growing fibres could be extracted. SANS data

of composite hydrogels showed the features of both SL micelles and fibroin (Figure 1A, red). Subtracting the SL signal from that of the composite gel yielded a signal very similar to that of a pure silk gel (Figure 2B), that could be fitted with the same model and parameters with a tendency towards longer and flatter fibres.

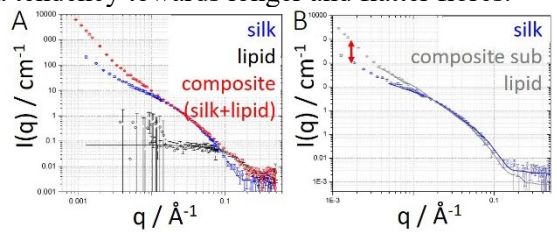


Fig. 1: A) SANS data for silk, sophorolipid and composite gels. B) SANS of silk (blue) and the signal resulting from the subtraction of lipid from the composite signal (grey).

DISCUSSION & CONCLUSIONS: SL does kinetically influence the growth of SF fibres. We could observe a tendency towards flatter fibres when SL micelles were present. More importantly we could show that SL molecules do not insert into the hydrophobic domains of fibroin, they keep their structure of charged This opens the way towards micelles. orthogonal hydrogels, where each compound can be stimulated separately. We propose that the underlying mechanism of fastened gelation is a depletion of water from the SF to the sugar headgroups Currently of SL. investigation is the difference seen in the low qrange (Figure 2B): we suppose that these differences have their origin either in the gel network or in the presence of larger and more β-sheet domains.

ACKNOWLEDGEMENTS: We acknowledge A Martel, L Porcar, R Schweins and S Prevost from ILL, and GB Messaoud from Sorbonne University. Funded by EU (grant No 731096).

REFERENCES: [1] Baccile *et al.*, J Phys Chem B 2015 119:13113-13133. [2] Martel *et al.*, J Am Chem Soc 2008 130(50):17070-17074. [3] Baccile *et al.* Langmuir 2016 32:10881–10894. [4] Nisal *et al.*, Biomacromolecules 2016 17:3318–3327.

Newly Designed Bilayered Scaffolds for Axonal Growth

Z. B. Ahi¹⁻³, R. Assunção-Silva^{2,3}, A. Salgado^{2,3}, K. Tuzlakoglu¹

¹Department of Polymer Engineering, Yalova University, Yalova, TR, ²Life & Health Sciences Research Institute, School of Health Sciences, University of Minho, Braga, PT, ³ICVS/3B's, PT Government Associate Laboratory, Braga/Guimarães, PT

INTRODUCTION: Spinal cord injury (SCI) is a devastating disease of the central nervous system (CNS) and because of the complex nature of the injured tissue; traditional treatment techniques are not efficient. Therefore biomaterial-based systems have been developed as alternative strategies to repair the damaged tissue [1]. The aim of this study is to evaluate whether the novel Collagen/PLGA bilayered scaffold is a potential tool for the treatment of SCI.

METHODS: Developed matrices consisting of two different layers. While the Coll/PLGA+laminin electrospun top layer processed by electrospinning acts as a carrier system for ASCs, the collagen bottom layer obtained by plastic compression method acts as a releasing system for NT3 and chABC. ASCs were cultured in top layer of the construct at a density of 5000 cells/cm2, for periods up to 7 days. Media were changed every 2 days. Cell metabolic activity was assessed by MTS assay, where DAPI and phalloidin were used to stain the nucleus and the F-actin filaments of cell cytoskeleton, respectively. For the assessment of axonal outgrowth, dorsal root ganglia (DRG) explant culture was cultured with matrices for 5 days. To stain the intermediate filaments of DRG neurons and nucleus, neurofilament (NF) and DAPI were used, respectively.

RESULTS: SEM micrographs revealed the complete integrity between two layers of developed dual structures (Fig.1.a). ASCs were able to adhere and proliferated on the matrices and the aligned fibers promoted the cell growth in such organized way. The bilayered matrices supported cells metabolic activity, inferred by the MTS assay. Likewise, the bilayered matrices promoted DRGs neurite outgrowth. The bilayered matrices that have Coll/PLGA+Laminin top layer appears to promote higher neurite growth.

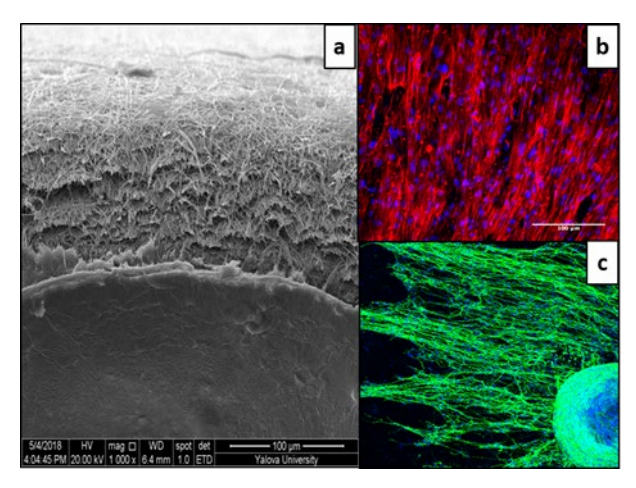


Fig. 1: a) SEM images of bilayered matrices, b) Confocal image of ASCs morphology (Blue:DAPI, Red:Phalloidin), c) Confocal image of morphology of DRG (Blue:DAPI, Green: Neurofilament).

DISCUSSION & CONCLUSIONS: The results from this study indicated that bilayered matrices are appropriate for ASCs adhesion and growth. Besides, presence of laminin promotes axonal growth significantly.

ACKNOWLEDGEMENTS: This work was supported by the Scientific and Technological Research Council of Turkey (TÜBİTAK) project #12M134. Z.B.Ahi acknowledges TUBITAK-BIDEB for the financial support given through 2214-A scholarship program.

REFERENCES: [1] Shrestha et al. Stem Cell Research & Therapy 2014, 5:91.

Investigating Dynamic Biological Processes with High-Speed, High-Resolution Correlative AFM-Light Microscopy

H. Haschke¹, T. Jaehnke¹

¹JPK BioAFM, Bruker Nano Surfaces, Berlin, DE

INTRODUCTION: The ability of atomic force microscopy (AFM) to obtain three-dimensional topography images of biological molecules and complexes with nanometer resolution and under near-physiological conditions remains unmatched by other imaging techniques. However, the typically longer image acquisition times required to obtain a single high-resolution image (~minutes) has limited the advancement of AFM for investigating dynamic biological processes.

METHODS: While recent years have shown significant progress in the development of high-speed AFM (HS-AFM), the ability to scan faster has typically been achieved at the cost of decreased scanner range and restricted sample size. As such, these HS-AFM systems have mainly been focused on studying single molecule dynamics and have been very limited in their ability to conduct live cell imaging.

RESULTS: JPK BioAFM has developed a new NanoWizard® ULTRA Speed 2 AFM which not only enables high-speed studies of timeresolved dynamics associated with cellular processes, it's latest scanner technologies and compact design also allow full integration of AFM into advanced commercially available light microscopy techniques. Thus, fast AFM imaging of 10 frames per second can be seamlessly combined with methods such as epifluorescence, confocal, TIRF, microscopy, and many more. Furthermore, with the new NestedScanner technology, cells, bacteria or structured surfaces with sample heights of up to 8 µm can now be examined at the highest scan speeds.

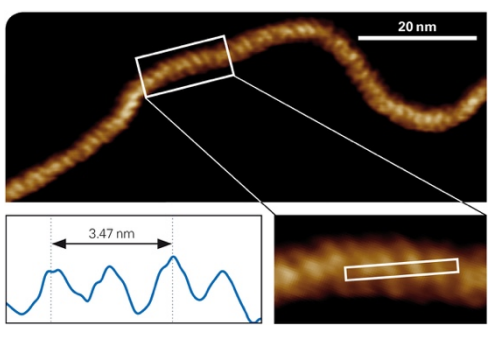


Fig. 1: Image of Plasmid-DNA with major and minor grooves (imaged in liquid.

DISCUSSION & CONCLUSIONS: We will present how the latest advances in the ULTRA Speed 2 AFM can be applied to study a widerange of biological samples, from individual biomolecules to mammalian cells and tissues in real-time, in-situ experiments. We will also describe how this unique system enables new research opportunities with high-speed, high-resolution correlative AFM-light microscopy.

REFERENCES: [1] Winkel et al., The Wide-Open Door: Atomic Force Microscopy 30 Years On, Microscopy Today, 2016, 24(6), pp. 12–17. [2] D. Stamov et al, BioScience AFM - Capturing Dynamics from Single Molecules to Living Cells, Microscopy Today, 2015 November, 18-25.